

MITIGATION OF BACTERIAL ADHESION  
ON METAL SURFACES BY  
SURFACE ROUGHNESS MODIFICATION



NORATIQA BINTI CHIK

اونيورسيٲي ملايسيا قهغ

UNIVERSITI MALAYSIA PAHANG

MASTER OF SCIENCE

UNIVERSITI MALAYSIA PAHANG

## UNIVERSITI MALAYSIA PAHANG

### DECLARATION OF THESIS AND COPYRIGHT

Author's Full Name : NORATIQA BINTI CHIK

Date of Birth : 27<sup>TH</sup> JULY 1991

Title : MITIGATION OF BACTERIAL ADHESION ON METAL SURFACES BY SURFACE ROUGHNESS MODIFICATION

Academic Session : SEM II 2020/2021

I declare that this thesis is classified as:

- CONFIDENTIAL (Contains confidential information under the Official Secret Act 1997) \*
- RESTRICTED (Contains restricted information as specified by the organization where research was done)\*
- OPEN ACCESS I agree that my thesis to be published as online open access (Full Text)

I acknowledge that Universiti Malaysia Pahang reserves the following rights:

1. The Thesis is the Property of Universiti Malaysia Pahang
2. The Library of Universiti Malaysia Pahang has the right to make copies of the thesis for the purpose of research only.
3. The Library has the right to make copies of the thesis for academic exchange.

Certified by:



(Student's Signature)

910727-02-5958

New IC / Passport Number  
Date: 14 JULY 2021



(Supervisor's Signature)

Dr. Wan Salwanis Bt. Wan Md. Zain

Name of Supervisor  
Date: 14 JULY 2021

NOTE: \* If the thesis is CONFIDENTIAL or RESTRICTED, please attach a thesis declaration letter.

### SUPERVISOR'S DECLARATION

We hereby declare that We have checked this thesis and in our opinion, this thesis is adequate in terms of scope and quality for the award of the degree of Master of Science.



---

(Supervisor's Signature)

Full Name : DR. WAN SALWANIS BINTI WAN MD. ZAIN

Position : SENIOR LECTURER

Date : 14 JULY 2021



---

(Co-supervisor's Signature)

Full Name : DR. WAN HANISAH BINTI WAN IBRAHIM

Position : SENIOR LECTURER

Date : 14 JULY 2021

## STUDENT'S DECLARATION

I hereby declare that the work in this thesis is based on my original work except for quotations and citations which have been duly acknowledged. I also declare that it has not been previously or concurrently submitted for any other degree at Universiti Malaysia Pahang or any other institutions.



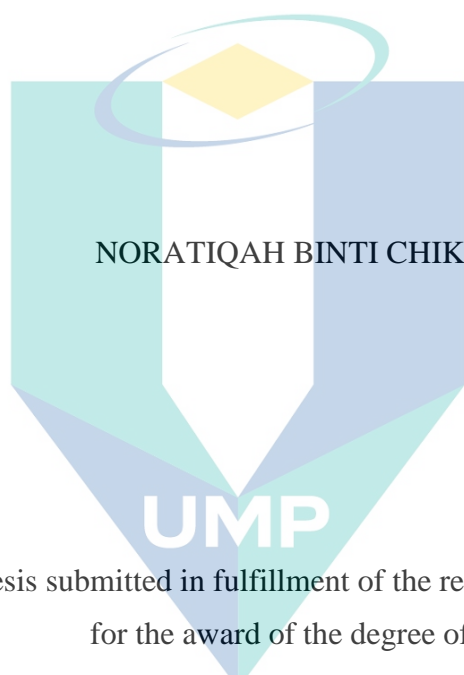
(Student's Signature)

Full Name : NORATIQAHA BINT CHIK  
ID Number : MKB 15008  
Date : 14 JULY 2021

اونيورسيتي ملايسيا قهغ

UNIVERSITI MALAYSIA PAHANG

MITIGATION OF BACTERIAL ADHESION  
ON METAL SURFACES BY  
SURFACE ROUGHNESS MODIFICATION



Thesis submitted in fulfillment of the requirements  
for the award of the degree of  
Master of Science

اونيورسيتي ملايسيا قهغ

UNIVERSITI MALAYSIA PAHANG  
UNIVERSITI MALAYSIA PAHANG

JULY 2021

## ACKNOWLEDGEMENTS

*In the name of Allah, the Most Gracious and the Most Merciful.*

First and foremost, praises and thanks to Allah the Almighty for the shower of blessing throughout my study. Thank you for giving me this opportunity and for keeping me strong to finish what I have started.

I would like to express my deepest and sincere gratitude to my supervisor Dr. Wan Salwanis Bt. Wan M. Zain for her endless supports, advice and motivations from the beginning until the end of my study. I would say my supervisor is my strength and without her guidance and encouragement, I probably could not complete this study. She helped a lot especially in thesis writing and never gave up to share her knowledge and opinions about the research. It has been a great pleasure and honor to be under her supervision. Thank you, Dr, I will always put your name and your family in my prayers (*InshaAllah*).

I also want to extend my thanks to Universiti Malaysia Pahang and FABSURFWAR teams for funding me throughout the study and giving me a chance to involve in the Visiting Fellow Program (Sponsored Researcher) at the University of Warwick for almost six months. It was like a dream comes true for me as I got to visit other countries and learned a lot of new things during the program. Besides that, special gratitude also goes to my postgrad's friends Huda, Sofia, Kira, Kak Aini, Nurul Atikah, Fida, Ashikin, Aishah, Ain, Kak Hajar and Kak Tasha for helping me especially during the lab work. I am so grateful to have them during the journey.

Finally, special thanks to all my family members that have been supporting me all the time and always be my side when the times get hard. My father Chik Bin Yom, my mother Che Mah Bt. Hasan, my brothers Abdul Rahim and Amiruddin and my sisters Hayati, Haliza and Hayani are all the special persons that always pray for me until I managed to complete this study successfully.

اونيورسيتي ملايسيا فاهڠ

UNIVERSITI MALAYSIA PAHANG

## ABSTRAK

Pencemaran-bio disebabkan oleh kelekatan bakteria telah menyebabkan kontaminasi terhadap alatan perubatan, bio-kakisan terhadap alatan industri dan banyak lagi. Kelekatan bakteria di atas sesuatu permukaan akan menghasilkan satu lapisan bakteria (biofilm) yang amat susah untuk dibasmi. Oleh itu, industri-industri telah menghabiskan berjuta ringgit untuk proses pembasmian dan penyucian 'biofilm' tersebut. Banyak faktor yang menyumbang kepada masalah kelekatan bakteria telah dikaji tetapi, faktor yang berkaitan dengan permukaan topografi mempunyai maklumat yang tidak konsisten dan kurang tepat. Oleh itu, kajian ini telah mengkaji kesan topografi terhadap kelekatan bakteria. Objektif kajian ini adalah untuk menilai kesan kepelbagaian ciri-ciri permukaan besi terhadap kelekatan bakteria yang juga akan dikaitkan dengan faktor-faktor lain seperti ciri-ciri bakteria dan faktor persekitaran. Bakteria *Escherichia coli* (*E. coli*) ATCC 8739 dan *Staphylococcus aureus* (*S. aureus*) ATCC 6838 telah digunakan dalam ujian kelekatan ke atas besi stainless steel AISI 316L (SS) dan titanium Gred 5 (TT) dimana ujian tersebut telah dijalankan selama 4 jam untuk setiap proses. Permukaan SS dan TT telah difabrikasi menggunakan teknik penggilapan (P-kontrol), pengisaran (G), laser millisaat (MI), dan laser ultracepat (UI). Ciri-ciri permukaan besi dan bakteria untuk kajian ini telah diuji sepenuhnya. UI mempunyai permukaan yang hidrofobik manakala kebanyakan permukaan G dan MI adalah hidrofilik. Dari segi ujikaji kekasaran, teknik G, MI dan UI telah menghasilkan permukaan yang mempunyai  $S_q$  (ukuran kekasaran) antara 98.34 nm – 720 nm untuk SS dan 88.92 nm – 630 nm untuk TT, serta ukuran sudut kontak (UKS-ukuran kebasahan permukaan) sebanyak  $70^\circ$  hingga  $146^\circ$ . *E. coli* ATCC 8739 telah dilaporkan mempunyai permukaan yang hidrofilik manakala *S. aureus* ATCC 6838 mempunyai permukaan hidrofobik dan kedua-duanya mempunyai caj permukaan yang negatif. Keputusan mengenai kesan pH dan kepekatan garam terhadap kelekatan bakteria telah menunjukkan apabila pH meningkat, kelekatan bakteria telah menurun sebanyak 44% - 75% manakala kenaikan kepekatan garam telah meningkatkan kelekatan bakteria ke atas permukaan SS dan TT sebanyak 10 kali ganda lebih. Ini adalah disebabkan perubahan pH dan kepekatan garam telah mempengaruhi caj dan kekuatan ion permukaan bakteria lalu memberi kesan terhadap kelekatan bakteria. Di samping itu, permukaan UI telah menunjukkan kelekatan *E. coli* ATCC 8739 dan *S. aureus* ATCC 6838 yang terendah di atas SS dan TT dengan pengurangan sebanyak 12% ke 98% apabila dibandingkan dengan permukaan P (kontrol). UI juga telah membuktikan mampu mengurangkan kelekatan *E. coli* ATCC 8739 ke atas SS dan TT sebanyak 10% - 91% pengurangan apabila dibandingkan dengan permukaan G dan MI. Penghasilan LIPSS (struktur berombak) dan serbuk besi yang tidak sekata (bersaiz nano) di atas permukaan UI selepas proses fabrikasi telah menyumbang kepada pengurangan bakteria dengan menghadkan titik sentuhan antara bakteria dan permukaan besi. Keseluruhannya, jika dibandingkan dengan permukaan P (kontrol), permukaan UI telah mencatatkan permukaan yang mempunyai kelekatan *E. coli* ATCC 8739 (20% - 98%) dan *S. aureus* ATCC 6838 (12% - 78%) yang paling rendah terutamanya pada permukaan UI-SS-0.10 dengan  $S_q = 298$  nm dan  $S_{ds} = 17039.43/\text{mm}^2$  dan permukaan UI-TT-0.10 dengan  $S_q = 210$  nm dan  $S_{ds} = 16456.30/\text{mm}^2$  dimana peningkatan hidrofobik dan kekasaran permukaan telah menjadi faktor utama kepada penurunan kelekatan bakteria.

## ABSTRACT

Bio-fouling caused by bacterial adhesion on metal surfaces creates contamination in medical equipment, bio-corrosion of industrial devices and many more. Bacterial adhesion on a surface will develop a biofilm which will be extremely difficult to remove. Therefore, industries had suffered from billions of dollars for the process of removing and cleaning the biofilm. Many factors that contributed to the bacterial adhesion had been studied but factors related to the surface topography are found inconsistent and not accurate. Hence, this study was investigating on the effect of surface topography towards bacterial adhesion. The objectives of this study are to evaluate the effect of varying surface properties towards the bacterial adhesion on the metal surfaces which also will be associated with other factors like bacterial properties and environmental factors. *Escherichia coli* (*E. coli*) ATCC 8739 and *Staphylococcus aureus* (*S. aureus*) ATCC 6838 were used in the adhesion test on stainless steel AISI 316L (SS) and Grade 5 titanium alloys (TT) where the test has been carried out for 4 hours for each process. SS and TT surfaces were fabricated by using the polishing technique (P-control), grinding (G), millisecond laser (MI) and ultrafast laser (UI). The characterizations of the metal and bacterial surfaces have been investigated. UI surfaces are mainly hydrophobic while G and MI surfaces are mostly hydrophilic. In terms of surface roughness, G, MI and UI techniques had produced  $S_q$  (root mean square roughness) ranging from 98.34 nm – 720 nm for SS and 88.92 nm – 630 nm for TT, while CAM (Contact angle measurement) for the surfaces varies between  $70^\circ$  to  $146^\circ$ . *E. coli* ATCC 8739 was reported to have a hydrophilic surface while *S. aureus* ATCC 6838 has a hydrophobic surface and both have negative surface charge. Based on the effect of pH and salt concentration towards the bacterial adhesion, the results showed that when pH increased the number of bacterial adhered on P-SS and P-TT had reduced about 44% - 75% while the increase of salt concentration had increased up to 10-fold of adhesion of both bacteria. This is because the changes of pH and salt concentration of bacterial solution had influenced the bacterial surface charge and the ionic strength thus, affecting the adhesion. Besides that, UI surfaces were found to have the lowest adhesion of *E. coli* ATCC 8739 and *S. aureus* ATCC 6838 on both UI-SS and UI-TT which is about 12% to 98% of reduction when compared to P surface (control). UI also had proved can reduce *E. coli* ATCC 8739 adhesion on both SS and TT with a 10% - 91% of reduction when compared to G and MI surfaces. The generation of LIPSS (ripples) and nano-sized irregular grains on the UI surfaces after the fabrication process had contributed to the bacterial reduction by minimizing the contact point between the bacteria and metal surfaces. Overall, the highest reduction for *E. coli* ATCC 8739 (20% - 98%) and *S. aureus* ATCC 6838 (12% - 78%) against polished surface was achieved with UI specifically at UI-SS-0.10 with  $S_q = 298$  nm and  $S_{ds} = 17039.43/\text{mm}^2$  and UI-TT-0.10 with  $S_q = 210$  nm and  $S_{ds} = 16456.30/\text{mm}^2$  which were mainly contributed due to the increase of hydrophobicity and roughness.



## TABLE OF CONTENT

**DECLARATION**

**TITLE PAGE**

**ACKNOWLEDGEMENTS** **ii**

**ABSTRAK** **iii**

**ABSTRACT** **iv**

**TABLE OF CONTENT** **v**

**LIST OF TABLES** **x**

**LIST OF FIGURES** **xi**

**LIST OF SYMBOLS** **xiv**

**LIST OF ABBREVIATIONS** **xvi**

**CHAPTER 1 INTRODUCTION** **1**

1.1 Background of Study 1

1.2 Motivation and Problem Statement 4

1.3 Research Objectives 6

1.4 Research Scopes 6

1.5 Significance of Study 7

1.6 Thesis Outline 8

**CHAPTER 2 LITERATURE REVIEW** **9**

2.1 Introduction 9

2.2 Biofilm Formation 10

2.3 Microorganism 13

2.3.1	<i>Escherichia coli</i>	14
2.3.2	<i>Staphylococcus aureus</i>	15
2.4	Bio-surface	16
2.4.1	Stainless Steel	17
2.4.2	Titanium	18
2.5	Surface Modifications	19
2.5.1	Polishing and Grinding	19
2.5.2	Laser Treatments	21
2.6	Factors of Bacterial Adhesion	24
2.6.1	Effect of Bacterial Properties	25
2.6.2	Effect of Metal Surface Properties	27
2.6.3	Effect of Environmental Condition	31
2.7	Summary	32
<b>CHAPTER 3 MATERIALS AND METHODS</b>		<b>34</b>
3.1	Introduction	34
3.2	Materials	36
3.2.1	Bacteria	36
3.2.2	Chemicals	36
3.2.3	Metals	36
3.3	Methods: Metals Fabrication	36
3.3.1	Polishing (Control Surface)	37
3.3.2	Grinding	38
3.3.3	Millisecond Laser Treatment	38
3.3.4	Ultrafast Laser Treatment	38
3.3.5	Metal Washing Process	39

3.4	Methods: Bacterial Preparation	40
3.4.1	Preservation of Stock Culture	40
3.4.2	Media Preparation	40
3.4.3	Germination of Stock Culture and Inoculum	41
3.5	Method: Adhesion Test	41
3.6	Analysis: Characterization of Metal Surfaces	42
3.6.1	Contact Angle Measurements (CAM)	42
3.6.2	Optical Profilometer	42
3.6.3	Scanning Electron Microscopy (SEM)	43
3.7	Analysis: Characterizations of Bacteria	43
3.7.1	Gram Staining	43
3.7.2	Bacteria Size Analyzer	43
3.7.3	Bacterial Adherence to Hydrocarbon (BATH) Technique	44
3.7.4	Salt Aggregation Test (SAT)	44
3.7.5	Zeta Potential Analyzer	44
3.8	Analysis: Bacterial Adhesion	45
3.8.1	Fluorescence Microscope	45
3.8.2	Scanning Electron Microscopy (SEM)	45

**CHAPTER 4 METAL AND BACTERIAL SURFACE CHARACTERIZATIONS**

4.1	Introduction	46
4.2	Metal Surface Characterizations	46
4.2.1	Contact Angle Measurement (CAM)	46
4.2.2	Surface Roughness	48
4.2.3	Surface Morphologies	56

4.3	Bacterial Characterizations	61
4.3.1	Gram Staining	61
4.3.2	Bacterial Size and Shape	62
4.3.3	Bacterial Hydrophobicity	63
4.3.4	Bacterial Surface Charge	65
4.4	Summary	66

## **CHAPTER 5 ASESSMENT OF BACTERIAL ADHESION** **68**

5.1	Introduction	68
5.2	Effect of Environmental Condition (pH and salt concentration) on the Bacterial Adhesion	69
5.2.1	Bacterial Adhesion on Stainless Steel	69
5.2.2	Bacterial Adhesion Titanium	72
5.2.3	Comparative Assessment of Bacterial Adhesion on Stainless Steel and Titanium	74
5.3	Effect of Surface Fabrication on the Bacterial Adhesion	75
5.3.1	Bacterial Adhesion on Stainless Steel	75
5.3.2	Bacterial Adhesion on Titanium	82
5.3.3	Comparative Assessment of Bacterial Adhesion on Stainless Steel and Titanium	88
5.3.4	Bacterial Adhesion on Ultrafast Laser Surfaces Fabricated under Argon Gas	96
5.4	Summary	97

## **CHAPTER 6 CONCLUSION AND RECOMMENDATIONS** **99**

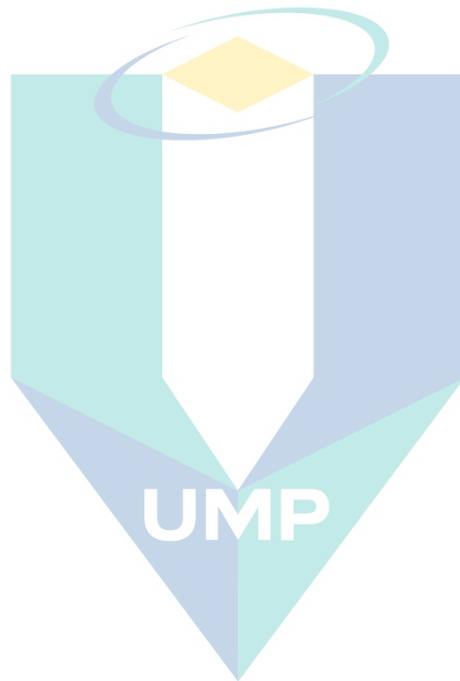
6.1	Conclusion	99
6.2	Recommendations	101

**REFERENCES**

**102**

**APPENDIX A LIST OF PUBLICATIONS AND AWARDS**

**121**



اونيورسيتي مليسيا قهغ

**UNIVERSITI MALAYSIA PAHANG**

## LIST OF TABLES

Table 2.1	Physical properties of stainless steel	17
Table 2.2	Physical properties of titanium	18
Table 2.3	The adhesion of bacteria on various surface roughness	29
Table 3.1	Symbols used for sample classification	37
Table 3.2	Parameters of millisecond laser and ultrafast laser in texturing the metal surfaces	39
Table 3.3	Composition of PBS solution	41
Table 4.1	Contact angle measurement of stainless steel AISI 316L and grade 5 titanium alloy surfaces	47
Table 4.2	Result of $S_q$ , $S_a$ , $S_{sk}$ , $S_{ku}$ , $S_{dr}$ and $S_{ds}$ of stainless steel AISI 316L	51
Table 4.3	Result of $S_q$ , $S_a$ , $S_{sk}$ , $S_{ku}$ , $S_{dr}$ and $S_{ds}$ of grade 5 titanium alloy	52
Table 4.4	All characterizations of <i>E. coli</i> ATCC 8739 and <i>S. aureus</i> ATCC 6838	66
Table 5.1	Data of bacterial adhesion on G-SS and surface parameters	77
Table 5.2	Data of bacterial adhesion on MI-SS and surface parameters	79
Table 5.3	Data of bacterial adhesion on UI-SS and surface parameters	81
Table 5.4	Data of bacterial adhesion on G-TT and surface parameters	83
Table 5.5	Data of bacterial adhesion on MI-TT and surface parameters	86
Table 5.6	Data of bacterial adhesion on UI-TT and surface parameters	88
Table 5.7	Average number of bacterial count based on the contact angle measurement (CAM) at different surface fabrication	94
Table 5.8	Number of <i>E. coli</i> ATCC 8739 and <i>S. aureus</i> ATCC 6838 adhesion on UI-SS and UI-TT surfaces fabricated under argon gas	97

اوپنیورسیتی ملیسیا فہق

UNIVERSITI MALAYSIA PAHANG

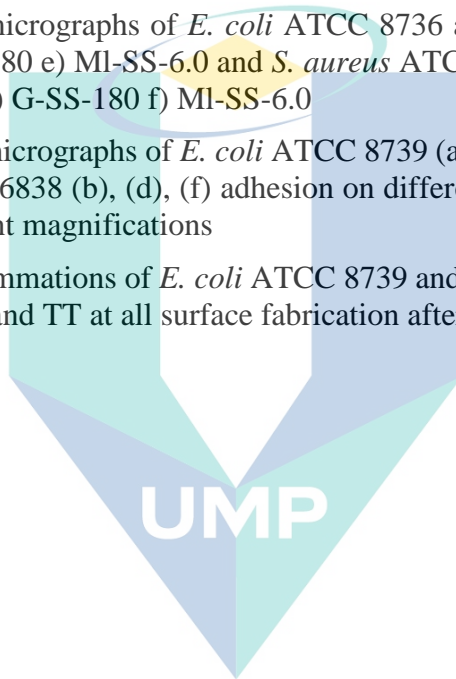
## LIST OF FIGURES

Figure 2.1	Steps of biofilm formation	11
Figure 2.2	The cross section of the membrane structures of <i>E. coli</i>	15
Figure 2.3	The cross section of the membrane structures of <i>S. aureus</i>	16
Figure 2.4	X-ray images of stainless steel used in broken bones a) screw and plates used to hold the broken ankle b) pins used to hold the broken elbow	17
Figure 2.5	X-ray images of titanium used as knee joint in orthopaedic implant	18
Figure 2.6	Schematic diagram of grinding process	21
Figure 2.7	Schematic diagram of ultrafast laser (femtosecond laser) treatment process	23
Figure 2.8	Schematic presentation of roughness profile for $S_a$ and $S_q$	30
Figure 2.9	Schematic presentation of roughness profile for a) $S_{sk}$ b) $S_{ku}$	30
Figure 3.1	Flow chart for the overall process of study	35
Figure 3.2	Schematic diagram of metal surfaces fabricated by a) polishing, grinding and ultrafast laser b) millisecond laser for stainless steel AISI 316L and grade 5 titanium alloys	37
Figure 4.1	Examples of drop shape image of distilled water on metals surfaces with the measurement of contact angle a) G-SS-180, 79.20° b) G-TT-180, 72.30° c) UI-SS-0.11, 145.70° d) UI-TT-0.01, 130.10°	48
Figure 4.2	3D-topography images of polishing (P) and grinding (G) surfaces. Warm colors (brown and yellow) depict surface with greater surface roughness and cold colors (blue and green) describes otherwise	53
Figure 4.3	3D-topography images of, millisecond laser (MI) surfaces. Warm colors (brown and yellow) depict surface with greater surface roughness and cold colors (blue and green) describes otherwise	54
Figure 4.4	3D-topography images of ultrafast laser (UI) surfaces. Warm colors (brown and yellow) depict surface with greater surface roughness and cold colors (blue and green) describes otherwise	55
Figure 4.5	SEM images of the common features available on the surfaces after various of fabrication techniques a) ultrafast laser surface at 500x magnification b) grinding surface at 2000x magnification c) ultrafast laser surface at 20000x magnification d) ultrafast laser surface at 20000x magnification	56
Figure 4.6	SEM micrograph of the surface morphologies of polishing (P) and grinding (G) surfaces at 2000x of magnification	57
Figure 4.7	SEM micrograph of the surface morphologies of millisecond laser (MI) surfaces at 2000x of magnification	58

Figure 4.8	SEM micrographs of the surface morphologies ultrafast laser (UI) surfaces at 20000x magnification. The red circle area highlighted the nano-size irregular grains formed on top of LIPSS	59
Figure 4.9	Image of Gram stained of a) <i>E. coli</i> ATCC 8739 (red colour), b) <i>S. aureus</i> ATCC 6838 (violet/purple colour) under 100x magnification of light microscope	62
Figure 4.10	Size and shape of bacterial under scanning electron microscope a) <i>E. coli</i> ATCC 8739 b) <i>S. aureus</i> ATCC 6838 at 4000x of magnification	63
Figure 5.1	Flourescence image of a) <i>E. coli</i> ATCC 8739 and b) <i>S. aureus</i> ATCC 6838 on UI-SS-0.11 after 4 hours of adhesion at 100x magnification	68
Figure 5.2	Effect of pH on the adhesion of <i>E. coli</i> ATCC 8739 and <i>S. aureus</i> ATCC 6838 on P-SS in the PBS solution with shaking 70 rpm for 4 hours	71
Figure 5.3	Effect of salt concentration (mol/L) on the adhesion of <i>E. coli</i> ATCC 8739 and <i>S. aureus</i> ATCC 6838 on P-SS in the PBS solution with shaking 70 rpm for 4 hours	71
Figure 5.4	Diagram of electrical double layer (EDL) around positively charged bacteria (depends on the bacterial strain)	72
Figure 5.5	Effect of pH on the adhesion of <i>E. coli</i> ATCC 8739 and <i>S. aureus</i> ATCC 6838 on P-TT in the PBS solution with shaking 70 rpm for 4 hours	73
Figure 5.6	Effect of salt concentration (mol/L) on the adhesion of <i>E. coli</i> ATCC 8739 and <i>S. aureus</i> ATCC 6838 on P-TT in the PBS solution with shaking 70 rpm for 4 hours	73
Figure 5.7	Number of <i>E. coli</i> ATCC 8739 and <i>S. aureus</i> ATCC 6838 adhesion on G-SS surface at different types of grit size after 4 hours of adhesion in the PBS solution with 70 rpm of shaking (pH 7.4 and 0.0137 mol/L of NaCl)	76
Figure 5.8	Number of <i>E. coli</i> ATCC 8739 and <i>S. aureus</i> ATCC 6838 adhesion on MI-SS surface at different types of power after 4 hours of adhesion in the PBS solution with 70 rpm of shaking (pH 7.4 and 0.0137 mol/L of NaCl)	78
Figure 5.9	Number of <i>E. coli</i> ATCC 8739 and <i>S. aureus</i> ATCC 6838 adhesion on UI-SS surface at different types of power after 4 hours of adhesion in the PBS solution with 70 rpm shaking (pH 7.4 and 0.0137 mol/L of NaCl)	81
Figure 5.10	Number of <i>E. coli</i> ATCC 8739 and <i>S. aureus</i> ATCC 6838 adhesion on G-TT surface at different types of grit size after 4 hours of adhesion in the PBS solution with 70 rpm shaking (pH 7.4 and 0.0137 mol/L of NaCl)	83



Figure 5.11	Number of <i>E. coli</i> ATCC 8739 and <i>S. aureus</i> ATCC 6838 adhesion on MI-TT surface at different types of power after 4 hours of adhesion in the PBS solution with 70 rpm shaking (pH 7.4 and 0.0137 mol/L of NaCl)	86
Figure 5.12	Number of <i>E. coli</i> ATCC 8739 and <i>S. aureus</i> ATCC 6838 adhesion on UI-TT surface at different types of power after 4 hours of adhesion in the PBS solution with 70 rpm shaking (pH 7.4 and 0.0137 mol/L of NaCl)	87
Figure 5.13	The average summation of <i>E. coli</i> ATC 8739 and <i>S. aureus</i> ATCC 6838 adhesion on SS and TT which undergone different surface fabrications	89
Figure 5.14	SEM micrographs of <i>E. coli</i> ATCC 8736 adhesion on a) P-SS c) G-SS-180 e) MI-SS-6.0 and <i>S. aureus</i> ATCC 6838 adhesion on b) P-SS d) G-SS-180 f) MI-SS-6.0	91
Figure 5.15	SEM micrographs of <i>E. coli</i> ATCC 8739 (a), (c), (e) and <i>S. aureus</i> ATCC 6838 (b), (d), (f) adhesion on different parts of UI-SS with different magnifications	92
Figure 5.16	The summations of <i>E. coli</i> ATCC 8739 and <i>S. aureus</i> ATCC 6838 on SS and TT at all surface fabrication after 4 hours of adhesion	96



اونيور سيطي ملايسيا قهغ

UNIVERSITI MALAYSIA PAHANG

## LIST OF SYMBOLS

$(\text{NH}_4)_2\text{SO}_4$	Ammonium sulphate
Ar	Argon gas
$S_q$	Average roughness
$\text{COO}^-$	Carboxylate ion
cm	Centimetre
°	Degree
°C	Degree Celsius
$S_{dr}$	Developed surface area ratio
$\text{Na}_2\text{HPO}_4 \cdot 7\text{H}_2\text{O}$	Disodium hydrogen phosphate
$\text{dyn/cm}^2$	Dyne per square centimetre
<i>E. coli</i> ATCC 8739	<i>Escherichia coli</i> ATCC 8739
$\text{Fe}^{2+}$	Ferrous ion/ iron
g	Gram
$\text{g/cm}^3$	Gram per cubic centimetre
Hz	Hertz
$\text{C}_6\text{H}_{14}$	Hexane
$\text{C}_{16}\text{H}_{34}$	Hexadecane
HCl	Hydrochloric acid
KHz	Kilohertz
$S_{ku}$	Kurtosis
L	Litre
<	Less than
$\mu\text{m}$	Micrometre
$\mu\text{L}$	Microlitre
Min	Minutes
$\mu\Omega/\text{cm}$	Microohm per centimetre
mm	Millilitre
mM	Millimolar
mS/cm	Millisiemens per centimetre
ml	Millilitre
mV	Millivolt

mm/s	Millimetre per second
mol/L	Mol per litre
mol L <sup>-1</sup>	Mol per litre
M	Molarity
>	More than
nm	Nanometre
N/mm <sup>2</sup>	Newtons per square millimetre
%	Percentage
ps	Picosecond
KCl	Potassium chloride
KH <sub>2</sub> PO <sub>4</sub>	Potassium dihydrogen phosphate
pH	Potential hydrogen
rpm	Rotation per minute
S <sub>q</sub>	Root mean square roughness
S <sub>dq</sub>	Root mean square slope
S <sub>sk</sub>	Skewness
<i>S. aureus</i>	<i>Staphylococcus aureus</i>
S <sub>ds</sub>	Summit density
NaOH	Sodium hydroxide
NaCl	Sodium chloride
SiC	Silicon carbide
mm <sup>2</sup>	Square millimetre
cm <sup>2</sup>	Square centimetre
V	Voltage
v/v	Volume per volume
W	Watt
w/v	Weight per volume
C <sub>8</sub> H <sub>10</sub>	Xylene

## LIST OF ABBREVIATIONS

BATH	Bacterial adherence to hydrocarbon
BSA	Bovine serum albumin
CAM	Contact angle measurement
DVLO	Derjaguin, Verwey, Landau and Overbeak
EDL	Electrical double layer
EPS	Extracellular polymeric substance
G	Grinding
HIC	Hydrophobic interaction chromatography
IEP	Isoelectric point
KIT	Karlsruhe Institute Technology
LB	Luria Bertani
LIPSS	Laser induced periodic structure
LTA	Lipoteichoic acid
MIC	Microbiologically influenced corrosion
MI	Millisecond laser
OD	Optical density
P	Polishing
PBS	Phosphate buffer solution
PIA	Polysaccharide intercellular adhesins
QS	Quorum sensing
SEM	Scanning electron microscopy
SS	Stainless steel AISI316L
TT	Titanium alloys grade 5
3D	Three dimensional
TPP	Two phase system
UI	Ultrafast laser
UV	Ultraviolet
XDVLO	Extended Derjaguin, Verwey, Landau and Overbeak

# CHAPTER 1

## INTRODUCTION

### 1.1 Background of Study

Bacteria are ubiquitous and easily attach to the exposed surfaces. Different surfaces and different types of bacteria will give disparities implications to the level of bacterial attachment and creates different problems in various industry ranging from contamination in medical devices, food industry, pharmacy sector, and marine science to bio-fouling or bio-corrosion of industrial equipment (Bohinc et al., 2016; Sheng et al., 2007). The attachment of bacterial colonies to a surface is termed as adhesion (Garrett et al., 2008) which often lead to biofilm formation where colonies of bacteria embedded in extracellular polymeric substances (EPS) (Olsen, 2015). EPS protects the bacteria and also able to prevent the access of certain antimicrobial agent or antibiotic (antibiotic-resistance) into the biofilm (Harimawan & Ting, 2016). Therefore, the biofilm can be extremely difficult to remove as well as the eradication of pathogen is difficult, time-consuming and expensive (Cunliffe et al., 1999). Hence, many industries were reported to suffer the ill-effect of biofilm especially in medical industry where 2% - 5% of implant recipients facing risk for serious implant-associated infections (Armentano et al., 2014; Wang & Tang, 2019). Fortunately, researchers had found that bacterial adhesion to the implant surfaces is the first stage in developing an implant-associated infection and the effective ways to overcome this problem is to mitigate the adhesion itself (Lu et al., 2020; Wassmann et al., 2017).

Adhesion of bacteria is mediated by various physico-chemical interactions between bacterial cell and substratum surface (Lu et al., 2016; Ortega et al., 2008). Generally, the mechanisms of the bacterial adhesion can be described into two phases which are physicochemical interaction and molecular and cellular interaction (An & Friedman, 2000; Anikieieva & Gordiyenko, 2014). The initial phase involved the movement of bacteria to a material surface (distance 5 nm – 50 nm between bacterial and surfaces) by the effect of physico-chemical forces, such as Brownian motion, van der

Waals attraction forces, gravitational forces and the effect of surface electrostatic charge and hydrophobic interaction (Abraham et al., 2015; Armentano et al., 2014; Gottenbos et al., 2002) between the two surfaces. In the second phase, molecular-specific interaction between bacterial surface structures and material surfaces become firmer due to the bridging function of the bacterial polymeric structure including capsules, flagella, fimbriae or pili and slime (Tuson & Weibel, 2013). The polymeric structures also called as adhesins which facilitate the process of the bacterial (Floyd et al., 2017) adhesion by binding to the material surfaces and form a biofilm afterwards. Shaikh et al. (2017) mentioned that, in order to prevent the formation of biofilm, it is important to control the bacterial adhesion since its initial phase which is during the physicochemical interaction between the bacteria and the surface.

Many factors play important role during the initial phase of adhesion of bacteria onto the material surfaces which all directly linked to the bacterial properties, material surface properties and environmental condition (Habimana et al., 2014; Katsikogianni & Missirlis, 2004). For a given material surface, different bacterial species and strains adhere differently since the characteristics of bacteria such as surface hydrophobicity, surface charge and bacterial size varies between species and strains (Katsikogianni & Missirlis, 2004). Besides that, surface roughness, surface hydrophobicity, surface morphologies (texture/pattern), and surface chemistry of a material surface also give significant effect on the process of the bacterial adhesion. In addition, the environmental condition such as pH, salinity (salt concentration), time, temperature and shear stress of the medium are another important factors that also dictates the adhesion (An & Friedman, 2000; Cunha et al., 2016).

Several strategies and approaches were introduced to discourage the initial adhesion of bacterial cells on the material surfaces. For instance, coating the surfaces with antibacterial metals (copper, silver), impregnation with antibiotics, chemical treatments and plasma-assisted modification (Chan et al., 2017; Shaikh et al., 2017). Unfortunately, considerable drawbacks to such approaches exist, including possibility of antibiotic resistance, toxicity to human cells and also the exhausted coating layers which can cause functionality loss due to the hydrolytic or thermal degradation (Chan et al., 2017; Jang et al., 2018). Then, modification of surface topography has become attention when a few studies reported a great improvement over adhesion after implementation of

surface texturing whilst controlling the topography and roughness within certain range (Bohinc et al., 2016; Zhang et al., 2018) The micro/nanoscale structures exhibited anti-adhesion properties which can inhibit the bacterial adhesion by reducing the contact area between the bacteria and the material surface (Kumar & Hiremath, 2019; Wu et al., 2018). Dantas et al. (2016) also mentioned that the initial attachment of bacteria on certain surfaces are assisted by surface irregularities and controlling the surface roughness is the essential steps in reducing the bacterial adhesion. On top of that, surface hydrophobicity and surface morphology as well as environmental factors (pH, salinity) also determined the initial progress of the bacterial adhesion (Orapiriyakul et al., 2018).

Although numerous studies have been performed to identify the relationship between bacterial adhesion and the surface properties of a material, there is still no fixed conclusion can be derived as adhesion are material and strain specific. For example, *S. epidermis* was discovered to preferentially adhere on rough modified stainless steel surfaces (Zhang et al., 2018). However, an increase in the roughness did not facilitate the adhesion of *S. mutants* on the ceramic surfaces (Song et al., 2015). These uncertain results are due to the distinctive material properties and bacterial properties studied in the tests. Therefore, in this research the effect of surface properties specifically surface roughness towards the bacterial adhesion on the different material surfaces was investigated in detail as well as studied other factors that are involved in this problem. This study was focusing on the mitigation of bacteria from Gram positive and negative types that are mostly found in the medical field (Bachirraho & Abouni, 2017). The bacteria were chosen based on the properties different, where the study is focused on understanding the effect of the bacterial size and shape, bacterial hydrophobicity and bacterial surface charge. While for material surface properties, factors involved are surface hydrophobicity, surface roughness and surface morphologies. In order to discuss the effect of surrounding, only pH and salinity have been studied to gain a better understanding on the effect of charge and ionic strength of a solution towards the bacterial adhesion process. All these factors were believed give huge impacts on the initial adhesion of bacteria onto the material surfaces.

## 1.2 Motivation and Problem Statement

The existence of bacteria colonies or biofilm on a surface has triggered researchers to deeply investigate the factors of bacterial adhesion as many industries have suffered from this problem. Bacterial infection in medical application became a major impediment to the long-term use of implanted or intravascular devices such as joint prostheses, heart valve, vascular valves, vascular catheters, contact lenses and dentures (Herman-Bausier et al., 2015; Lu et al., 2016). Besides that, bio-fouling and bio-corrosion are the worldwide problems caused by the biofilm in the industrial application which leads to metal deterioration and equipment failure (AlAbbas et al., 2012). Consequently, patients with implant-associated infection need to invest more money for the treatments while other industries encountered with a heavy cost in cleaning and maintenance their equipment due the biofilm phenomenon.

Stainless steel and titanium are the most common metallic materials used in the development of both medical devices and industrial equipment (Carvalho et al., 2013). Both stainless steel and titanium are widely used in orthopedic, cardiovascular, dentistry and craniofacial implants (Kumar & Hiremath, 2019) while, industrial equipment such as water distribution pipes, reactor and food storage are mostly made up of stainless steel (Vishwakarma, 2020). Adhesion of bacteria on these metals had created aforementioned problems. Besides that, there are many bacteria related to the implant-associated infection but the most common pathogen are *Escherichia coli* (*E. coli*) and *Staphylococcus aureus* (*S. aureus*) (Bachirraho & Abouni, 2017). Both *S. aureus* and *E. coli* contributed about 33% - 43% and 4% - 7% to this infection, respectively, and were easily found in the human body as well as in the domestic pipeline and wastewater (Barros et al., 2019; Tasneem et al., 2018). On the other hand, these two bacteria have distinctive properties in term of Grams types, size and shape (Zituni et al., 2013). As mentioned in the introduction part, different bacterial species will adhere differently on a surface hence, it is interesting to investigate the adhesion of both types of bacteria on the different metals like stainless steel and titanium and study the best way to reduce this bacterial adhesion problem.

Lu et al. (2016) has stated that surface topography can be a key in controlling the formation of the biofilm. Crawford et al. (2012) also had emphasized the effect of surface topography is predominant in the bacterial adhesion phenomenon when two samples with



practically identical surface chemistry (hydrophobicity, charge) were identified, exhibited greatly different bacterial adhesion profiles due to differences in surface configuration and roughness. Surface roughness is the main parameter for characterizing the surface topography besides skewness, kurtosis, root mean square gradient/slope, developed interfacial area ration, and summit density (Cheng et al., 2019). Roughness within submicron to nanometer range was reported as highly effective in reducing and combating the initial adhesion of bacteria on a surface (Jang et al., 2018). This is because, surface modification with nano-roughness and nano-features could reduce the contact area between the micron-sized bacteria with the original surface as well as create surface with bactericidal effect which subsequently can reduce the adhesion of bacteria (Xu et al., 2017).

However, the results founds are inconsistent because some studies said that bacterial prefer to adhere on nano-smooth surfaces with roughness between 45.2 nm to 172.5 nm (Wu et al., 2018; Yoda et al., 2014) while some of them found on nano-rough surface (380 nm – 730 nm) (Achinas et al., 2019; Duarte et al., 2009). Such contradictory results happened because the change of surface roughness is often accompanied by changes in surface hydrophobicity (Cheng et al., 2019) which also a dominant factor that influenced the bacterial adhesion. The indefinite correlation between nano-scale surface roughness and surface hydrophobicity towards bacterial adhesion have led to less accuracy of results and suitable surface to reliably inhibit the formation of biofilm has not been discovered yet. Apart from that, the range of surface roughness from micro to nano that suitable for bacterial removal also are not being informed in details.

Precisely, to date, there is no exact single surface with designed roughness that can eliminate all kind of bacteria and it is far from possible. Therefore, this study was focused to eliminate and to control bacteria with varying properties by means of controlling surface properties. Current work was emphasized surface fabrication (surface finishes) technique such as polishing, grinding, millisecond laser and ultrafast laser texturing on two different materials (stainless steel and titanium) as to structure the surface with roughness within the range of sub-micron to nanometer. Simultaneously, taking into account other factors such as bacterial properties (size, shape, hydrophobicity, charge) and environmental conditions (pH, salinity).

### 1.3 Research Objectives

The objectives of the study are described in detail through the following explanations. This study consists of three objectives which are:

- i. To fabricate and characterize the stainless steel AISI 316L and Grade 5 titanium alloys surfaces at varying hydrophobicity and degree of roughness within designated value.
- ii. To characterize the bacterial properties of *Escherichia coli* ATCC 8739 and *Staphylococcus aureus* ATCC 6838.
- iii. To evaluate the effect of varying surface properties towards the bacterial adhesion on the stainless steel AISI 316L and Grade 5 titanium alloys surfaces with respect to the properties of bacterial and the environmental factors.

### 1.4 Research Scopes

In order to achieve the objectives, this study was divided into several scopes, which are:

- i. Fabrication of stainless steel AISI 316L and Grade 5 titanium alloys were using four different types of surface texturing which are i) polishing (control surface), ii) grinding (grit size, 180 – 1500), iii) millisecond laser texturing (power, 3.0 W – 7.8 W) iv) ultrafast laser texturing (power, 0.04 W - 0.12 W). The fabrication process was designed to generate different surfaces structures and surface properties of the metals such as surface hydrophobicity/hydrophilicity ( $70^{\circ}$ -  $150^{\circ}$ ) and surface roughness (less than  $1\ \mu\text{m}$ ).
- ii. Characterization of the fabricated surfaces (stainless steel AISI 316L and Grade 5 titanium alloys) for determination of surface hydrophilicity/hydrophobicity (contact angle measurement (CAM)), surface roughness ( $S_q$ ,  $S_a$ ,  $S_{sk}$ ,  $S_{ku}$ ,  $S_{dr}$ ,  $S_{ds}$ ) and surface morphology using Scanning Electron Microscopy (SEM).
- iii. Characterization of *Escherichia coli* ATCC 8739 and *Staphylococcus aureus* ATCC 6838 for determination of Gram types, size, surface hydrophilicity/hydrophobicity and surface charge.

- iv. Analysis of the bacterial adhesion on the polished surfaces (control) with the effect of varying environmental conditions such as pH (4, 5, 6, 7.4, and 9) and salt concentration (0.001, 0.01, 0.1, 0.135 and 0.2 mol L<sup>-1</sup>).
- v. Study on the bacterial adhesion on the different fabricated surfaces (polishing, grinding, millisecond laser texturing, ultrafast laser texturing) in which the number of bacterial adhered per square area (cm<sup>2</sup>) was examined using ImageJ software and fluorescence microscope to determine the surface (range of roughness) with less bacterial adhesion.

### 1.5 Significance of Study

In the medical application, patients with implant associated-infection were treated with antibiotics, drugs and other chemical solutions. However, in a certain condition the antibiotics do not work anymore towards the patients due to the antibiotic resistance developed by the biofilm that adhered on the implant surfaces. Thus, the situation leads to the overuse of chemicals (drugs, antibiotics) which can become toxic and affect the health condition of human body. Therefore, instead of using a chemical to combat the bacterial infection problem, this study has come out with a physical approach as an alternative where the surface of the material will be structured with different types of fabrication process in order to identify a surface that could inhibit the adhesion of bacteria and subsequently avoid the biofilm formation. Hence, the use of chemicals in medical industry which related to the implant associated-infection could be reduced as well as the treatment costs.

Besides that, this physical approach is a green approach and produced zero waste especially for the fabrication using ultrafast laser treatments. Throughout the ultrafast laser treatment process (power > 0.10 W), molten materials called nano-sized metallic particles will be redeposited on the laser fabricated surface, creating patterns and nano particles with tailored roughness. Interestingly, the nano-sized metallic particles are permanent once the surface is cooled down, thereby it will diminish the generation of waste (water pollution) from its fabrication process. Furthermore, the laser surface treatments (millisecond laser and ultrafast laser) are very flexible process where the parameters used during the fabrication process can be controlled and adjusted easily.

They are also less time consuming because the process is very quick and a lot of samples can be produced within a short time.

## 1.6 Thesis Outline

This thesis is organized into six chapters. The first chapter briefly introduced the background study of this research followed by the motivation, problem statement, objectives, scopes and the significance of the study. Chapter two provides the literature review regarding the microorganism (*Escherichia coli*, *Staphylococcus aureus*) and metals (stainless steel, titanium) used in this study. Furthermore, it provides important insight of biofilm formation and the factors of the bacterial adhesion. Chapter three describes the materials and methods that involved throughout the study where the research method was divided into four sections. All four sections are methods for metal preparation, bacterial preparation, adhesion test, and analysis. The results for surface characterizations (contact angle measurement, surface roughness, surface morphology) and bacterial characterizations (gram staining, bacterial size, hydrophobicity, surface charge) are comprehensively discussed in chapter four. Next, in chapter five the results of the bacterial adhesion are critically assessed. The effect of surrounding which involving of pH and salt concentration and also the effect of surface fabrication give disparities results towards the level of bacterial adhesion. Therefore, a lot of discussion and arguments has been done in this chapter. Lastly, the conclusion of this study is written in chapter six as well as a few recommendations for future study.

اونيورسيتي ملايسيا فهغ

UNIVERSITI MALAYSIA PAHANG

## CHAPTER 2

### LITERATURE REVIEW

#### 2.1 Introduction

Implant-associated infection has become one of the main failures form of artificial joint replacement in medical application. In orthopaedic implants, it has been shown that aseptic loosening and infection remain major complication (Eid, 2016; Kobayashi et al., 2008) and the average rate of infection is 2% - 5% (Darouiche, 2004). In addition, more than 1 million of primary hip and primary knee arthroplasties are performed each year in USA and it has been increasing every year but, between 0.5% until 2.5% of them will become infected within 10 years (Neoh et al., 2012). Similarly, in dentistry, 52.5% of dental implant ruination was also caused by the bacterial infection (Eick et al., 2017). All the implant associated-infection was originated from the biofilm that build up in the human body and makes the bacteria resistance to natural host defence system and significantly decreases the antibiotic susceptibility (Bagherifard et al., 2015). Consequently, lead to implant failure through poor biocompatibility, material degradation and inflammation.

Bio-fouling is another phenomenon related to the biofilm formation. Bacterial adhesion on a material with the presence of conditioning film followed by proliferation and encapsulation in EPS is a condition that can lead to bio-fouling phenomena (Achinas et al., 2019). Bio-fouling can affect the efficiency of a variety of engineered system such as water distribution pipes, water treatment membranes, cooling tower and heat exchanger (Li & Logan, 2004). Meanwhile, the growth of biofilm can develop the so-called microbiologically influenced corrosion (MIC) of the metals (Yang et al., 2014) where the microbial metabolic activities increase the rate of corrosion of industrial facilities especially in the oil and gas industry (AlAbbas et al., 2012) thus, created bio-corrosion phenomenon. In addition, other industries for example food, maritime, and agriculture also faced similar problem. The formation of biofilm on equipment surfaces are very serious issues caused it leads to cross contamination, food spoilage, transmission

of disease (Ortega et al., 2008) product spoilage, pipe blockages, reduced production efficiency and equipment failure (Garrett et al., 2008).

Owing to all the problems related to biofilm, significant steps must be done in order to exterminate the formation of the biofilm. Adhesion of bacterial to a certain surface is an essential step to biofilm formation (Lorite et al., 2011; Woo et al., 2020) therefore, it is important to understand the mechanism of biofilm and study all the factors which related to the bacterial adhesion phenomenon. Accordingly, this chapter onwards will cover the deeper explanations about the biofilm formation, types of microorganisms and types of metal used in this study. Then, the factors involved in the bacterial adhesion process including bacterial properties, surface properties and environmental condition also have been revealed and discussed in detail.

## 2.2 Biofilm Formation

Bacterial adhere to a certain surface and developed biofilm. Biofilm is a group of microorganisms which composed by single or multiple microbial species. The important requirements for the growth of biofilm are the existence of bacterial and a surface. Note that, a biofilm will not form when one of these components is excluded (Dunne, 2002). Bacteria within a biofilm are more resistant against external factors such as detergent, antibiotic treatments, biocides and host defense responses than planktonic (shown in Figure 2.3) cells (McCarty et al., 2014). Consequently, developed aforementioned problems which are implant-associated infection in medical applications and bio-fouling and bio-corrosion in industrial applications. Biofilm secreted a matrix called EPS which protect them from unfavorable environment conditions thus, become difficult to eliminate (Kokare et al., 2008). The formation of biofilm occurs step by step, involving four stages which are initial attachment, growth and proliferation, maturation and detachment (Achinas et al., 2019; McCarty et al., 2014). The whole process of biofilm formation was summarized in Figure 2.1.

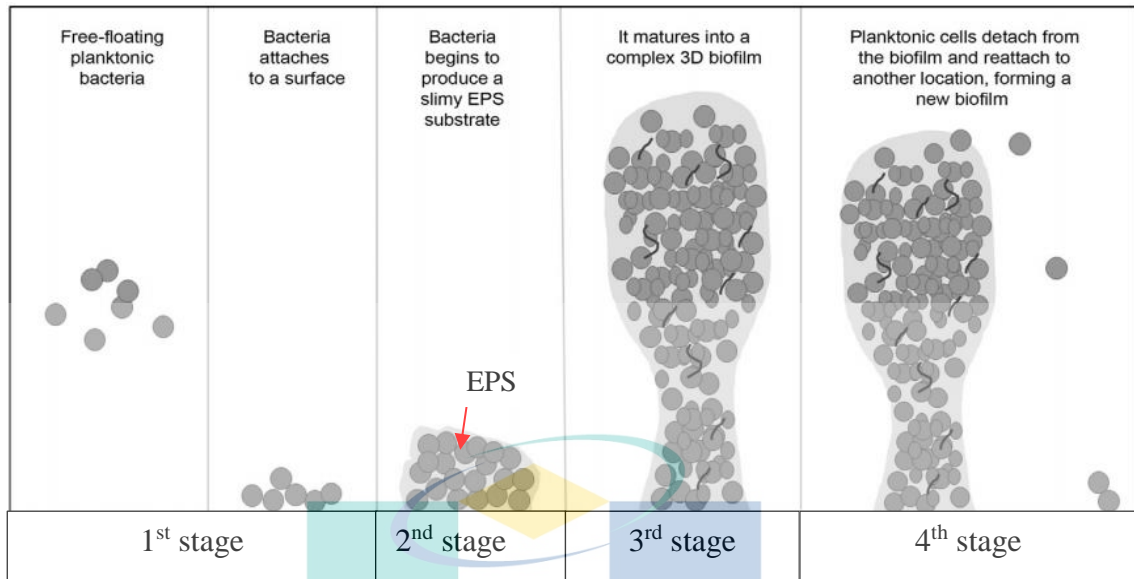


Figure 2.1 Steps of biofilm formation

Source: McCarty et al. (2014)

Generally, before adhesion occur bacteria exist in planktonic form which is freely existing in bulk solution. Exposed surfaces in the bulk medium developed a layer called conditioning layer due to the adsorption of macromolecules (lipids, proteins and polysaccharides) on the surface. The layer modifies the chemical and physicochemical (hydrophobicity, electrical charges) characteristics of the surface and facilitates the accessibility of bacteria. The first stage in the biofilm formation is the process where free-floating planktonic bacteria are moved from bulk liquid to the conditioned surface (50 nm – 5 nm). It is reversible process affected by the combination of hydrodynamic forces and physicochemical forces such as van der Waals, Brownian motion, electrostatic forces, gravitational forces, acid-base and hydrophobic interaction between the bacteria and the surface. Then, once the bacteria get attached with the surface, the appendages of the bacteria such as flagella, fimbriae and pili will strengthen the attachment of the bacteria to the surface. The initial attachment of bacteria is a crucial step in the biofilm formation. According to Wang et al. (2015) the process took 2 to 4 hours to occur and after 4 hours the bacterial cells will become irreversibly attached. During this initial stage, it will specify whether the transporting bacterial cells will adhere or not to the surface and all are depends on the surface properties (charge, hydrophobicity or wettability, topography and roughness, morphology, chemical composition) bacterial properties (charge, hydrophobicity) and local environment conditions (pH, temperature, salinity, pressure). Therefore, the factors of initial adhesion of bacterial to a surface become the

highlighted topic in this research as to avoid the formation of biofilm (Achinas et al., 2019; AlAbbas et al., 2012; Garrett et al., 2008; Kokare et al., 2008; Lorite et al., 2011; McCarty et al., 2014).

The second stage involves the irreversible process where division of the adhered bacteria occurs and forming a micro colony. During this stage, a slime-adhesive organic substance called as extracellular polymeric substances (EPS) was secreted by the bacterial cells, enclosed the cell colonies within it and form what is known as biofilm. EPS has heterogenous composition that includes exopolysaccharides, proteins, nucleic acid, lipids, glycoproteins and other polymeric compounds. The EPS which also called as extracellular matrix provides shelter to the colonies of bacterial and protects them from any antimicrobial agents, disinfectants and unfavorable environmental conditions. Thus, the biofilm cells become extremely difficult to eliminate as they exhibit enhanced resilience compared to planktonic cells. Besides that, EPS that covers the cells changes the physicochemical characteristics of the cell such as hydrophobicity, surface charge and polymeric properties. These alteration helps in cellular recognition and promotes the adhesion and aggregation as well as allow the biofilm to grow to form different layers of cell clusters on the surface (Achinas et al., 2019; Floyd et al., 2017; Harimawan & Ting, 2016; McCarty et al., 2014).

At the third stage the biofilm continues to expand, form different layer of cell clusters and developed into a matured complex biofilm. During this stage, molecules known as auto inducers (chemical and peptide signals in high concentrations) are used as signalling molecules to communicate from cell to cell through a process called quorum sensing. Quorum sensing (QS) is a mechanism involves cell density-dependent control of gene expression. When the population density is reached the threshold level, signaling molecules (auto inducer) produced by the bacteria will activate the bacteria receptor and release the extracellular signals. This communication system allows sharing of genetic information between bacteria by transduction, conjugation and transformation and make the EPS matrix to adapt various situations. On the other hand, there are channels formed between different colonies within the three-dimensional structure of EPS which allow nutrients to venture deep into the biofilm and prevent the bacterial growth termination. (Achinas et al., 2019; Dewasthale et al., 2018; Donald, 2017; Garrett et al., 2008; Khatoon et al., 2018; Li & Tian, 2012).



The last stage possesses the detachment of the planktonic cells from the mature biofilm due to the oversaturation of the cells, nutrients starvation and excessive waste products. At this stage, pieces of biofilm break away and the cells are dispersed into the surrounding fluid. This situation enables the cells to colonize to new area and form new biofilm. Commonly, a biofilm is consisted of two distinct layers which are base film layer where the bacterial cell exists and the surface film where they get dispersed into the surrounding for expansion and continued existence. The limitation of sources in the biofilm triggered the bacterial cells to produce enzymes (dispersin B, deoxyribonuclease) that can degrade the EPS layer which is the surface film, thereby releasing the bacterial cells to the surrounding. (Achinas et al., 2019; Dewasthale et al., 2018; Donald, 2017; Khatoon et al., 2018; McCarty et al., 2014). Generally, without the protective biofilm environment the bacterial cells are easier to remove and more susceptible to the antimicrobial agents therefore, by controlling the adhesion of bacteria since the initial process the development of biofilm could be largely prevented.

### 2.3 Microorganism

Many bacteria contributed to the medial implant-associated infection and bio-fouling or bio-corrosion of industrial equipment problems. In medical application, ten million of medical devices (joint replacement device, spinal fixation devices, artificial ligaments) are used each year but a significant proportion of each devices become colonized by bacteria and directly lead to implant-associated infection (Long, 2008). The most common bacteria found are *Staphylococcus epidermis*, *Staphylococcus aureus*, *Enterococcus faecalis*, *Escherichia coli*, *Streptococcus viridans*, *Klebsiella pneumonia*, *Proteus mirabilis* and *Pseudomonas aeruginosa* (Chen et al., 2013). Meanwhile, bio-fouling and bio-corrosion of equipment usually caused by the formation of biofilm from various type bacteria such as *Pseudomonas fluorescens*, *Escherichia coli*, *Pseudomonas vesicularis*, *Corynebacterium* and *Arthrobacter* (Fletcher, 1994; Nguyen et al., 2012). Nevertheless, in this study *Escherichia coli* and *Staphylococcus aureus* will be studied because it has been reported that the large proportion of implant-associated infections are caused by *Staphylococcus aureus* which percentage about 33% - 43% while *Escherichia coli* contributed about 4% - 7% of infections (Barros et al., 2019; Ribeiro et al., 2012). On the other hand, *Escherichia coli* also a common bacterium isolated from the bio-fouling and bio-corrosion of industrial equipment. Both bacteria have different properties

particularly in Grams type and size in which are assume will work differently on the adhesion process (Zituni et al., 2013) . Katsikogianni and Missirlis (2004) indicated that different bacterial species and strains have different physicochemical properties thus, adhere differently on the surface.

### 2.3.1 *Escherichia coli*

*E. coli* is a gram-negative bacterium with a rod shaped and can grow under aerobic and anaerobic conditions (Farmer et al., 2010; Shewaramani et al., 2017). Figure 2.2 showed the cross section of the membrane structures of *E. coli* which has thin peptidoglycan. Besides that, *E. coli* is a type of bacterium that lives in human intestines and most of the strains are harmless except when they are in the form of big clusters or biofilm (Shewaramani et al., 2017). Gram-negative bacteria contributed about 15% in orthopaedic implant infection with *E. coli* became the second most common cause of the infection after *Pseudomonas aeruginosa* (Hsieh et al., 2009). It contributed in various extra-intestinal diseases such as urinary tract infections and bacteremia that could result in orthopaedic implant infection (Crémet et al., 2012). On the other hand, *E. coli* also involved in bio-fouling problem as reported in Zhao and Chen (2017), where the deposition of *E. coli* on the membrane surface of bioreactors and its pores in the waste water treatments had led to membrane fouling which significantly shortens the lifespan of the membrane, reduces the filtration flux, increases energy consumption and cleaning costs. In addition, Pratikno and Titah (2017) expressed that *E. coli* also caused serious problem in marine bio-fouling such as accelerated the corrosion of marine metals which is termed as bio-corrosion. Bio-fouling and bio-corrosion are caused by the formation of biofilm on surfaces. *E. coli* has been investigated to have specialized virulence factors such as adhesins, polysaccharide coatings, siderophores, proteases, toxins and serum-resistance proteins which facilitates the organisms to colonize or invade host tissues, destroy host defense mechanisms and adhere on targeted surfaces (Crémet et al., 2012). Biofilm is the key component to the persistent of *E. coli* on the biomedical devices and industrial equipment where EPS secreted by them help to protect the microorganisms from any antimicrobial agents. On the other hand, *E. coli* also consisted proteinaceous appendages such as flagella and pili that mediate the initial attachment by facilitating motility and anchoring to a surface of a material (Floyd et al., 2017).

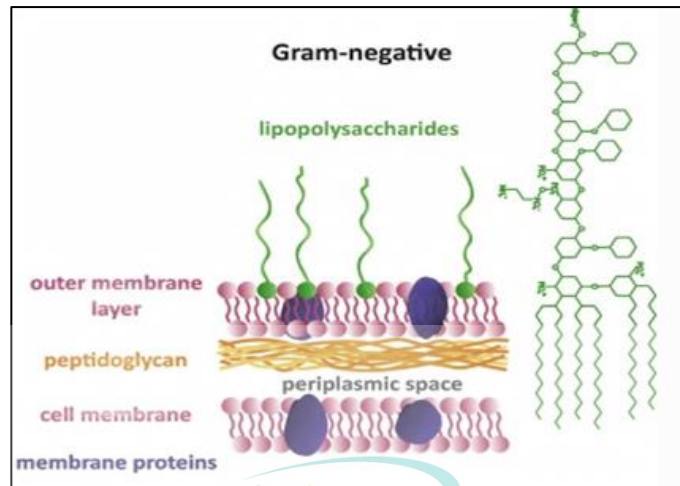


Figure 2.2 The cross section of the membrane structures of *E. coli*  
Source: Pajerski et al. (2019)

### 2.3.2 *Staphylococcus aureus*

*S. aureus* is a gram-positive with a spherical (coccus) shaped and also can grow under aerobic and anaerobic condition (Farmer et al., 2010). Figure 2.3 showed the cross section of the membrane structures of *S. aureus* which has thicker peptidoglycan than *E. coli*. Healthy people carry the *S. aureus* in their nose and throat (50%), on their hands (5% - 30%) and in wounds (Eni et al., 2010). *S. aureus* is a nosocomial pathogen that can cause variety of human disease in which two-thirds of all pathogens in orthopedic implant infections are coming from *S. aureus*. It had become the primary causative agents of infection affecting bone, osteomyelitis and septic arthritis, which involve the inflammatory destruction of joint and bone (Ribeiro et al., 2012). All the infections are extremely difficult to treat because of the ability of *S. aureus* to easily form small colonies and grow into biofilms. Besides that, *S. aureus* comprises of several cell-surface adhesion molecules that enables it to bind to bone matrix which called as adhesins. Generally, specific tissues need specific adhesins for colonization onto biomaterials (implant devices) (Harris & Richards, 2006; Ribeiro et al., 2012). The types of adhesins include fibrinogen-binding protein, fibronectin-binding proteins and collagen-binding adhesins (Arciola et al., 2004). These adhesins have been recognized as critical virulence factors in incriminated in various stages of infection, including early colonization, invasion, tissue localization and cell internalization (Harris & Richards, 2006). Furthermore, it has been reported that polysaccharide intercellular adhesins (PIA) are another factor that required for biofilm formation and bacterium-bacterium adhesion in which this adhesin is accountable for the production of EPS that makes up the biofilm (Ribeiro et al., 2014).

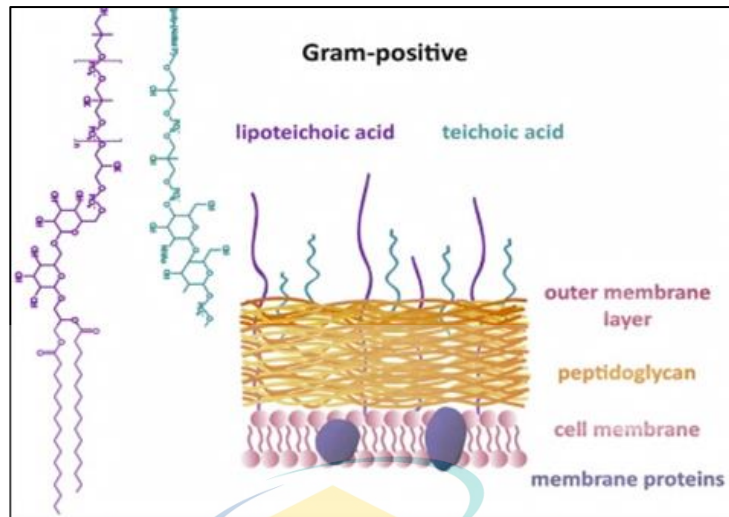


Figure 2.3 The cross section of the membrane structures of *S. aureus*  
 Source: Pajerski et al. (2019)

## 2.4 Bio-surface

Adhesion of bacteria to a surface is the first step in the biofilm formation. Bacteria can easily adhere on any exposed surfaces like on metals, plastics, polymers, ceramics, glass woods and sands. Yuan et al. (2017) demonstrated that *E. coli* had covered almost 60% of untreated polystyrene surface during the study of *E. coli* adhesion on polymeric substrates. *S. aureus* and *P. aeruginosa* have been found adhered on 45S5 bioactive glass based on Shaikh et al. (2017) study, while higher adhesion of *S. epidermidis* and *S. sanguinis* were discovered on zirconia which is a ceramic-like surface in a study regarding bacterial adhesion on zirconium oxide dental implants (Wassmann et al., 2017). There are more surfaces that have been studied with regards to the bacterial adhesion problem such as aluminum, copper, cobalt-chromium, nickel and polyethylene (Cheung et al., 2007; Tuson & Weibel, 2013). However, the most materials used in medical and industrial devices and always correlated with implant-associated infection and bio-fouling problems are stainless steel and titanium (Bezek et al., 2019). Studies found that, bacteria are capable to adhere and form biofilm on any medical and industrial contact surfaces such as stainless steel and titanium (Bagherifard et al., 2015; Lorenzetti et al., 2015). Hence, in this study stainless steel and titanium have been thoroughly investigated.

### 2.4.1 Stainless Steel

Stainless steel is the name of iron-based alloys known for their corrosion and heat resistance. It primarily made of iron and carbon and other added elements such as chromium, nickel, silicon, manganese and nitrogen (Cunat, 2004). Table 2.1 shows the physical properties of stainless steel. In medical application, type AISI 316L stainless steel is commonly used in surgical procedures to replace biological tissue or to help stabilize a biological structure due to its corrosion resistance ability (Ribeiro et al., 2012). It is largely used in implant division for instance as stent in cardiovascular, as bone fixation (plate, screw, pin) in orthopaedic, and as an artificial eardrum in otorhinology implant (Bagherifard et al., 2015; Hermawan et al., 2011). Figure 2.4 shows the examples of X-ray images of stainless steel used in bone fixation. In industrial application, stainless steel used as food storages, tanks, reactors, water distribution pipes and many more (Vishwakarma, 2020). All these medical and industrial devices are easily adhered by bacteria thus contributed to the implant-associated infection and bio-fouling or bio-corrosion phenomenon.

Table 2.1 Physical properties of stainless steel

Physical Properties	Data
Melting point	1371 °C – 1399 °C
Density	7.99 g/cm <sup>3</sup>
Yield strength	170 MPa
Co-efficient of expansion	16 x 10 <sup>-6</sup> /°C
Modulus of elasticity	200 GPa

Sources: Harvey, (2011)

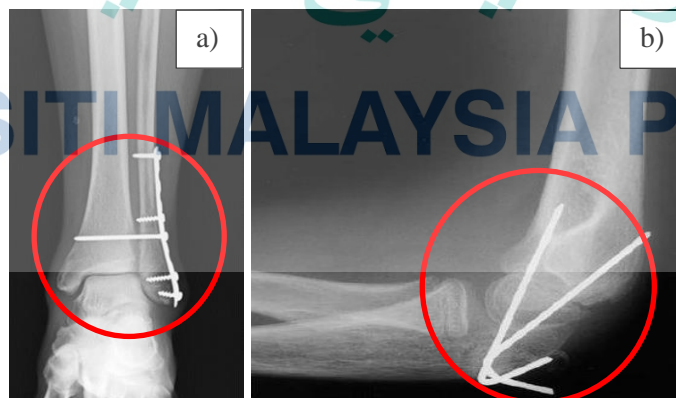


Figure 2.4 X-ray images of stainless steel used in broken bones a) screw and plates used to hold the broken ankle b) pins used to hold the broken elbow

Source: Long (2008)

## 2.4.2 Titanium

Titanium is a strong alloy with light weight features (Fernandes et al., 2015). It is a transition metal in periodic table of elements which denoted by symbol Ti. Table 2.2 displays the details about the physical properties of titanium. Compared to stainless steel, titanium is more difficult to deform as it has high yield strength of measurement with 1100 MPa (Table 2.1 and 2.2). Besides that, titanium especially grade 5 titanium alloys are recognized for their excellent tensile strength, pitting corrosion resistance, highly durable and resistant to loads (Hermawan et al., 2011). Like AISI 316L stainless steel, grade 5 titanium alloy also is highly compatible in human body and has been applied in various medical applications as implant devices ranging from cardiovascular to craniofacial division. Generally, it has been used for artificial heart valve in cardiovascular implant, artificial joints such as hip joint and knee joint in orthopedic implant and also for a filling and dental restoration wiring in dentistry (Hermawan et al., 2011; Long, 2008). Figure 2.5 displayed the X-ray images of titanium used as knee joint. Therefore, both metals which are AISI 316L stainless steel and grade 5 titanium alloy has been chosen to be studied in this research as they were the most common metals applied in both medical and industrial applications.

Table 2.2 Physical properties of titanium

Physical Properties	Data
Melting point	1660 °C
Density	4.51 g/cm <sup>3</sup>
Yield strength	1100 MPa
Co-efficient of expansion	8.9 x 10 <sup>-6</sup> /°C
Modulus of elasticity	116 GPa

Source: Fernandes et al. (2015)

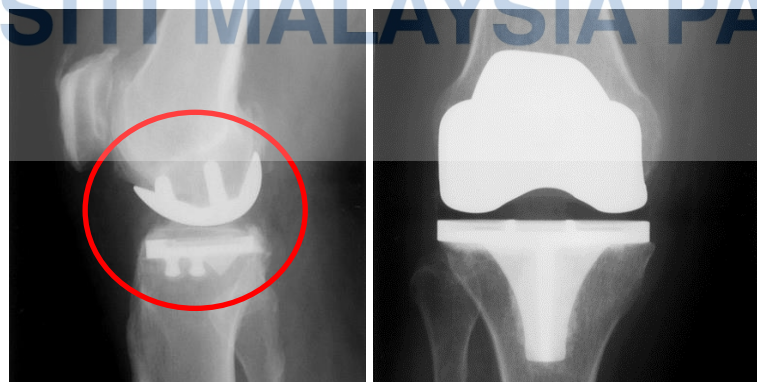


Figure 2.5 X-ray images of titanium used as knee joint in orthopaedic implant

Source: Taljanovic et al. (2003)

## 2.5 Surface Modifications

Researchers had come out with various of surface modification techniques to avoid or reduce the initial adhesion of bacterial especially on medical and industrial devices. One of the famous strategies that have been implemented was the use of biocides, with the development of coatings on the surface that release antimicrobials or kill micro-organisms by contact (Shaikh et al., 2017). Many clinical trials have been performed using this method but, the long-term extensive use of biocides on coatings were reported could lead to increased antibiotic resistance (Desrousseaux et al., 2013; Shaikh et al., 2017). Other surface modifications such as polymer brush coatings and polyethylene glycol-based coatings were investigated can improve the non-fouling behavior of the surface (Keskin et al., 2019; Muszanska et al., 2014). However, they have drawback in cell cytotoxicity and stability aspects in which the use of iron (e.g. silver) and copper catalyst in polymer brush coating are not desirable in medical applications while the long-term stability of polyethylene glycol-based coatings is still has to be developed (Keskin et al., 2019). Practically, it is impossible to develop a surface that can prevent colonization by all bacteria, at the same time being harmless to humans and the environment if there are chemicals involved in the surface modification process (Callow & Callow, 2011). Therefore, in this study physical surface modifications have been highlighted as a method to reduce the initial adhesion of bacteria on metal surfaces and at the same time avoiding any damage to human body and environment. Surface modification through fabrication process could modify the topography, structures and roughness of a surface. It is believed that controlling the surface roughness, topography and structures could mitigate the initial adhesion of bacteria (Lu et al., 2016). Therefore, the metals surfaces were being modified through fabrication process using polishing, grinding and laser treatment techniques.

### 2.5.1 Polishing and Grinding

Surface that has submicron to nanometre range of surface roughness has been reported could resist the adhesion of bacteria (Jang et al., 2018). Polishing and grinding processes had produced average surface roughness ( $S_a$ ) about  $0.08\ \mu\text{m}$ -  $0.09\ \mu\text{m}$  and  $0.18\ \mu\text{m}$  -  $0.4\ \mu\text{m}$ , respectively based on the study from Hilbert et al. (2003) and Khare and Agarwal (2015) The ability of polishing and grinding process to generate surfaces

between micro to nano-roughness could assist in the inhibition of initial adhesion of bacteria on a surface. On the other hand, both techniques are easy to conduct, create durable surface and long lasting. Thus, polishing and grinding are the perfect fabrication process to be studied.

Polishing and grinding remove materials from a specimen with increasing grit grinding paper and polishing compound which is usually performed on a rotating wheel plate (Rudawska, 2019). Generally, grinding is the first step of mechanical material removal and then followed by polishing. In the grinding process, the damaged or deformed surface material will be removed using fixed abrasive particles that contain grains and attached to the grinding wheel (Hou & Komanduri, 2003). Figure 2.6 shows the schematic diagram of grinding process. The common abrasive particle used is silicon carbide (SiC) abrasive paper which is primarily used for grinding cast iron, austenitic stainless steel and hardened tool steel. SiC abrasive paper has different grit sizes and the standard grit size is usually from 60 to 2000 (Zhou, 2018). The higher the grit number is equivalent to a finer abrasive, which creates smoother surface finishes while the lower grit number represents coarse abrasives that scrape off material much quicker (Kwak, 2005). Usually, the process will start with a coarser abrasive paper to a finer size where different grit sizes will leave the surface with different microstructure and micro to nano-roughness. A study from Zhou (2018) showed the average roughness ( $S_a$ ) of AISI 304L stainless steel was 1.84  $\mu\text{m}$ , 0.77  $\mu\text{m}$  and 0.34  $\mu\text{m}$  after been fabricated with SiC abrasive paper at grit size of 60, 180 and 400, respectively. Meanwhile, polishing is a finishing process of creating a smooth and shiny surface by using diamond abrasive after the finest grinding step (Rudawska, 2019). The polishing process is repeated by different sizes of diamond abrasive (30, 15, 9, 6, 3, 1, 0.25  $\mu\text{m}$  of sizes - standard size) until mirror surface finishing is obtained (Nassar & Nassar, 2012). Most of the devices used in medical and industrial applications like implant tools and reactors or tanks have polished surface finish. Harris et al. (2007) stated that polished stainless steel and standard titanium alloy are extensively used for hospital furniture, devices, and equipment, as well as for implants such as intramedullary nails, osteosynthesis screws and plates, and external fixation devices.



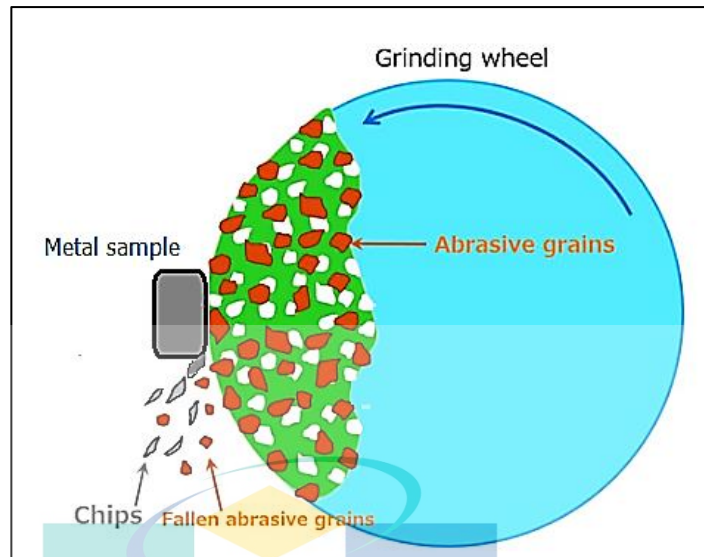


Figure 2.6 Schematic diagram of grinding process

Source: Zhou (2018)

## 2.5.2 Laser Treatments

Laser treatments is a promising approach for the surface modification of different materials. Various studies from previous research had mentioned that laser surface modification could reduce the adhesion of bacterial on any surfaces. For example, Pflöging et al. (2009) stated that laser-assisted modification of polystyrene surfaces can control protein adsorption and cell adhesion (no bacterial cells observed when the laser fluences were set more than  $9\text{mJ}/\text{cm}^2$ ), Cunha et al. (2016) described femtosecond laser surface texturing of titanium as one of the significant methods to reduce the adhesion of *S. aureus* and biofilm formation about 2-fold (compared to polished specimen) and Shaikh et al. (2017) explained that femtosecond laser induced surface modification for prevention of bacterial adhesion on 45S5 bioactive glass with almost 98% of reduction. Besides of capable in generating nano-roughness, nano-structures and nano-topography surfaces (Epperlein et al., 2017), laser surface processing is a direct process which provides uniformity compared to other surface modification techniques such as sand blasting and machining. The process also very precise, fast, flexible and contamination free, from product development to finishing (Chantal et al., 2011). Furthermore, it does not have any issue of poor adherence of surface with bulk material or cells body and has better surface properties in term mechanical, corrosion, wear and wettability compared to other surface modification like surface coating (Indira et al., 2016). On the hands, the characteristics of a material such as surface roughness or structures can be modified

efficiently and smoothly by using proper laser processing parameters like laser power, frequency, fluences and scanning speed (Indira et al., 2016). To date, laser also was used for structuring the implant material in medical application as to replace the traditional method like grid-blasting, acid-etching and anodic oxidation (Shah et al., 2016). It provides distinct advantages for instance, the localised elevation of temperature and reaction with ambient oxygen results in a thicker oxide layer which influences the osteoconductive behaviour and facilitates tissue bonding as well as process of melting and re-solidification at the surface lead to an enlarge contact surface area with benefits for biomechanical anchorage of implanted devices (Shah et al., 2016). Hence, in this study, millisecond laser and ultrafast laser are being selected for the laser surface modification process.

Millisecond laser and ultrafast laser treatments remove material from the surface or bulk and can produce multi-levels surface with microstructures or nanostructures easily (Nuutinen et al., 2012). Both lasers are pulsed laser which is a promising alternative to chemical method for the surface modification. Millisecond laser has long pulse duration (in millisecond range) than ultrafast laser which generates quite a significant heat-affected zone in the material (Hamad, 2016). Jaeggi et al. (2011) explained that, this is because of the pulse duration is longer than the thermalization time of most metals. Meanwhile, ultrafast laser which also known as femtosecond laser emits optical ultrashort pulses with duration below 1 picosecond (ps) (Chantal et al., 2011). Due to the ultrashort pulse length, ultrafast laser can deposit energy to a material in a controllable manner on a time scale faster than another laser like picosecond laser and millisecond laser (Buividas et al., 2012). The schematic diagram of the ultrafast laser treatment process can be seen at Figure 2.7. Based on the figure 2.7, femtosecond laser was focused on the sample (stainless steel) surface through the objective lens. The exposure time of the laser beam was controlled by a fast-mechanical shutter and the reflector mirror amplified and delivered the laser beam to the samples (Yang et al., 2012).

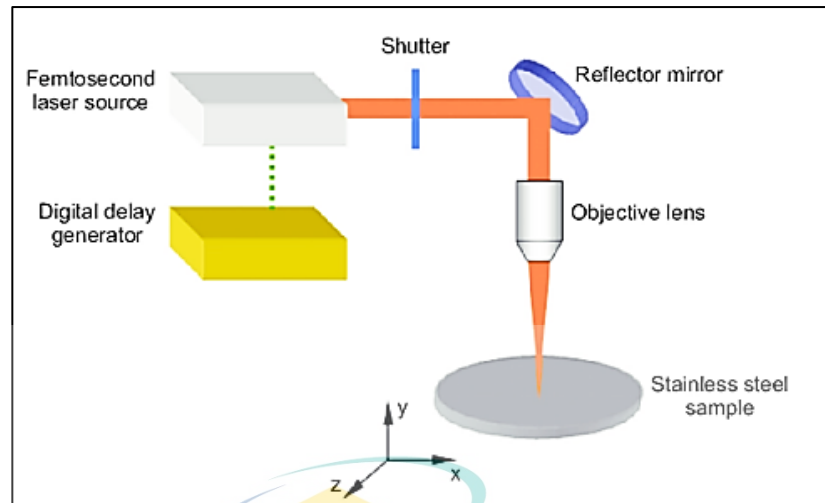


Figure 2.7 Schematic diagram of ultrafast laser (femtosecond laser) treatment process

Sources: Yang et al. (2012)

During the interaction of the ultrafast laser pulse with materials, heat conduction is limited. Thus, the material will be ablated within a well-defined area with minimized mechanical and thermal damage of the ablated area (Chantal et al., 2011; Hamad, 2016). Ultrafast laser with short pulses has succeeded in machining surface with nano-roughness with good quality. For example, Epperlein et al. (2017) reported the successful ablation of femtosecond laser in producing nanostructure surface on steel with roughness  $S_q$  from 4 nm to 10 nm and  $S_z$  16 nm to 60 nm. On the other hand, the process also generated a small amount of molten material or also called as nano-sized irregular grain on the laser surfaces due to the heat diffusion (Phillips et al., 2015). This small heat-affected zone contains low level of thermal defects, which is common in femtosecond laser processing and sometime could increase the surface roughness up to  $S_q$  900 nm (Phillips et al., 2015). Different parameters of laser treatments process such as power, scan speed, frequency and wavelength can influence the roughness, topography and structure of the metal surfaces. In this study, power was varied to structure the surface and usually with high power, the heat entering the material surface will increase thus, deep structuring process could occur.

## 2.6 Factors of Bacterial Adhesion

The adhesion of microbial cells to material surfaces in aqueous media is an important phenomenon in both medical and engineering system (Sheng et al., 2007). There are various factors involved in the initial adhesion of bacteria such as bacterial properties, material surface properties and the environmental factors (AlAbbas et al., 2012; Katsikogianni & Missirlis, 2004; Ribeiro et al., 2014). However, understanding the theoretical model regarding the bacterial phenomenon is utmost important. A few theoretical models have been implemented to describe the net physicochemical interaction between a cell and a flat surface which are, thermodynamic theory, DVLO (Derjaguin, Verwey, Landau and Overbeek) theory and extended DVLO (XDVLO) theory (Faisal et al., 2012). The thermodynamics approach has been used to describe bacterial attachment to surfaces by taking into account the various types of attractive and repulsive interactions, such as van der Waals, electrostatic or dipole which can be expressed in term of free energy (Katsikogianni and Missirlis, 2004). However, the thermodynamics approach ignores the electric double layer interaction with the bacteria which caused the theory is invalid since the bacterial cells have a positive and negative surface charge (AlAbbas et al., 2012). Therefore, DVLO theory has been introduced as it displays a balance between two additive factors, which are van der Waals interaction and repulsion interaction from the overlap between the electrical double layer of the cells and surfaces (Trevor et al., 2008). The extended DVLO (XDVLO) theory was suggested since the hydrophobic and hydrophilic interaction was included in the theory as well as other four fundamental interaction energies such as, van der Waals, electrostatic, Lewis acid-base and Brownian motion forces (AlAbbas et al., 2012; Katsikogianni & Missirlis, 2004). XDVLO-based analyses have provided support for the importance of the properties of both surfaces (bacteria and material) and colloids adhesion but, it is not been tested rigorously using a wide range of bacteria and surfaces (Li & Logan, 2004). These physiochemical theories do help in explaining some observation and manifest the complexity of interaction between bacteria and a surface however, it has not been overall successful in predicting all the various attachment behavior observed in bacterial adhesion system.

### 2.6.1 Effect of Bacterial Properties

Among the bacterial properties involved in the adhesion, bacterial types, bacterial surface hydrophobicity and bacterial surface charge are often the determining factors (Habimana et al., 2014; Katsikogianni & Missirlis, 2004). Different bacterial types will adhere differently on a material surface as physicochemical characteristics of bacteria are different between species and strains (Habimana et al., 2014). These variations are linked to differences in cell wall structures and the presence of bio-molecules on the bacterial cell wall (Beveridge, 2001). Bacteria can be classified into Gram-positive or Gram-negative based on the cell wall structures. The Gram-positive bacteria is made up of thick peptidoglycan layer (~ 30 nm) which consisted a network of crosslinking carbohydrates and peptides (see Figure 2.3). The cell wall also acts as a tough and flexible barrier which capable of withstanding any external stress. Hence, when experiencing irregular surface structure during the adhesion process the cells are quite difficult to damage or encounter cell rupture and lysis. The outer surface of Gram-positive cell is usually covered with appendages covalently attached to either peptidoglycan layer (i.e. cell wall protein, teichoic acid, polysaccharides) or the inner plasma membrane (lipoteichoic acid) (Beveridge, 2001; Habimana et al., 2014). Meanwhile, Gram-negative bacteria consists of thinner peptidoglycan layer (~ 10 nm), which is covered by an outer membrane consisting of proteins (i.e. adhesins), lipopolysaccharide and phospholipid (see Figure 2.2) (Beveridge, 2001; Habimana et al., 2014). The differences of the bio-molecules on the cell wall of Gram-negative and Gram-positive bacteria will influence the surface hydrophobicity or surface charge of bacteria thus, contributing to the bacterial adhesion. For example, Schar-Zammaretti and Ubbink (2003) has reported that the teichoic acid and lipoteichoic acid which can be found only on Gram-positive bacteria confer hydrophobic properties to the bacterial surface whereas polysaccharides (Gram-negative bacteria) render the bacterial surface hydrophilic. On the other hand, the proteinaceous appendages including pili and flagella (adhesins) will initiate the adhesion by establishing bridges between the bacteria and material surface (AlAbbas et al., 2012).

Surface hydrophobicity of bacteria is another important physical factor involved in the initial adhesion of bacteria. Bacteria with hydrophobic properties prefer hydrophobic surfaces while those with hydrophilic characteristics prefer hydrophilic surfaces. Between these two distinct properties, the hydrophobic bacteria adhere to a

greater extent than hydrophilic bacteria with stronger binding strength (Ma et al., 2012). The hydrophobicity of a bacteria varies according to bacteria species and is always influenced by the bacterial structure, bacterial age and growth medium (Ribeiro et al., 2014). A decrease in adhesion and hydrophobicity of *E. coli* during the exponential phase about 1-fold was mentioned in Walker et al. (2005) study. This was ascribed to the hydrophilic proteins on the outer membrane of *E. coli* that decrease with the culture age which consequently lead to a decrease in hydrophobicity and the adhesion. Meanwhile, cell surface hydrophobicity of *Pseudomonas* sp also was found to decreased with increasing cellular age based on the study from Kuntiya et al. (2005). Furthermore, Kuntiya et al. (2005) also demonstrated by changing the medium composition through the addition of sodium chloride (0.5% w/v) resulted in a decrease of the cell surface hydrophobicity about 42%. Hydrophobicity of bacteria can be examined through evaluation of ability of bacteria to adhere onto hydrocarbons (i.e. hexadecane, hexane, chloroform, xylene) or polystyrene, contact angle measurement, salt aggregation test, partitioning of bacteria in an aqueous two-phase system, hydrophobic interaction chromatography, latex particle agglutination test and direction spreading (An & Friedman, 2000).

Apart from bacterial structure and bacterial surface hydrophobicity, bacterial surface charge also plays a significant role in the bacterial adhesion phenomenon. Most bacteria gain a surface electric charge in aqueous suspension due to the ionization of their acid-base cell wall functional groups (Katsikogianni & Missirlis, 2004). Most bacterial in aqueous suspension have a net negative charge on the cell wall at neutral pH. Nevertheless, different bacterial species have different magnitude of surface charge and they are influenced by the bacterial surface structure, pH and ionic strength of the suspending buffer, growth medium and bacterial age (Katsikogianni & Missirlis, 2004; Ribeiro et al., 2014). The surface charge of a bacteria can be determined by zeta potential measurement (electrokinetic potential), electrophoretic mobility, colloidal titration and electrostatic interaction chromatography (An & Friedman, 2000). In order to measure the surface charge of a bacteria, the pH of the bacterial suspension could be varied from acidic to basic such as from pH 3 to pH 9. The pH also can be specified to 7.4 (fluid in human body) for determining the surface charge of a bacteria in human body (Carlos et al., 2013). Carlos et al. (2013) expressed that at different pH, different surface charge of mycobacterial cell has been measured, the surface charge (zeta potential) of

mycobacterial cell was constant at pH 6 to pH 8 (-25 mV) and increased to -40 mV at pH 9. Besides that, the surface charge of the bacteria is greatly influenced the adhesion force by controlling the electrostatic interaction and resulted in stronger repulsive/ attractive forces in the cell-metal surface interaction (Renner & Weibel, 2011). During adhesion, negatively charged bacteria will attach to positive charge surface while positively charged bacteria will attach to negative charge surface and resulted in the formation of electrical double layer (Li & Logan, 2004). For example, study from Oh et al. (2018) had shown that the adhesion of negative zeta potential of *S. aureus* and *E. coli* O157:H7 decreased on the substrates with negative zeta potential due to the similar of surface charge. Thus, this finding points out the importance of electrostatic interactions in the context of bacterial adhesion.

### 2.6.2 Effect of Metal Surface Properties

The factors influencing bacterial adhesion to material surfaces include surface hydrophobicity, surface roughness or physical configuration and surface charge (An & Friedman, 2000; Ribeiro et al., 2014). In this study, surface hydrophobicity and surface roughness will be highlighted as both are reported to have significant effects upon the initial adhesion of bacteria on a material surface. Material surface hydrophobicity is a major feature that influences the interaction between material surface and the bacteria (Achinas et al., 2019). The hydrophobicity of a material surface has been evaluated mainly by contact angle measurement (CAM) which is based on the angle of water droplets form on the surface. A high CAM represents surface with hydrophobic (CAM > 90 °) feature while a low CAM represents hydrophilic (CAM < 90 °) surface (Habimana et al., 2014). In general, metal surfaces have high surface energy and hydrophilic surface however, the different configurations of metal surface structures could change the hydrophilicity or hydrophobicity of a metal (An & Friedman, 2000). This in line with study from Bohinc et al. (2016) where the CAM of stainless steel increased to 91° (hydrophobic) after undergone 3D polishing treatment compared to the untreated surface which has 72° (hydrophilic) of CAM value. Besides that, depending on the hydrophobicity level of both bacterial and material surfaces, bacteria adhere differently to material with different hydrophobicity (An & Friedman, 2000). Katsikogianni and Missirlis (2004) reported that diamond-like carbon coated PVC exhibited lower level of *S. epidermis* (hydrophobic bacteria) adhesion due to reduction of hydrophobicity in

comparison to the uncoated PVC. On the other hand, Bohinc et al. (2016) showed that the surface hydrophobicity of stainless steel at each surface treatment are different thus, the adhesion of *E. coli* ATCC 35218 on each surface are varied with the lowest adhesion was on 3D polished surface ( 2-fold of reduction) as it has high hydrophobic surface while *E. coli* ATCC 35218 is a hydrophilic bacteria. Moreover, Charville et al. (2008) also found that the pretreatment of the PVC surface with bovine serum albumin (BSA) originated a decrease of hydrophobicity and reduced the adhesion of hydrophobic *S. aureus* and *S. epidermis*.

Material surface roughness or physical configurations are other factors that influenced the initial adhesion of bacteria to the material surface (Wassmann et al., 2017). Roughness is a surface irregularity which results from the various machining process such as grinding, polishing, lasering and cutting and can be measured by stylus profilometer or optical profilometer (An & Friedman, 2000). These irregularities form surface finish with different pattern and textures (Lima & Almeida, 2017). It plays an important role regarding the interaction with the bacterial adhesion (De Giorgi et al., 2016). However, until recently there are conflicting reports arises regarding the kind of surface roughness that are able to reduce the initial adhesion of bacteria on metal surfaces. Bagherifard et al. (2015) showed that the increase in the surface roughness ( $S_q$ ) of stainless steel from  $0.13 \mu\text{m}$  to  $10.10 \mu\text{m}$  had increased the adhesion of *E. coli* about 25%. This is because, rough surface has a greater surface area and the depressions in the roughened surface provide more favorable site for colonization. This statement also has been supported by Wu et al. (2011) which stated that, surface roughness encourages the adhesion of bacteria as *S. epidermis* increased about 5-fold after the surface roughness ( $S_a$ ) of titanium alloy increase from  $0.006 \mu\text{m}$  to  $0.830 \mu\text{m}$ . However, some literature said that bacterial also tend to adhere on smooth surfaces based on the condition that suits the adhesion process (Elbourne et al., 2019; Li & Logan, 2004). Therefore, it is necessary to find out the specific surface roughness that can significantly reduce the bacterial adhesion. Table 2.3 listed other studies regarding the bacterial adhesion on different magnitudes of surface roughness.



Table 2.3 The adhesion of bacteria on various surface roughness

Surface material	Roughness ( $S_q$ )	Microorganisms	Influence on adhesion	Reference
Stainless steel with different finishes	9 – 145 nm	Indigenous bacteria from poultry rinse	Higher attachment on rougher surfaces	(Arnold & Bailey, 2000)
Stainless steel	0.03 – 0.89 $\mu\text{m}$	<i>P. aeruginosa</i> , <i>P. putida</i> , <i>D. desulfuricans</i> , <i>Rhodococcus</i> spp.	Attachment increased with higher roughness, bacteria tend to align with scratches of similar dimension	(Medilanski et al., 2002)
Titanium implant	0.35 and 0.81 $\mu\text{m}$	Indigenous oral microbiota	Rougher surface harbored 25 times more bacteria	(Bollenl et al., 1997)
Stainless steel	0.01 - 1 $\mu\text{m}$	<i>S. thermophilus</i>	No statistical difference	(Boulangé-Petermann et al., 1997)
Stainless steel	0.66 – 1.2 $\mu\text{m}$	<i>L. monocytogenes</i>	No difference	(Flint et al., 2000)
Stainless steel	0.1 – 0.9 $\mu\text{m}$	<i>P. aeruginosa</i>	Smoothest surface had 100 times adhesion more than roughest surface	(Vanhaecke et al., 1990)

Source: Cheng et al. (2019)

Roughness parameters can be calculated in three-dimensional (3D) forms in which an area of a surface will be calculated instead of a straight line (Gadelmawla et al., 2002). The 3D roughness includes amplitude, spatial, hybrid, functional, feature and other 3D parameters (Deltombe et al., 2014). However, in this study only amplitude and hybrid parameters will be focused on as both are the most important features to characterize surface structures and the topography. Amplitude parameters used to measure the vertical characteristics of the surface deviation and the parameters include average roughness ( $S_a$ ), root means square roughness ( $S_q$ ), skewness ( $S_{sk}$ ) and kurtosis ( $S_{ku}$ ) (Naylor et al., 2016; Whip, 2017).  $S_a$  is the average of the individual height (asperities) and depths from the arithmetic mean elevation of the profile while  $S_q$  is the square root of the sum of the squares of the individual height and depths from the mean line (Figure 2.8). In this study, parameter  $S_q$  will be emphasized because it is more sensitive to occasional highs and lows reading while  $S_a$  simply averages them (Gadelmawla et al., 2002). On the other hand,  $S_{sk}$  is used to measure the symmetry of the profile about the mean line (Gaussian distribution) and is sensitive to occasional deep valleys or high peaks (Figure 2.9 (a)). A negative value of  $S_{sk}$  indicates that the surface

is made up of valleys, whereas a surface with positive skewness is said to contain mainly peaks and asperities (Gadelmawla et al., 2002). Meanwhile,  $S_{ku}$  is a measure of sharpness of profile peaks (Figure 2.9 (b)) (Whip, 2017). Gadelmawla reported that, if  $S_{ku} < 3$  the distribution curve is to be platykurtic and has relatively few peaks and low valleys however, if  $S_{ku} > 3$  the distribution curve is said to be leptokurtic and has many peaks and low valleys (Figure 2.9 (b)).

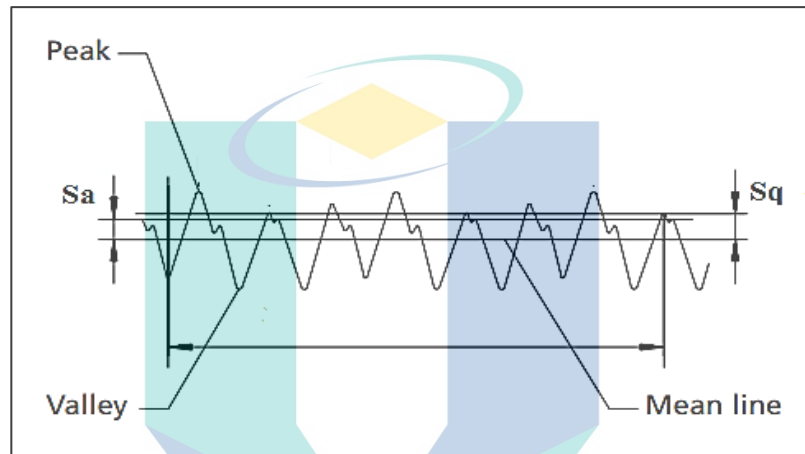


Figure 2.8 Schematic presentation of roughness profile for  $S_a$  and  $S_q$   
Source: Gadelmawla et al. (2002)

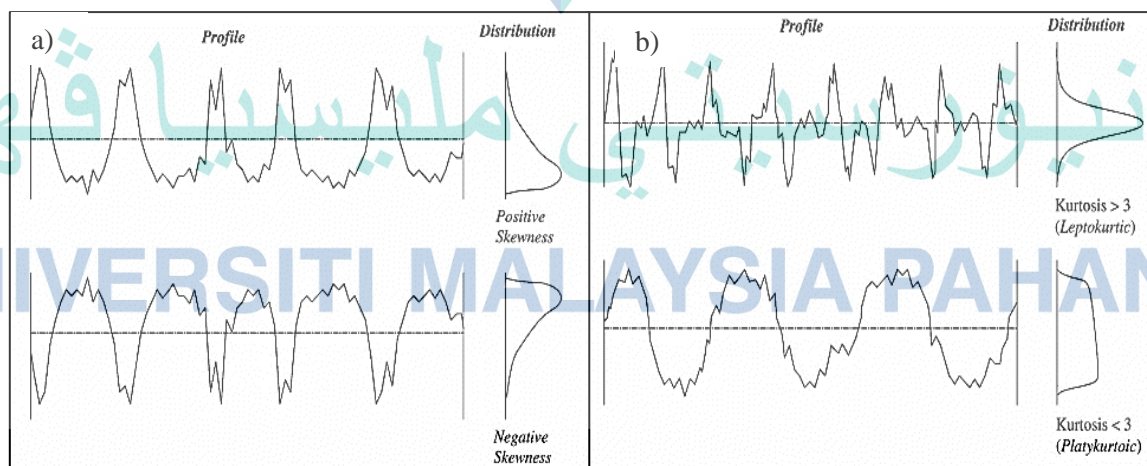


Figure 2.9 Schematic presentation of roughness profile for a)  $S_{sk}$  b)  $S_{ku}$   
Source: Gadelmawla et al. (2002)

Meanwhile, hybrid parameters explain relative characteristics between amplitude and spatial properties where spatial parameters used to measure the horizontal characteristics of the surface deviations (Deltombe et al., 2014; Suh et al., 2003). In this study, the hybrid parameters comprise of developed interfacial area ratio ( $S_{dr}$ ) and summit density ( $S_{ds}$ ).  $S_{dr}$  is used to measure the total surface area over a given sampling area and  $S_{ds}$  calculated the number of summits or peaks (above all eight nearest neighbour) per unit area of the surface (Suh et al., 2003). All these amplitude and hybrid parameters were used to characterize the structures and topography of a surface and relate to the bacterial adhesion process.

### 2.6.3 Effect of Environmental Condition

In general environment, factors like pH, salt concentration (salinity), temperature, time of exposure, bacterial concentration, the presence of antibiotics and the associated flow conditions can affect bacterial adhesion (An & Friedman, 2000). Nevertheless, in this study only pH and salt concentration have been focused as both are related to surface charge of bacteria and can influence the bacterial adhesion.

pH plays an intrinsic role in bacterial growth and the optimal range (pH 6.5 – 7.2) highly depends on type of bacteria. The change in electrolyte pH influences the microbial cell surface charge (AlAbbas et al., 2012). Usually, bacteria are negatively charged, but a few strains have been reported that exhibits a net positive charge due to pH change. Bacteria respond to changes in internal and external pH by adjusting the activity and synthesis of proteins associate with many different cellular processes (Sehar & Naz, 2016). Studies have shown that a gradual increase in acidity, increases the chances of cell survival in comparison to a sudden increase by rapid addition of hydrochloric acid (HCl) (Achinas et al., 2019; Ribeiro et al., 2014). This means that bacterial are less resistant to large pH fluctuation when compared to small pH differences.. Sheng et al. (2008) had suggested to vary the pH of bacteria solution from pH 3 to pH 9 which is from acidic to basic as to observe the effect of different pH towards the bacterial adhesion. Meanwhile, as this study is focussing on implant-associated infection, the pH range also will be specified to pH of human body which is 7.4 in order to analyse the bacterial adhesion in normal human body. Based on Sheng et al. (2008) study, the adhesion forces of *Pseudomonas* sp. and *Desulfovibrio singaporenus* at pH 9 were higher than those at pH

7 due to the increase in the attraction between the irons ( $\text{Fe}^{2+}$ ) and the negative carboxylate groups. On the other hand, Hamadi et al. (2005) investigated the adhesion of *S. aureus* ATCC 25923 to glass at different pH values and observed that the bacterial adhered strongly in the pH range 4 to 6 and weakly at acidic (pH 2 and 3) and alkaline condition. Different bacterial types and strains have different properties thus, the adhesion was varied at different pH value. Other studies also reported that changes in pH can have marked effect on the bacterial adhesion (Katsikogianni & Missirlis, 2004; Ribeiro et al., 2014)

Salt concentration (salinity) such as NaCl and KCl are always related to ionic strength. The effect of electrolyte ionic strength has been investigated extensively as it is one of the factors contributed to the bacterial adhesion. Study from AlAbbas et al. (2012) have shown an increase of bacterial adhesion in NaCl concentration that range from 0 M to 0.2 M. Similarly, Cowell et al. (1998) also mentioned that increasing of NaCl from 0.8% to 1.0% (w/v) had increased adhesion of all bacterial tested which are *P. aeruginosa*, *S. marcescens*, *F. meningosepticum*, *S. maltophilia* and *S. intermedius*. However, there are several studies that concluded no correlation between bacterial attachment to hydrophobic surfaces and changes salt concentration (Katsikogianni & Missirlis, 2004; Li & Logan, 2004). This could be due the microbial metabolism and what kind of microbe is used for the research study. Shephard et al. (2010) had suggested to vary the NaCl concentration between 0.001 mol/L to 0.3 mol/L as it is the suitable range for the bacterial growth and it covers the estimated salinity for the human body, domestic sewage and industrial sewage. The NaCl concentration in human body is 0.135 mol/L thus, the concentration will be included as to study the effect of bacteria adhesion at human salt concentration.

## 2.7 Summary

Biofilm formation can be avoided if the adhesion of bacteria on a surface is controlled since the initial stage of the process. This is because, during the initial stage of the biofilm formation, bacterial cells will specify whether to adhere or not to the surface and all are depends on the factors of surface properties, bacterial properties and local environment conditions. It has been reported that the large proportion of implant-associated infections are caused by *S. aureus* and *E. coli* which percentage of infection

about 33% - 43% and 4% - 7%, respectively. On the other hand, *E. coli* also a common bacterium isolated from the bio-fouling and bio-corrosion of industrial equipment. Hence, *E. coli* and *S. aureus* have been selected to be studied in this research. Besides that, stainless steel and titanium surfaces were investigated in the subsequent works as they were the main materials used in medical and industrial devices and always correlated with the implant-associated infection and bio-fouling problems.

Chemical and physical surface modification can be used in reducing the adhesion of bacterial on a surface. However, physical surface modification approaches have been applied as this method can avoid any damage to the human body as well as contamination to the environment. The fabrication of metal surfaces selected are polishing, grinding, millisecond laser and ultrafast laser treatment. All these methods have the ability to produce surfaces between micro to nano-roughness while the process itself are easy to conduct, long lasting, fast and flexible. The effect of the fabricated surface properties will dictate the adhesion process which will vary accordingly upon the bacterial properties, and the environmental factors. Factors of bacterial properties comprised of bacterial types, hydrophobicity and surface charge while material surface properties included surface hydrophobicity and surface charge. On the other hand, pH and salt concentration are the factors involved in environmental condition.

اونيورسيتي مليسيا قهغ

UNIVERSITI MALAYSIA PAHANG

## CHAPTER 3

### MATERIALS AND METHODS

#### 3.1 Introduction

This chapter focus on all the methods and procedures that have been performed in this study and the overall experimental work is summarized in Figure 3.1. Three types of materials have been used in this study which are bacteria, chemicals and metals and the explanation about all the materials can be referred at section 3.2. Section 3.3, 3.4 and 3.5 which covered the methods for the metal's fabrication, biological works, and adhesion test, respectively. Section of metals fabrication consisted the types of metals fabrication (grinding, polishing, millisecond laser treatment, ultrafast laser treatment) and metal washing process while, biological work section comprised of preservation of stock culture, media preparation and germination of stock culture and inoculum. Finally, sections 3.6, 3.7 and 3.8 provide details of all the analysis used in characterizing the metals and bacterial surfaces and also in analyzing the bacterial adhesion.

اونيورسيتي مليسيا قهغ

UNIVERSITI MALAYSIA PAHANG

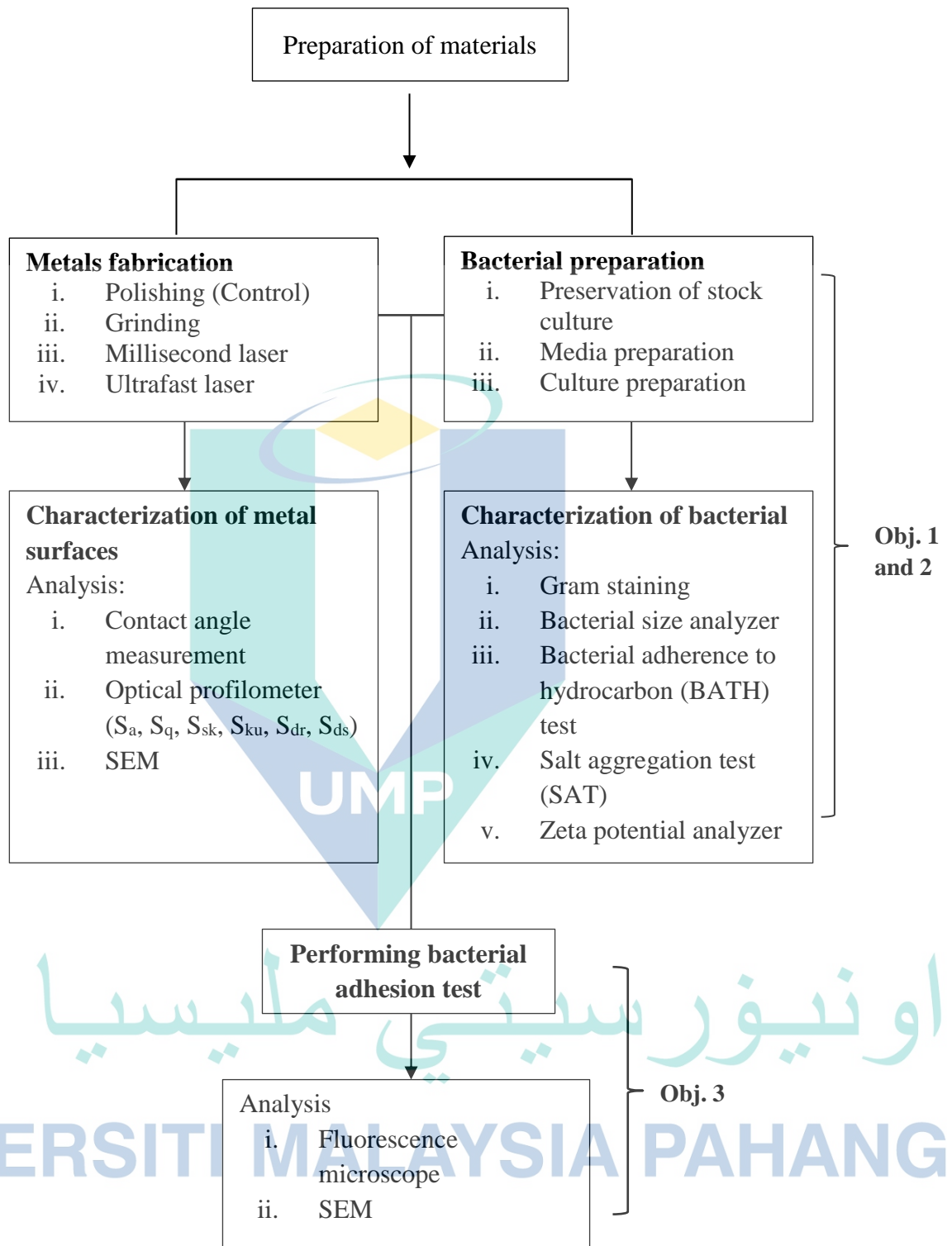


Figure 3.1 Flow chart for the overall process of study

## 3.2 Materials

### 3.2.1 Bacteria

Bacterial strains used in this study are *Escherichia coli* ATCC 8739 (*E. coli*) and *Staphylococcus aureus* ATCC 6838 (*S. aureus*). All the bacteria were obtained from the culture collection of Centre Laboratory of Universiti Malaysia Pahang and kept in the FKKSA laboratory chiller at 4 - 6 °C prior to the experiment.

### 3.2.2 Chemicals

Yeast extract, agar powder, Gram staining kit, potassium chloride (KCl), ammonium sulphate ((NH<sub>4</sub>)<sub>2</sub>SO<sub>4</sub>), sodium hydroxide (NaOH), hydrochloric acid (HCl) and ethyl alcohol (purity 99.7%) were purchased from R&M Chemical (Essex, UK). Glutaraldehyde and peptone from caseins were purchased Sigma Aldrich (St. Louis, USA). Potassium dihydrogen phosphate (KH<sub>2</sub>PO<sub>4</sub>) and disodium hydrogen phosphate (Na<sub>2</sub>HPO<sub>4</sub>·7H<sub>2</sub>O) were purchased from Merck KGaA (Darmstadt, Germany). Meanwhile, xylene, n-hexane, n-hexadecane were purchased from Acros Organics (New Jersey, USA) and sodium chloride (NaCl) was from Fisher Scientific (Loughborough, UK). Yeast extracts, agar- agar powder and peptone from caseins were of biological grade and other chemicals were of analytical grade.

### 3.2.3 Metals

Stainless steel AISI 316L and Grade 5 titanium alloys metals were used in this research. The surface of both metals was fabricated with different types of treatment process in order to get different microstructure or nanostructure surfaces and being tested in the bacterial adhesion test. Types of fabrication process will be explained in the following section.

## 3.3 Methods: Metals Fabrication

Surfaces of stainless steel AISI 316L and Grade 5 titanium alloys which also denoted as SS and TT had been fabricated with four different types of fabrication process which are polishing (P), grinding (G), millisecond laser (MI) and ultrafast laser (UI)



treatment process. All the metals were cut into small pieces (size can be referred at Figure 3.2) and proceed with the surface fabrication. Meanwhile, prior to the polishing and grinding process, the metals were mounted using acrylic resin in order to fix and protect the metal edges while performing the process. Table 3.1 displayed the symbols used to classify the samples and Figure 3.2 showed the schematic diagram of the fabricated metals.

Table 3.1 Symbols used for sample classification

Types of Fabrication	Stainless Steel (SS)	Titanium (TT)
Polishing (P)	P-SS	P-TT
Grinding (G)	G-SS	G-TT
Millisecond Laser (MI)	MI-SS	MI-TT
Ultrafast Laser (UI)	UI-SS	UL-TT

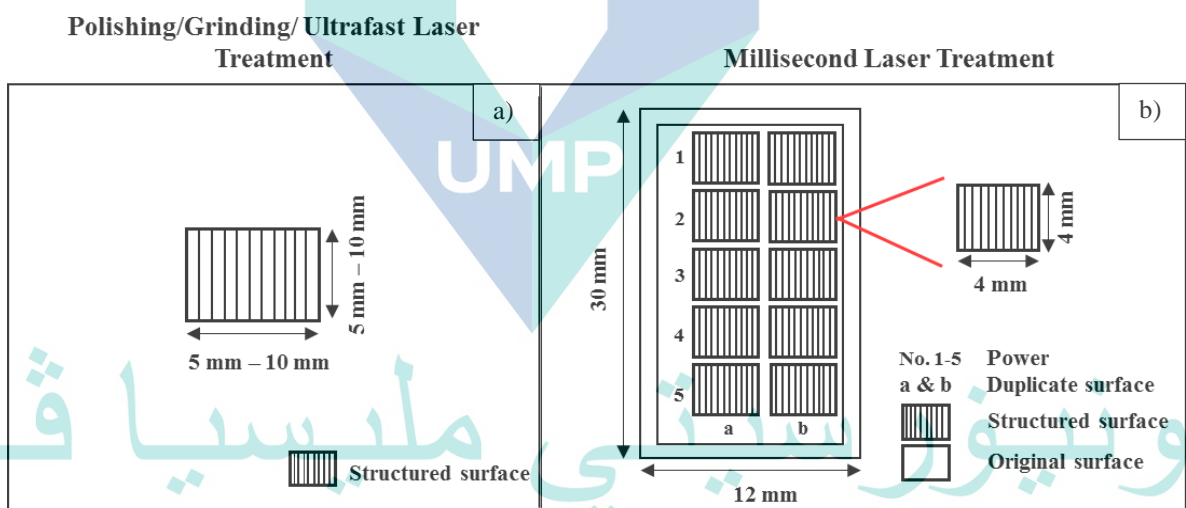


Figure 3.2 Schematic diagram of metal surfaces fabricated by a) polishing, grinding and ultrafast laser b) millisecond laser for stainless steel AISI 316L and grade

### 3.3.1 Polishing (Control Surface)

Polishing is a method to improve the surface finish of a metal where the surface will be ground (grinding) first until the finest surface was achieved. The metal samples were then polished on polishing cloths loaded with lubricant (diamond extender) and 1  $\mu$ , 3  $\mu$  and 6  $\mu$  smaller diamond abrasives until the mirrored surface finishing was obtained. After each polishing step, the metals were rinsed with distilled water in order

to remove the compound residues on the metal surfaces and the same process was repeated for other metal. Polished surface is a control surface in this study.

### **3.3.2 Grinding**

Five different grit sizes of 180 (coarse), 600, 800, 1200 and 1500 (superfine) silicon carbide (SiC) abrasive papers were used to grind the metal surfaces. Various grit sizes were chosen to achieve different surface structures (rough to smooth) on the metals. A higher grit size number indicates a finer abrasive paper, and grinding process starts with a smaller (course) grit size to the higher specific grit size (i.e 1500). After the process the metal surfaces were flush off using warm water to remove any unwanted abrasive particles attached to it. This process was repeated for different grit sizes and also the different types of metals.

### **3.3.3 Millisecond Laser Treatment**

Metal treatment by millisecond laser (ML-MF-A01, Herolaser) with maximum power of 30 W was conducted at Faculty of Mechanical Engineering laboratory, UMP. The laser operation was performed by setting the parameters as shown in Table 3.2. Stainless steel surface was structured at power of 4.2 W (14%), 5.1 W (17%), 6.0 W (20%), 7.0 W (23%) and 7.8 W (26%) while, power applied to the titanium surface was 3.0 W (10%), 4.2 W (14%), 5.4 W (18%), 6.6 W (22%) and 7.8 W (26%) as can be seen in Table 3.2. Stainless steel and titanium have different of mechanical properties, microstructure and processing parameters due to the elements contained in the metals (Mertens et al., 2014; Tolosa et al., 2010) therefore, different power was applied to these surfaces to achieve a comparable metal surface structures (i.e visibility of surface structures, width of laser lines and gap between the laser lines).

### **3.3.4 Ultrafast Laser Treatment**

Ultrafast laser treatment was performed at Karlsruhe Institute of Technology (KIT, Germany) using a micromachining workstation (PS450-TO, Optec) equipped with an ultrafast fiber laser (Tangerine, Amplitude Systems) operating with an average power of 35 W and pulse duration 380 fs. Laser surface texturing was carried out under ambient

air (24°) and the parameters used for the surface texturing of all metals was listed in the Table 3.2 below. The laser beam for LIPSS generation was guided through a beam expander (2-fold) and the scan head (Newson Engineering BV) was used together with an f-theta lens with a focal length of 100 mm (Klotzbach et al., 2016). Titanium surface cannot be structured at 0.04 W because it needs more power for the texturing process as it consists high yield strength than stainless steel (Table 2.1 and Table 2.2). After the laser treatment, the achieved surface structure was characterized by scanning electron microscopy (SEM EVO 50, Carl Zeiss).

Table 3.2 Parameters of millisecond laser and ultrafast laser in texturing the metal surfaces

Types of Laser Treatments	Types of Metals	Power (W)	Scanning Speed (mm/s)	Pulse Duration	Frequency (KHz)	Wavelength (nm)
Millisecond Laser	MI-SS	4.2	50	5 ms	0.05	1100
		5.1	50	5 ms	0.05	1100
		6.0	50	5 ms	0.05	1100
		7.0	50	5 ms	0.05	1100
		7.8	50	5 ms	0.05	1100
	MI-TT	3.0	50	5 ms	0.05	1100
		4.2	50	5 ms	0.05	1100
		5.4	50	5 ms	0.05	1100
		6.6	50	5 ms	0.05	1100
		7.8	50	5 ms	0.05	1100
Ultrafast Laser	UI-SS	0.04	10-20	380 fs	200	515
		0.10	10-20	380 fs	200	515
		0.11	10-20	380 fs	200	515
	UI-TT	0.12	10-20	380 fs	200	515
		0.10	10-20	380 fs	200	515
		0.11	10-20	380 fs	200	515
		0.12	10-20	380 fs	200	515

### 3.3.5 Metal Washing Process

For cleaning purposes, all metals were placed in an ultrasonic bath for 15 minutes using distilled water for by washing with 70% ethanol for additional 10 minutes. The samples were dried under UV light in a pre-sterilized bench for 5 minutes and ready to be used in bacterial adhesion test.

### 3.4 Methods: Bacterial Preparation

#### 3.4.1 Preservation of Stock Culture

For long term preservation, the culture was kept in 20% (v/v) glycerol at -80 °C. For use in subsequent microbial work, *E. coli* ATCC 8739 and *S. aureus* ATCC 6838 stock were stored in the chiller at 4 °C - 6 °C, transferred to an agar plate and incubated for 24 hours at 37 °C.

#### 3.4.2 Media Preparation

##### 3.4.2.1 Luria Bertani (LB) Broth

10 g of peptone from casein, 5 g of yeast extract, and 10 g of NaCl were dissolved in 1 L of distilled water. The solution was adjusted to pH 7 with 0.1 M of NaOH and 0.1 M of HCl and stirred for 15 minutes. The solution was autoclaved at 121 °C for 20 minutes.

##### 3.4.2.2 Luria Bertani (LB) Agar

10 g of peptone from casein, 5 g of yeast extract, 10 g of NaCl, and 15 g of agar powder were mixed in 1 L of distilled water. The pH was adjusted to 7 and stirred for 15 minutes using a hot magnetic plate, followed by autoclaving at 121 °C for 20 minutes. The solution was allowed to cool until 50 °C before being transferred into the petri dish and solidify at room temperature under the sterile environment. The agar plates were kept in 4 °C of chiller for the subsequent use.

##### 3.4.2.3 Phosphate Buffer Solution

PBS (0.1 M) solution was prepared according to the chemical composition listed in the Table 3.3. The pH of the solution was adjusted with 0.1 M NaOH and 0.1 M HCl before it was autoclaved at 121 °C for 20 minutes. Then, the solution was stored at room temperature for further use.

Table 3.3 Composition of PBS solution

Chemicals	Amounts
KH <sub>2</sub> PO <sub>4</sub>	0.024 g
Na <sub>2</sub> HPO <sub>4</sub> -7H <sub>2</sub> O	0.268 g
KCl	0.02 g
NaCl	0.8 g (0.0137 mol L <sup>-1</sup> )
Distilled water	998.0 mL
pH	7.4

#### 3.4.2.4 Saline Solution

0.85 g of NaCl was dissolved in 1 L of distilled water and stirred on a magnetic plate until become homogenous. The solution was autoclaved at 121 °C for 20 minutes.

#### 3.4.3 Germination of Stock Culture and Inoculum

A loopful of refrigerated stock culture was transferred to a petri dish containing LB agar and incubated at 37 °C for 24 hours. A colony of germinated cells was transferred to a 250 mL shake flask containing 50 mL LB broth, then incubated at 30 °C and shook at 200 rpm for 12 hours. The cells were then centrifuged at 5000 g for 5 minutes, washed twice with saline solution (0.85% (w/v) NaCl), and re-centrifuged for 5 minutes (Jamai et al., 2001). The supernatant was discarded and the pellet was transferred into 100 mL of PBS solution. The optical density (OD) of the bacterial suspension (PBS solution with bacterial cell) was adjusted until achieved approximately ~1.0 at 600 nm prior to the adhesion test.

#### 3.5 Method: Adhesion Test

Adhesion was carried out in a glass container (6 cm x 9 cm x 7 cm) containing a baby cradle-like holder to place the metal slides (2.5 cm x 7.6 cm x 0.1 cm) in the upright vertical position. The metal slides (metal and glass slide) were suspended in the 70 ml of bacterial suspension (OD: ~1.0 at 600 nm) and were shaken at 70 rpm and 30 °C for 4 hours. Samples were taken after 4 hours and lightly washed with PBS solution in the incubator shaker (10 min, 70 rpm, 30 °C) to remove the non-adherent or loosely adherent bacteria from the metal surfaces (Cunha et al., 2016). Then, the samples were kept in the chiller (15 °C) overnight before being observed under the fluorescence microscope.

During this adhesion test, polished samples (control) were tested with different condition of bacterial suspension, where the pH and NaCl concentration of the PBS solution was adjusted to pH 4, 5, 6, 7.4, and 9 (Sheng et al., 2008) and 0.001, 0.01, 0.1, 0.135 and 0.2 mol L<sup>-1</sup>, (Shephard et al., 2010) respectively. Meanwhile, all the laser structured (MI and UI) and ground (G) metal samples that have different surface structures each were evaluated with the same pH (pH 7.4) and NaCl concentration (0.0137 mol L<sup>-1</sup>) of the PBS solution as displayed in Table 3.3. The overall process was alternately repeated for two to three times with different types of bacteria (*E. coli* ATCC 8739 and *S. aureus* ATCC 6838) and metals (stainless steel and titanium). Samples were immersed in 2 % of glutaraldehyde solution for 30 minutes and subjected to ethanol dehydration to fix the bacteria and stored in 4 °C until further processed.

### **3.6 Analysis: Characterization of Metal Surfaces**

#### **3.6.1 Contact Angle Measurements (CAM)**

Contact angle generally used to evaluate the degree of wettability when a solid and liquid interacts (Yuan & Lee, 2013). The measurement of contact angle on metal surfaces was performed using sessile drop method (Tiab & Donaldson, 2012) with drop-shape analyzer (DSA 100, KRUSS). The analyzer comprises of the sample table with up to three moving axes, a CCD video system, optical system and manually software-controlled dosing system. 2 µL of distilled water was dropped onto a metal surface and the image of drop was magnified, photographed, and the contact angle at both left and right was measured using an image analysis program (DSA3 1.72b IEEE1394b) with an accuracy of ± 0.1 °. All the measurements were made at room temperature which is 24 °.

The analysis was repeated three times for each metal sample.

#### **3.6.2 Optical Profilometer**

The optical profilometer machine (ContourGT, Bruker) was used to measure the metal surface roughness in three-dimensional (3D) image and also the surface topography. The magnification of the objective lens was set to 50x magnification, covering an area of 0.5 mm x 0.5 mm using stitching algorithm technique. The optical profiler's software (Bruker Vision64) operates the data of the surface image and calculate

the sample roughness. Then, the surface roughness parameters for all the samples which are  $S_a$  (roughness average),  $S_q$  (root mean square (RMS) roughness),  $S_{sk}$  (skewness),  $S_{ku}$  (kurtosis),  $S_{dq}$  (root mean square (RMS) surface slope),  $S_{dr}$  (developed surface area ratio) and  $S_{ds}$  (summit density) were analysed. The measurement of the surface roughness parameters was taken three times for each sample.

### 3.6.3 Scanning Electron Microscopy (SEM)

All metals surfaces that have been fabricated were observed under SEM EVO 50, Carl Zeiss scanning electron microscope for observing the surface structures and morphology before being tested in the bacterial adhesion test.

## 3.7 Analysis: Characterizations of Bacteria

### 3.7.1 Gram Staining

A smear of bacterial culture was fixed on the clean glass slide and allowed to dry. The smear was covered with crystal violet for 1 minute followed with Gram's iodine for 1 minute after being washed with distilled water. Next, 95% of ethyl alcohol was used to decolourize the smear (decolourization process). Finally, safranin was added for 1 minute followed by washing with distilled water. The smear was then examined under the light microscope with 100x magnification.

### 3.7.2 Bacteria Size Analyzer

Sizes of *E. coli* ATCC 8739 and *S. aureus* ATCC 6838 were measured using scanning electron microscopy (SEM EVO 50, Carl Zeiss) and analysed with ImageJ software. Prior to the test, the bacterial samples were centrifuged at 5000 x g for 5 min followed by cell washing with 0.85% (w/v) of NaCl. The samples then were fixed in 2% of glutaraldehyde (1 hour, 4 °C), centrifuged at 5000 x g for 5 minutes and were dehydrated in an ethanol series of 30%, 50%, 70%, 80%, 90%, 100% (each step for 10 minutes excepting 100% ethanol treatment was for 30 minutes). The samples were left to dry and coated with Pt/Pd coating before been viewed using scanning electron microscopy (SEM). The images of bacteria captured were used for measuring their size

assisted by ImageJ software where 100 of bacteria were selected randomly for each SEM image.

### 3.7.3 Bacterial Adherence to Hydrocarbon (BATH) Technique

BATH technique was performed by centrifuging 15 ml of bacterial solution from 10 hours of culture at 5000 x g for 5 min, followed by washing with saline solution (0.85 % (w/v) NaCl). The bacterial cells (living and old cells) were re-suspension in 15 ml of PBS and OD were adjusted to ~1.0 ( $A_0$ ) at 600 nm using UV-Vis spectrophotometer (Hitachi, U-1800 spectrophotometer). Then, 4 ml of bacterial suspension were mixed with 1 ml of solvent (n-hexane, n-hexadecane and xylene) for 2 min. The water and organics phase were allowed to separate for 15 min and then, the OD of the aqueous phase was measured ( $A$ ) at 600 nm (Bohinc et al., 2016; Rosenbeg, 1984; Zita & Hermansson, 1997). The process was repeated three times for each bacterium. The percentage of bacterial hydrophobicity was calculated by the following equation 3.1:

$$\% \text{ of hydrophobicity} = (1 - (A + A_0)) \times 100 \quad 3.1$$

### 3.7.4 Salt Aggregation Test (SAT)

10  $\mu$ L of the bacterial suspensions (OD ~1.0 at 600 nm) were mixed with an equal volume of ammonium sulphate of various molarities which are set at 0.2 M, 1.8 M, and 3.2 M at pH 6.8 on a glass slide and observed for aggregation after left for 1 min at room temperature. The lowest concentration causing bacterial agglutination was called as salting out aggregation test (SAT) value. Cell surface hydrophobicity is inversely correlated with SAT value (Beveridge, 2001). Three repetitions were performed for each bacterium.

### 3.7.5 Zeta Potential Analyzer

Cell surface charge for *E. coli* ATCC 8739 and *S. aureus* ATCC 6838 was measured as zeta potential using Zeta Potential Analyser (Zetasizer Nano Series Nano-Z, Malvern) (Halder et al., 2015). The bacterial cells (10 hours of culture) were harvested by centrifugation at 5000 x g for 5 min, washed twice with saline solution, re-suspended in PBS and adjusted the bacterial suspension to ~1.0 (600 nm). The pH of the bacterial



suspensions was altered to 4, 7.4 and 9 and vortexed vigorously to ensure the cellular clumps were totally disrupted. The zetametry measurement was conducted at 150 V and 20 °C, where the bacterial suspensions were injected into the glass capillary, and the time cell suspension spent moving to the anode were monitored by optical microscopy on the zetameter (Carlos et al., 2013). The process was repeated three times for each bacterium.

### **3.8 Analysis: Bacterial Adhesion**

#### **3.8.1 Fluorescence Microscope**

After the bacterial adhesion test, metal substrates were examined under fluorescence microscope (BX53 Fluorescence Microscope, Olympus) to determine the number of adhered bacteria. Prior to the viewing process, a 1/1000 dilution of dye in which 2 µL of SYTO9 (3.34 mM) dye was dissolved in 2 mL of PBS solution was prepared. 10 µL drops of the dye solution then were placed on top of the bacterial smear, followed by washing with distilled water. The samples were examined under fluorescence microscope using 20x and 100x magnifications. Five different locations were observed for each magnification. Subsequently, the number of attached bacteria per square area (cm<sup>2</sup>) was determined using ImageJ software based on the image obtained from the fluorescence microscope.

#### **3.8.2 Scanning Electron Microscopy (SEM)**

The adhered bacteria on the metal samples were observed under SEM EVO 50, Carl Zeiss scanning electron microscope. The samples were soaked in 2% of glutaraldehyde solution and at 4 °C for 30 minutes and subjected to dehydrate in an ethanol series; 30%, 50%, 70%, 80%, 90%, 100% (each step for 10 minutes excepting 100% ethanol treatment was for 30 minutes). The samples were left to dry for a few minutes and then were kept in the desiccator to remove extra moisture. Subsequently, the metals plates were mounted on the aluminum stubs using carbon tape, coated (Kashi et al., 2014) with Pt/Pd using Ion sputter coater E-1030, Hitachi before being observed.

## CHAPTER 4

### METAL AND BACTERIAL SURFACE CHARACTERIZATIONS

#### 4.1 Introduction

This chapter comprised of the surface characterizations of metals and bacterial for investigating the physicochemical properties of both surfaces. The analyses of metals include contact angle measurement (CAM), surface roughness and surface morphologies while gram staining, bacterial size, bacterial hydrophobicity and bacterial surface charge are carried out for the determination of the bacterial surface characterizations.

#### 4.2 Metal Surface Characterizations

As mentioned in the methodology part, the surfaces of stainless steel AISI 316L and (SS) grade 5 titanium alloys (TT) were fabricated by using polishing, grinding, millisecond and ultrafast laser surface texturing. Grinding (G) samples were treated with five different grit papers while the millisecond laser (MI) samples were varied with five different laser power. Meanwhile, ultrafast laser (UI) samples were treated with four different laser power for stainless steel and three laser power for titanium, produced in natural and argon gas environment. Polished (P) surfaces with mirror finishing is used as a control element to compare the degree of adhesion with other tested surfaces. All the metal surfaces have different surface structures based on the fabrication process thus, produced varying surface properties for each metal.

##### 4.2.1 Contact Angle Measurement (CAM)

The surface hydrophobicity of metal samples were analysed by measuring the contact angle of the surfaces using the sessile drop method (Huhtamaki et al., 2018). Based on Bohinc et al. (2016) and Han et al. (2016) studies, metal is considered to have hydrophilic surface if CAM smaller than  $90^\circ$  and hydrophobic if greater than  $90^\circ$ . Table 4.1 showed the CAM values for all the structured surfaces of SS and TT. In general, most of grinding and millisecond laser surfaces have hydrophilic surfaces with CAM values

between 72.30 ° - 89.10 ° except for G-1200, G-1500 (both SS and TT) MI-6.0 and MI-7.8 (SS only) which were slightly hydrophobic (CAM: 90.70° - 96.10°). The hydrophobicity of the surfaces was then improved by the ultrafast laser treatment where almost all the UI surfaces are hydrophobic with the CAM is more than 100° which is between 100.65° - 145.70°. Studies from the previous research also found that the CAM value for grinding surfaces was ranged between 75° - 97° which is quite similar with the G samples in this study (Bohinc et al., 2016; Prajitno et al., 2016). Most of the laser treated surfaces especially ultrafast laser or femtosecond laser were observed to have hydrophobic surfaces, for instance study from Schwibbert et al. (2019) and Giannuzzi et al. (2019) reported the CAM value was found around 120.5° and 124° – 160°, respectively. However, Huang et al. (2018) expressed that different laser texturing parameters (power, pulses) applied to a surface can give various result of CAM as different surface micro and nano structures will be produced. Thus, surfaces treated by millisecond laser and sample UI-0.04 experienced hydrophilic surfaces because they might undergo different surface textures, pattern, roughness and topography which led to different CAM value.

Table 4.1 Contact angle measurement of stainless steel AISI 316L and grade 5 titanium alloy surfaces

Types of Fabrication	Stainless steel AISI 316L			Grade 5 titanium alloy		
	Samples	Contact Angle (°)	Condition	Samples	Contact Angle (°)	Condition
Polishing	P (C)	83.00	Hydrophilic	P (C)	72.70	Hydrophilic
Grinding	G-180	79.20	Hydrophilic	G-180	72.30	Hydrophilic
	G-600	84.30	Hydrophilic	G-600	79.90	Hydrophilic
	G-800	89.10	Hydrophilic	G-800	84.80	Hydrophilic
	G-1200	92.30	S. hydrophobic	G-1200	93.20	S. hydrophobic
	G-1500	96.10	S. hydrophobic	G-1500	95.30	S. hydrophobic
Millisecond laser	MI-4.2	83.20	Hydrophilic	MI-3.0	79.70	Hydrophilic
	MI-5.1	85.50	Hydrophilic	MI-4.2	80.90	Hydrophilic
	MI-6.0	90.70	S. hydrophobic	MI-5.4	82.70	Hydrophilic
	MI-7.0	94.00	S. hydrophobic	MI-6.6	87.50	Hydrophilic
	MI-7.8	88.80	Hydrophilic	MI-7.8	86.00	Hydrophilic
Ultrafast laser	UI-0.04	89.40	Hydrophilic	-	-	-
	UI-0.10	140.22	Hydrophobic	UI-0.10	100.65	Hydrophobic
	UI-0.11	145.70	Hydrophobic	UI-0.11	130.10	Hydrophobic
	UI-0.12	129.50	Hydrophobic	UI-0.12	134.20	Hydrophobic

\*All data are represented as average taken from three replications with ±10% of standard error.

\*S. hydrophobic is stands for slightly hydrophobic.

Furthermore, SS surfaces was observed to have high CAM values than TT which presumably influenced by the surface energy (Kalin & Polajnar, 2014). Goebel et al. (2004) mentioned that, high contact angle is caused by the low surface free energy on the metal which resulting a weak attraction between the solid (metal) and the liquid (liquid droplet) phase. Results obtained were also supported by the drop shape image shown in Figure 4.1. According to Yuan and Lee (2013), when a surface has low contact angle or hydrophilic surface the liquid droplet will spreads on the surface (Figure 4.1 (a, b)) while for high contact angle or hydrophobic surface a bead form of liquid will be produced (Figure 4.1 (c, d)).

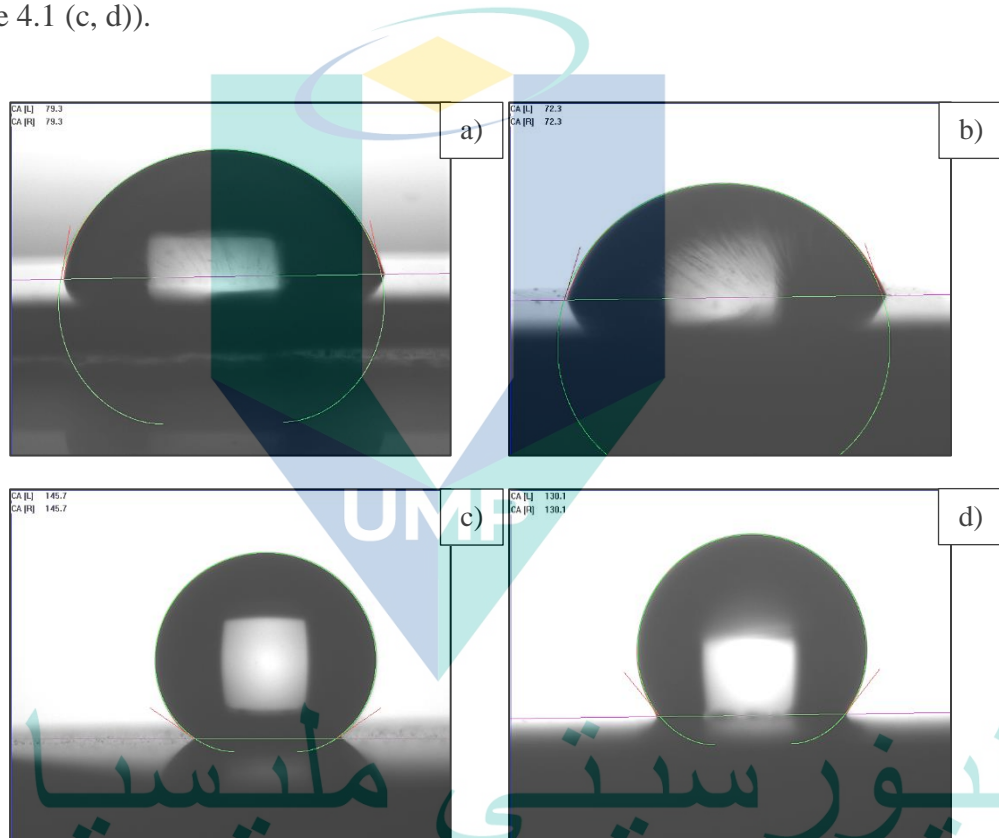


Figure 4.1 Examples of drop shape image of distilled water on metals surfaces with the measurement of contact angle a) G-SS-180, 79.20° b) G-TT-180, 72.30° c) UI-SS-0.11, 145.70° d) UI-TT-0.01, 130.10°

#### 4.2.2 Surface Roughness

Different surface modification, structures and features of SS and TT was produced during the fabrication process and the data roughness parameters has been presented in Table 4.2 and 4.3. Meanwhile, the topography images of both metals were analyzed using 3D optical profilometer as shown in Figure 4.2, 4.3 and 4.4. The surface parameters examined was surface average roughness ( $S_a$ ), root mean square roughness

( $S_q$ ), skewness ( $S_{sk}$ ), kurtosis ( $S_{ku}$ ), developed interfacial area ration ( $S_{dr}$ ) and summit density ( $S_{ds}$ ) (Deltombe et al., 2014).  $S_q$ ,  $S_a$ ,  $S_{sk}$  and  $S_{ku}$  (amplitude parameters) were used to measure vertical characteristics of the surface deviations where  $S_q$  and  $S_a$  represented the average roughness of a surface (Löberg et al., 2010).

Data displayed in Table 4.2 and 4.3, depicted the roughness ( $S_q$  and  $S_a$ ) obtained after the fabrication process. Most of the surfaces (G, MI, UI) had increased in roughness measurement when compare to P (control) of SS and TT which have  $S_q$  between 90.80 nm - 97.26 nm and  $S_a$  between 51.30 nm - 68.41 nm with an exception to MI-TT-3.0. UI-0.11 and UI-0.12 of both metals were observed to have rougher surface finishing than other surfaces with  $S_q$  and  $S_a$  were recorded between 630 nm – 910 nm and 490 nm – 700 nm, respectively. This gave an increase between 5-fold – 8-fold ( $S_q$ ) and 8-fold – 9-fold ( $S_a$ ) compare to control surfaces. On the other hand, all G samples showed the decrease of  $S_q$  and  $S_a$  from 269.48 nm to 175.15 nm and 207.14 nm to 132.89 nm, respectively with regards to the used of courser (180) to finer (1500) abrasive paper. During grinding process, heightened peaks was removed thereby provides a smoother surface compares to before treatment. In contrast,  $S_q$  and  $S_a$  of MI samples (SS and TT) was increased from 88.92 nm to 358.57 nm and 48.19 nm to 256.28 nm, respectively with the increase of laser power from 3.0 W to 7.8 W. Introduction of laser causing rearrangement of the melted metal on the laser line resulting in homogenous a controlled roughness on the lasered surfaces. At 3D-topography images in Figure 4.3, it is clearly shown that MI surfaces had increased in roughness where additional peaks were formed on top of the surface especially at MI-7.8 of both metals during the laser treatment as the laser power increase.

Two additional parameters which are  $S_{sk}$  and  $S_{ku}$  which also describe the surface roughness profile are being observed in this study. Skewness ( $S_{sk}$ ) is used to measure the symmetry of the surface profile about the mean line (Gadelmawla et al., 2002). Generally, with Gaussian distribution surface or symmetrical topography, the  $S_{sk}$  is zero while surface with high peaks and valleys filled in have positive  $S_{sk}$  and surface revealing more pits and valleys than peaks have negative  $S_{sk}$  (Suh et al., 2003). Meanwhile, kurtosis ( $S_{ku}$ ) describes the sharpness of height distribution of the surface profile and surface with Gaussian distribution surface has  $S_{sk}$  value of 3 (Mohamad et al., 2013). A narrow height distribution or spiky surface has  $S_{sk}$  value greater than 3 ( $S_{ku} > 3$ ), while a well spread

out height distribution or bumpy surface has  $S_{sk}$  value less than 3 ( $S_{ku} < 3$ ) (Blateyron, 2013). Therefore, referring to Table 4.3 most of the TT samples at all types of fabrication have negative  $S_{sk}$  showing that the surfaces were dominated by valleys, pits and scratches rather than peaks (Figure 4.2, 4.3, 4.4) except for G-1200, MI-7.8 and UI-0.12 samples that have  $S_{sk}$  value nearly to zero which means the surface has approximately symmetrical height distribution. On the other hand, some of SS samples have positive  $S_{sk}$  which explaining that the surfaces have many peaks and valley filled in. Furthermore, the kurtosis value for all the samples (SS and TT) was mostly more than 3 ( $S_{ku} > 3$ ), indicating that most of the peaks are sharp and spiky (narrow height distribution) especially MI-SS-6.0 ( $S_{ku}$ : 50.15) and MI-TT-3.0 ( $S_{ku}$ : 68.17) surfaces and the topography profile in Figure 4.2, 4.3 and 4.4 offer further insight the detail features of the samples. Generally, the homogeneity of the surfaces was more pronounce on the TT surfaces rather than SS, especially during grinding and millisecond laser treatment. This condition might be contributed to the hardness of TT which is really strong (Agripa & Botef, 2019) than SS where it can withstand heat produced through friction and laser ablation thus, easily to structure.

$S_{dr}$  and  $S_{ds}$  are hybrid parameters which describe the shape of a surface by the combination of amplitude and spatial properties (Wennerberg et al., 2015).  $S_{dr}$  expresses the percentage of additional surface area which resulted from the surface texture (Fabre et al., 2011) while  $S_{ds}$  or summit density characterizes the number of peak (above all eight nearest neighbours) per unit area on the sample surfaces (Wennerberg et al., 2015). Based on the results displayed in Table 4.2 and 4.3,  $S_{dr}$  and  $S_{ds}$  at UI samples are the highest compared to P, G and MI surfaces with  $S_{dr}$  was ranged between 4.65% – 76.63% and  $S_{ds}$  between 16171.76/mm<sup>2</sup> - 26945.58/mm<sup>2</sup>. This showing that the UI surfaces have high percentage of additional surface area as well as number of peaks. The topography images of UI surfaces especially at UI-0.11 (Figure 4.4) were covered by rich picture of pronounce peaks and less valleys features at both SS and TT. The peaks pattern was observed being more uniform than P, G and MI surfaces.

Table 4.2 Result of  $S_q$ ,  $S_a$ ,  $S_{sk}$ ,  $S_{ku}$ ,  $S_{dr}$  and  $S_{ds}$  of stainless steel AISI 316L

Samples	$S_q$ (nm)	$S_a$ (nm)	$S_{sk}$	$S_{ku}$	$S_{dr}$ (%)	$S_{ds}$ (1/mm <sup>2</sup> )
P (C)	97.26 ± 10.78	68.41 ± 9.92	0.85 ± 0.03	7.61 ± 2.07	0.08 ± 0.00	4230.62 ± 880.58
G-180	269.48 ± 10.12	207.14 ± 7.74	-0.44 ± 0.14	5.58 ± 0.52	0.49 ± 0.01	2627.25 ± 34.63
G-600	265.72 ± 11.99	207.42 ± 8.76	-0.50 ± 0.11	4.25 ± 0.16	0.28 ± 0.00	1985.25 ± 11.57
G-800	212.55 ± 21.05	163.15 ± 17.89	0.17 ± 0.23	4.02 ± 0.19	0.36 ± 0.01	2525.29 ± 122.00
G-1200	176.60 ± 46.11	131.97 ± 22.06	0.05 ± 0.29	6.44 ± 0.52	0.31 ± 0.03	2288.04 ± 52.66
G-1500	175.15 ± 2.87	132.89 ± 2.80	0.22 ± 0.02	4.49 ± 0.13	0.31 ± 0.01	2412.39 ± 37.90
MI-4.2	98.34 ± 3.48	67.58 ± 1.80	0.65 ± 0.04	17.07 ± 0.73	0.11 ± 0.01	3461.86 ± 3.45
MI-5.1	99.47 ± 11.13	70.76 ± 10.78	0.52 ± 0.48	25.73 ± 20.27	0.08 ± 0.00	3889.07 ± 682.00
MI-6.0	115.64 ± 2.94	73.20 ± 0.49	-1.52 ± 1.28	50.15 ± 23.36	0.23 ± 0.01	3378.05 ± 330.29
MI-7.0	207.17 ± 2.49	139.80 ± 0.61	-0.28 ± 0.19	23.63 ± 7.48	0.84 ± 0.01	5658.88 ± 349.25
MI-7.8	358.57 ± 6.67	256.28 ± 6.87	-0.29 ± 0.00	3.97 ± 0.06	1.72 ± 0.05	7540.22 ± 18.93
UI-0.04	190.00 ± 20.00	140.00 ± 0.00	2.34 ± 1.59	25.04 ± 18.17	5.30 ± 0.02	16171.76 ± 488.10
UI-0.10	298.00 ± 19.60	264.00 ± 17.40	-0.55 ± 0.05	1.96 ± 0.04	4.65 ± 0.42	17039.43 ± 112.32
UI-0.11	650.00 ± 78.00	510.00 ± 80.00	-0.06 ± 0.06	3.56 ± 0.06	30.80 ± 1.74	19868.05 ± 28.27
UI-0.12	720.00 ± 40.00	650.00 ± 20.00	0.59 ± 0.32	1.95 ± 0.02	60.83 ± 0.98	26945.58 ± 154.72

\*All data are represented as average taken from three replications.

Table 4.3 Result of  $S_q$ ,  $S_a$ ,  $S_{sk}$ ,  $S_{ku}$ ,  $S_{dr}$  and  $S_{ds}$  of grade 5 titanium alloy

Samples	$S_q$ (nm)	$S_a$ (nm)	$S_{sk}$	$S_{ku}$	$S_{dr}$ (%)	$S_{ds}$ (1/mm <sup>2</sup> )
P (C)	90.80 ± 15.20	51.30 ± 11.44	-4.51 ± 0.72	37.04 ± 9.61	0.30 ± 0.00	3346.27 ± 59.07
G-180	365.01 ± 28.14	287.69 ± 24.47	-0.48 ± 0.06	4.26 ± 0.71	0.69 ± 0.02	2965.01 ± 49.67
G-600	254.70 ± 6.14	195.27 ± 2.44	-0.56 ± 0.18	9.63 ± 3.02	0.41 ± 0.01	2497.77 ± 53.64
G-800	226.33 ± 57.10	175.18 ± 48.98	-0.89 ± 0.55	21.25 ± 17.57	0.30 ± 0.01	2474.37 ± 95.23
G-1200	205.66 ± 2.48	159.60 ± 2.52	0.10 ± 0.01	3.81 ± 0.18	0.65 ± 0.14	2508.74 ± 27.53
G-1500	204.10 ± 7.21	157.15 ± 7.06	-0.15 ± 0.11	5.28 ± 1.73	0.52 ± 0.01	3099.11 ± 51.66
MI-3.0	88.92 ± 6.00	48.19 ± 7.14	-5.62 ± 1.61	68.17 ± 34.19	0.12 ± 0.02	2965.94 ± 1094.04
MI-4.2	92.40 ± 2.21	52.79 ± 1.61	-4.06 ± 0.28	45.45 ± 9.25	0.17 ± 0.02	4912.55 ± 289.42
MI-5.4	146.75 ± 7.97	96.11 ± 6.94	-1.24 ± 0.07	11.47 ± 1.68	0.45 ± 0.07	7086.16 ± 315.05
MI-6.6	213.01 ± 2.00	161.00 ± 1.78	-0.46 ± 0.01	4.22 ± 0.01	0.69 ± 0.02	8053.78 ± 75.38
MI-7.8	270.26 ± 3.85	208.64 ± 2.30	0.27 ± 0.02	3.75 ± 0.03	0.94 ± 0.02	7458.29 ± 18.58
UI-0.10	210.00 ± 0.01	155.00 ± 0.01	-0.63 ± 0.22	5.99 ± 3.00	5.77 ± 0.35	16456.30 ± 1.01
UI-0.11	910.00 ± 0.00	700.00 ± 10.00	-0.24 ± 0.01	3.38 ± 0.00	49.64 ± 5.66	20670.31 ± 2.83
UI-0.12	630.00 ± 3.20	490.00 ± 5.70	1.63 ± 0.03	3.67 ± 0.09	76.63 ± 1.32	19031.06 ± 0.07

\*All data are represented as average taken from three replications



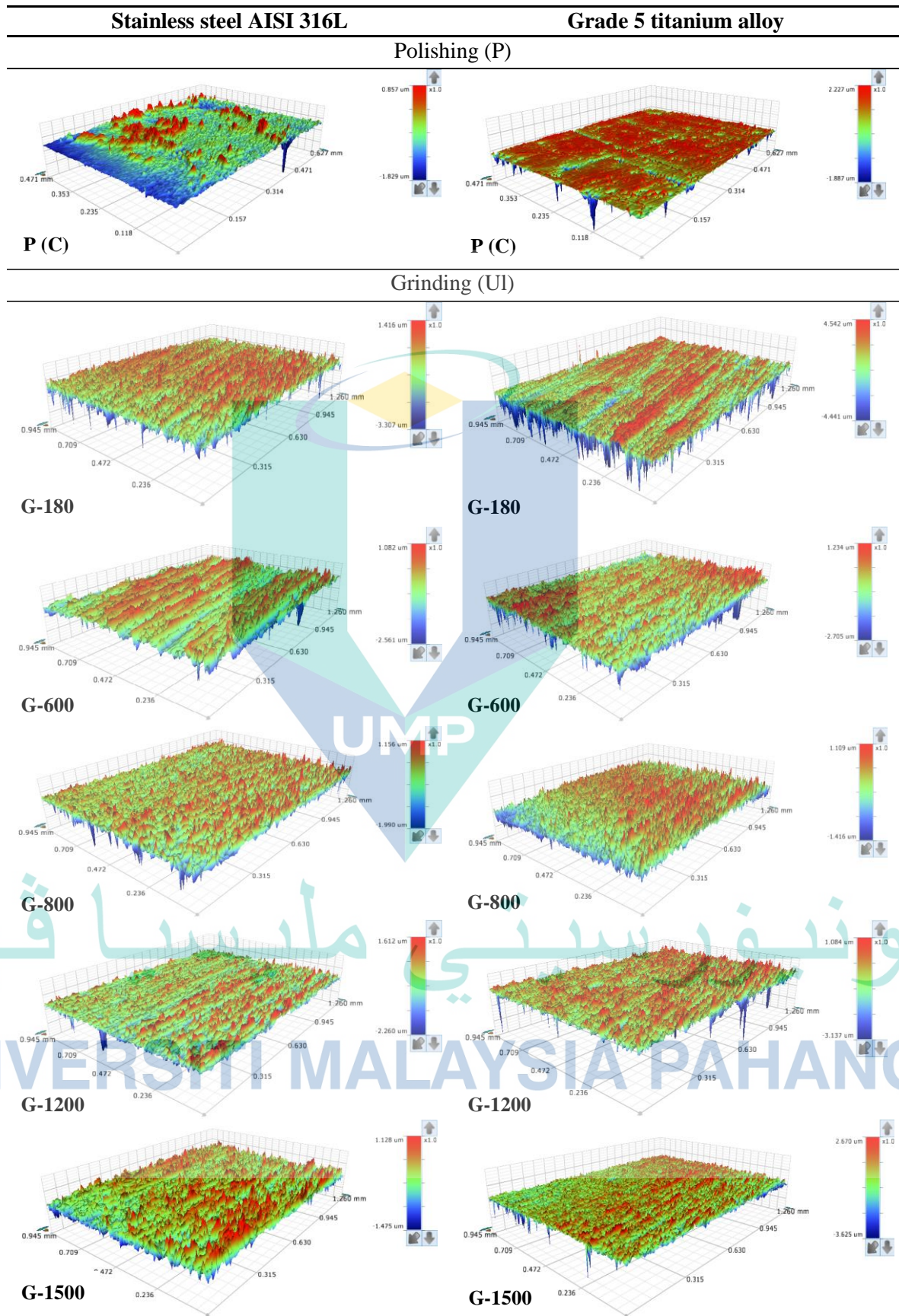


Figure 4.2 3D-topography images of polishing (P) and grinding (G) surfaces. Warm colors (brown and yellow) depict surface with greater surface roughness and cold colors (blue and green) describes otherwise

**Stainless steel AISI 316L**

**Grade 5 titanium alloy**

**Millisecond laser (MI)**

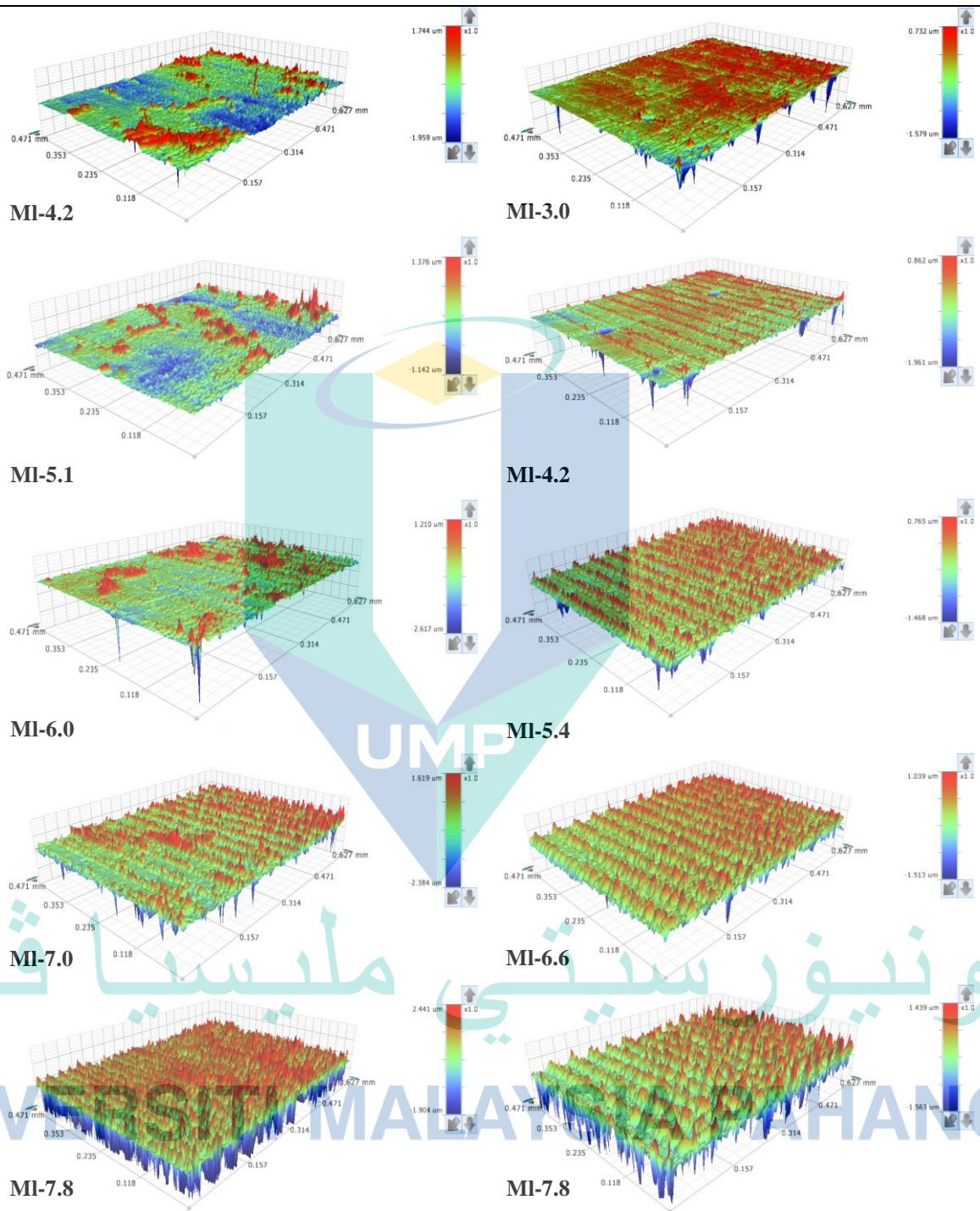


Figure 4.3 3D-topography images of, millisecond laser (MI) surfaces. Warm colors (brown and yellow) depict surface with greater surface roughness and cold colors (blue and green) describes otherwise

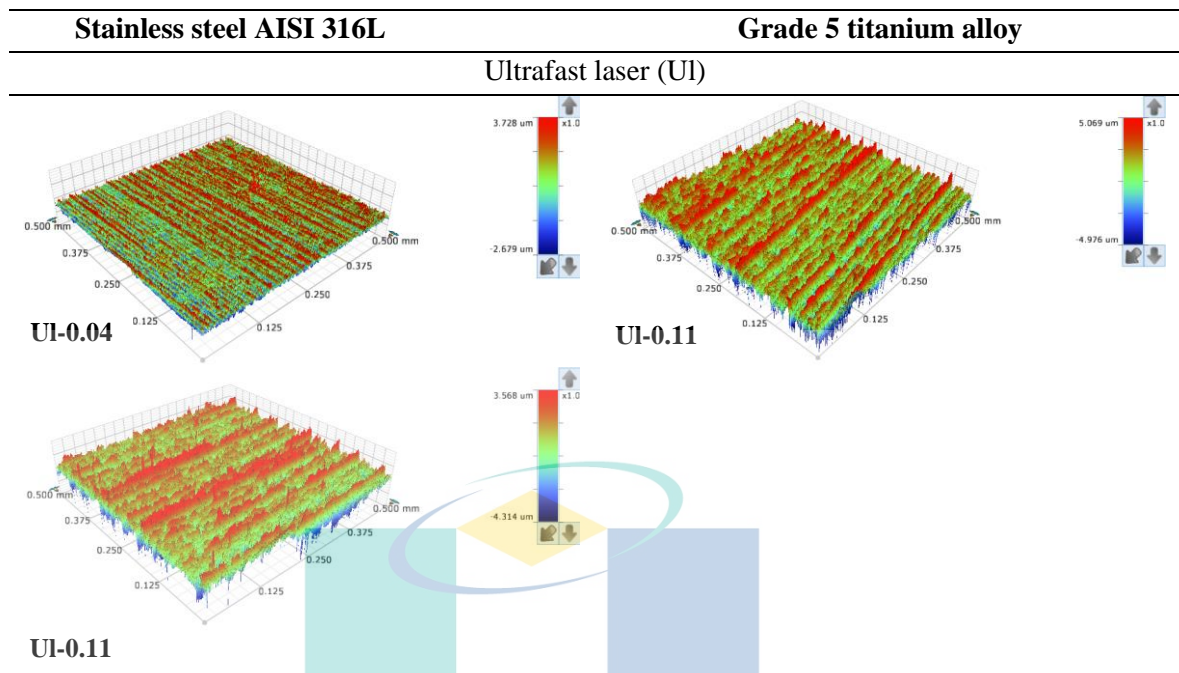


Figure 4.4 3D-topography images of ultrafast laser (UI) surfaces. Warm colors (brown and yellow) depict surface with greater surface roughness and cold colors (blue and green) describes otherwise

Overall, ultrafast laser treatment was observed can produce significant features towards the SS and TT surfaces where  $S_q$ ,  $S_a$ ,  $S_{dr}$ , and  $S_{ds}$  parameters measured were high compared to surfaces fabricated by polishing, grinding and millisecond laser. Similarly, study from Rajab et al. (2018) on the laser fabrication towards stainless steel surfaces with laser power about 0.20 W and scanning speed 10 mm/s had also discovered high roughness measurement which is between 200 nm - 1300 nm for  $S_q$  and 100 m - 1160 nm for  $S_a$ . But, in Maharjan (2019) study surface roughness of a metal were reduced to 203 nm for  $S_q$  and 119 nm  $S_a$  as the laser power increase to 30 W. Calignano et al. (2012) stated that, apart from the laser power other parameters such as scanning speed, frequency, wavelength and pulses are also another main factors that can control and varied the roughness of a surface. Therefore, different parameter used in laser processing can influence the topography profile of a surface in which various results of  $S_q$ ,  $S_a$ ,  $S_{sk}$ ,  $S_{ku}$ ,  $S_{dr}$  and  $S_{ds}$  will be produced.

### 4.2.3 Surface Morphologies

Fabrication definitely changed the surface finish of a metal. Figure 4.6, 4.7 and 4.8 show SEM micrograph of the surface morphologies and surface textures of SS and TT after the polishing, grinding, millisecond laser and ultrafast laser treatments. Figure 4.5 illustrates the SEM images of all the common features that available on the fabricated surfaces.

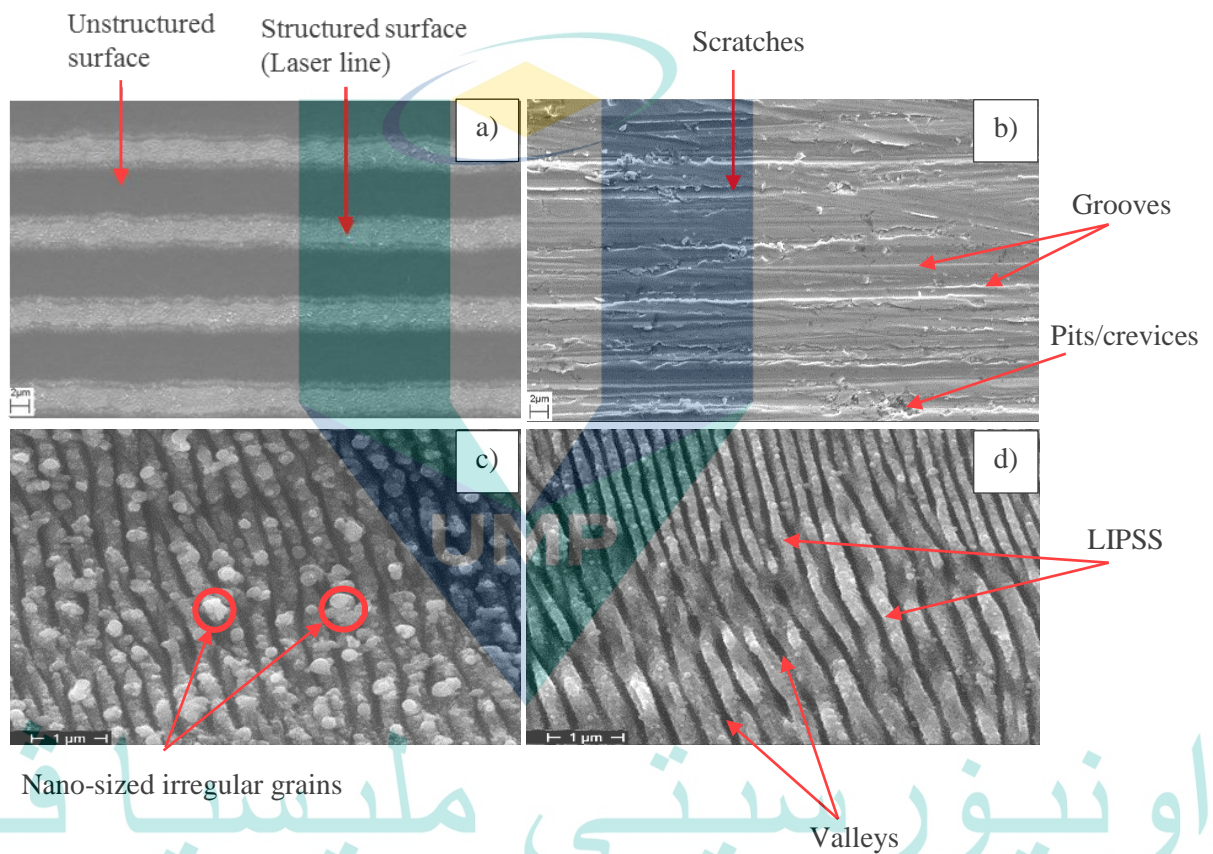


Figure 4.5 SEM images of the common features available on the surfaces after various of fabrication techniques a) ultrafast laser surface at 500x magnification b) grinding surface at 2000x magnification c) ultrafast laser surface at 20000x magnification d) ultrafast laser surface at 20000x magnification

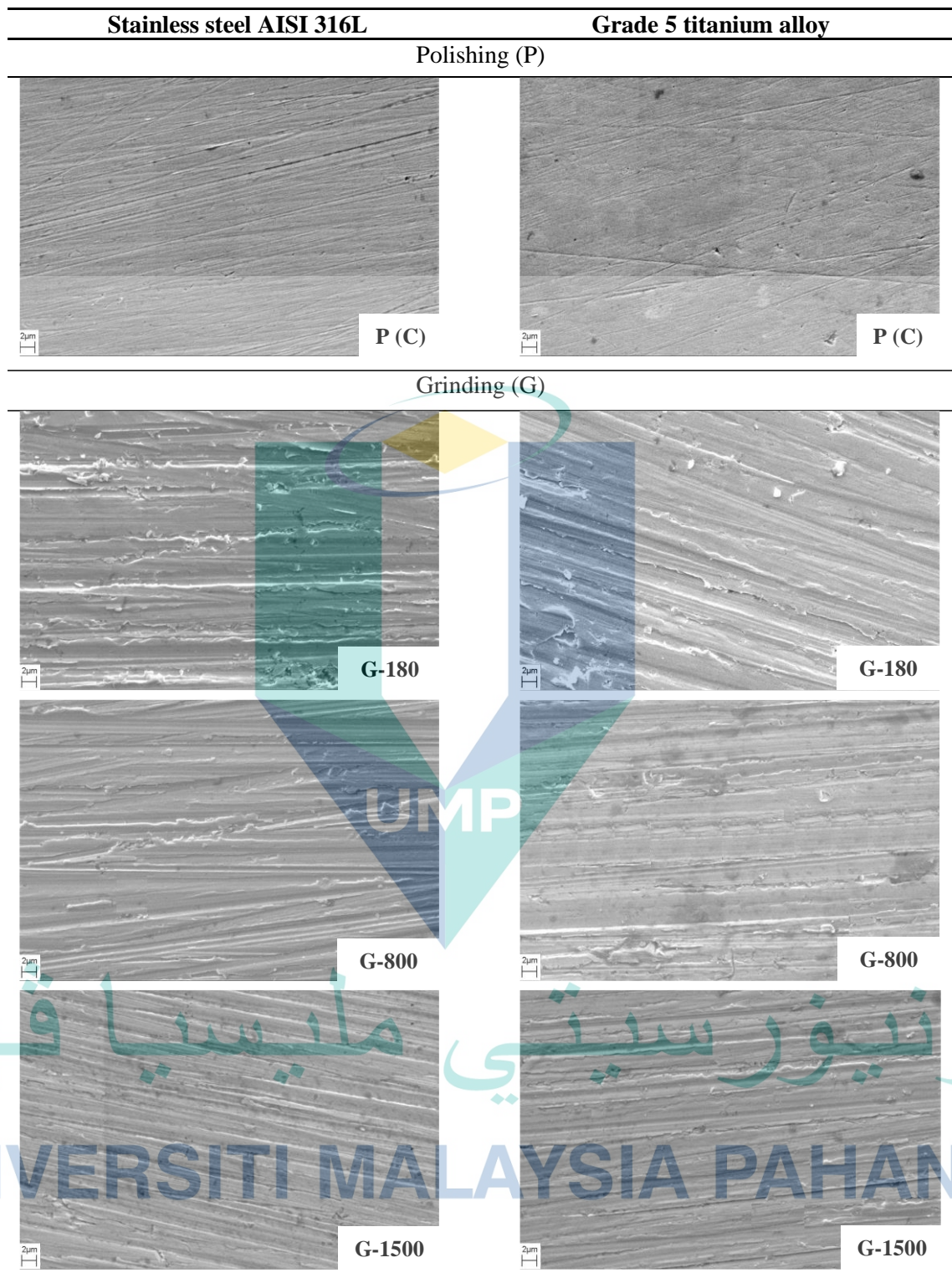


Figure 4.6 SEM micrograph of the surface morphologies of polishing (P) and grinding (G) surfaces at 2000x of magnification

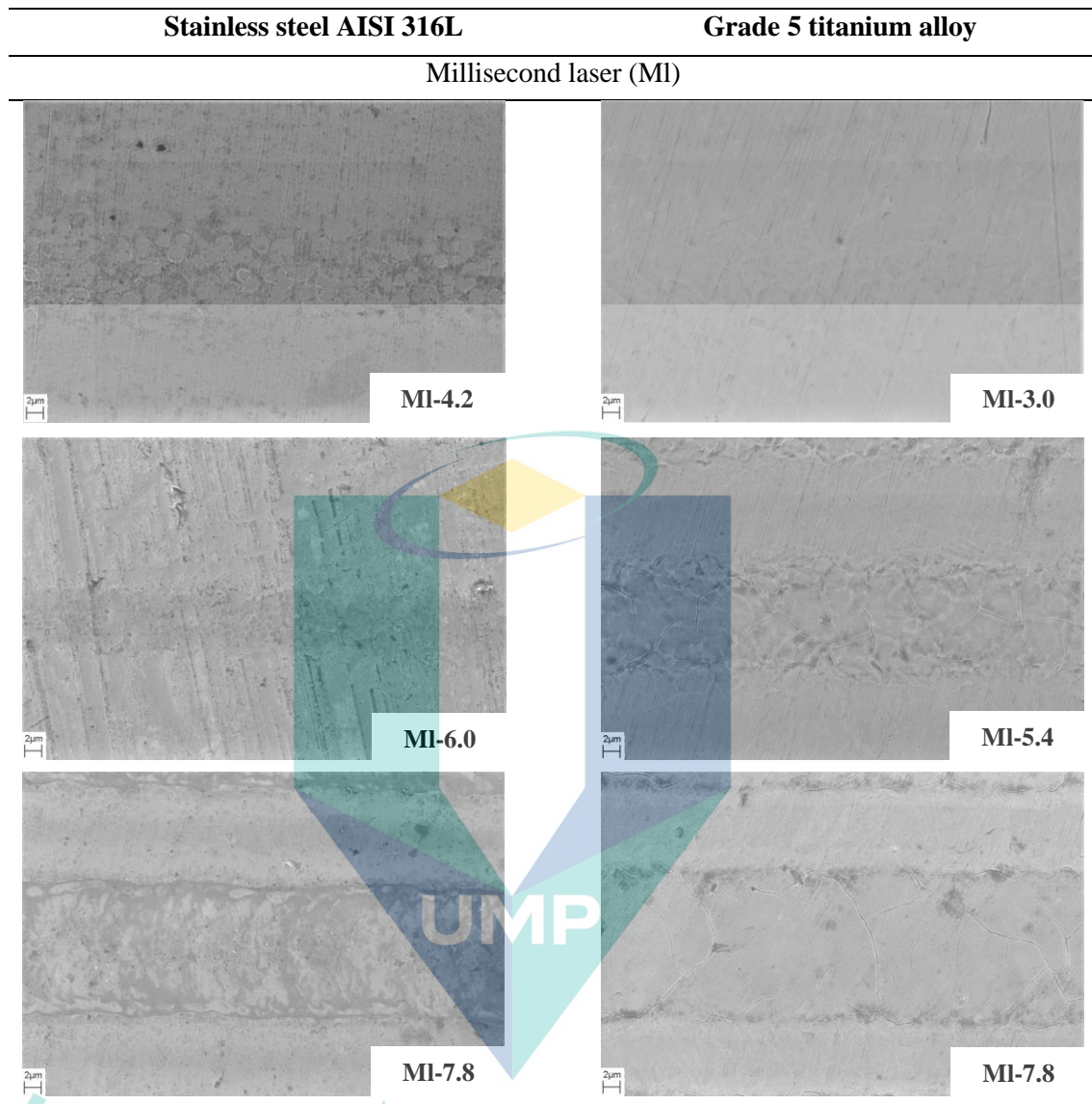


Figure 4.7 SEM micrograph of the surface morphologies of millisecond laser (MI) surfaces at 2000x of magnification

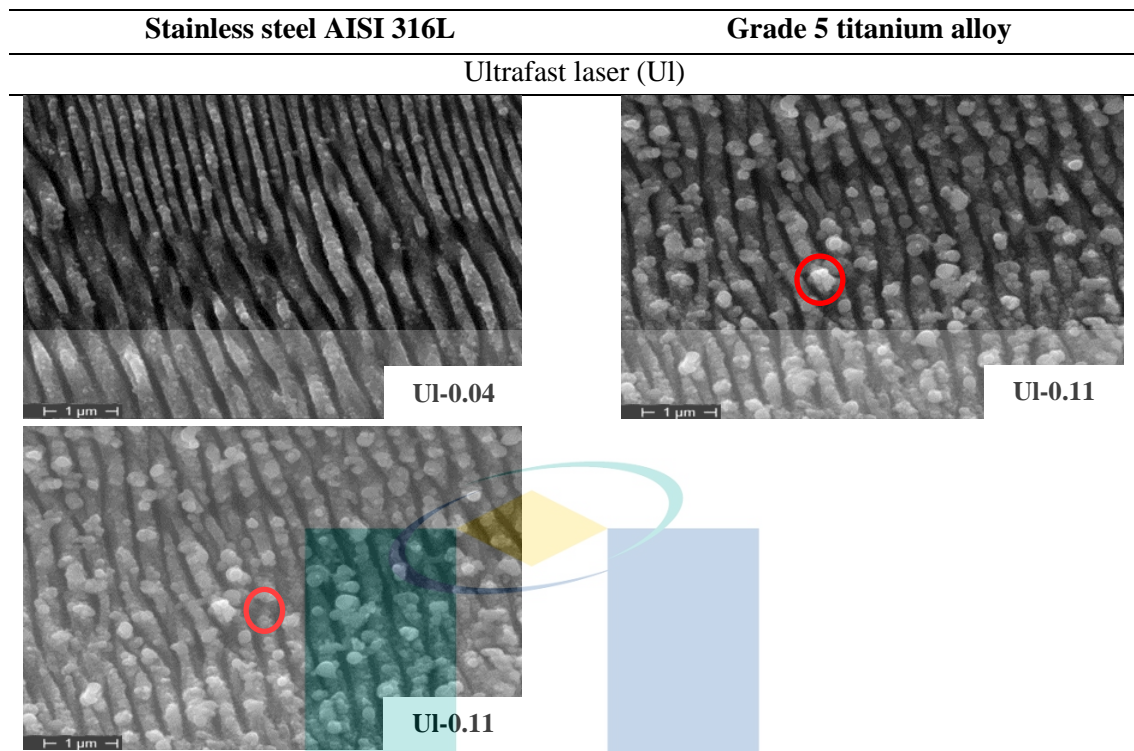


Figure 4.8 SEM micrographs of the surface morphologies ultrafast laser (UI) surfaces at 20000x magnification. The red circle area highlighted the nano-size irregular grains formed on top of LIPSS

Generally, polishing process generates smooth surfaces by removing the small irregularities on top of it (Jaritngam et al., 2020) which contributed to the reduction of roughness measurement therefore, in Figure 4.6 P samples were observed to have finer surface structures compared to others. Small scratches can be found on P-TT presumably caused by the abrasive tool scratching the surfaces (Lin & Kao, 2004). Nevertheless, the condition is acceptable because it does not pose significant effects on the surface roughness measurement (refer Table 4.2 and 4.3). Decreasing the grit size of abrasive paper (courser to finer) during grinding process produced irregular surface textures with a lot of grinding marks such as grooves, pits, and heavy scratches on SS and TT from sample G-180 until G-800 (Figure 4.6). However, when fine abrasive paper has been used, the surface waviness and scratches of both metals managed to be reduced especially at G-1500. Other study also emphasized that, surface pattern of grinding samples are always proportional to the grit size of abrasive paper used in the study (Zanatta et al., 2017).

Besides that, in order to study the effect of surface structured on the bacterial adhesion, different laser power was used to modify the surfaces of MI and UI samples. Based on Figure 4.7, laser line with size between 11  $\mu\text{m}$  and 23  $\mu\text{m}$  can be observed on the MI-6.0 and MI-5.4 surfaces and only a few scratches and cracks formed on the laser line. Then, when high laser power (7.8 W) was introduced to the MI-7.8 surfaces of both metals the scratches becomes more visible and rougher as well as the size of the laser line become bigger until 29  $\mu\text{m}$  - 34  $\mu\text{m}$ . On the other hand, as demonstrated in Figure 4.8 ultrafast laser treatment generated a so-called laser induced periodic surface structures (LIPSS) texture (shown in Figure 4.3). LIPSS was term as self-organized structures or ripples which was formed under varied laser fluence and pulses (Maragkaki et al., 2017). The LIPSS coverage on all metal surfaces are quite uniform and exhibited some waves, line breaks and Y-bifurcations. The size of the LIPSS is about 0.20  $\mu\text{m}$  and the distance between LIPSS line is approximately 0.086  $\mu\text{m}$ . Valleys, crevices and pits can be seen clearly formed between the LIPSS line. As the laser power increase to 0.10 W the additional of nano-sized irregular grains (red circle) with size between 0.083  $\mu\text{m}$  and 0.112  $\mu\text{m}$  were formed on the LIPSS (Figure 4.5). The nano-sized irregular grains were produced during the laser re-melting (Temmler & Pirch, 2020) ablation process, depending on the amount of deposited energy dose and the depolarization of the incident light (Phillips et al., 2015). At 0.04 W, there were absentees of the nano grains on the LIPSS lines which due to the insufficient of energy (power) introduced to the surface.

The existence of LIPSS features and the formation of nano-grains on the UL surfaces was proved can enhance the surface hydrophobicity (CAM) and surface roughness ( $S_q$ ,  $S_a$ ) of the metal samples (SS and TT) as the results of the CAM and roughness measurement of UL surfaces in this study are the highest than other surfaces. This is supported by the study from Truong et al. (2010) which had reported an enhancement of surface roughness ( $S_q$ ) from 3.79  $\mu\text{m}$  (as-received) to 5.84  $\mu\text{m}$  (laser treated) as well as study from Žemaitis et al. (2020) where the wettability (CAM) of the steel had changed to superhydrophobic after treated by the ultrafast laser which consisted of LIPSS and nanostructures features on the surface with the improvement of CAM from 4° (untreated steel) to 150°. Study from Jalil et al. (2020) also found that nanostructures that covered the LIPSS had further improve the hydrophobicity and roughness of the metallic surfaces. Therefore, it can be concluded that certain surface topography (structure) of a material can influences the surface hydrophobicity especially surface



treated by ultrafast laser machine. Overall, after the fabrication process all P, G, MI and UI samples have surface roughness ( $S_q$  - focused parameter) between 97.26 nm – 720 nm for SS and 90.80 nm - 910 nm for TT. Most of UI samples have hydrophobic surface after the fabrication except for UI-SS-0.04 with CAM ranged from 100.65° to 145.70° for both SS and TT while, P, G and MI samples have hydrophilic and slightly hydrophilic surface..

### 4.3 Bacterial Characterizations

Biofilm formation on a material surface is a complicated process (Bohinc et al., 2016) nevertheless, with proper understanding of the relationship between surfaces and the bacterial adhesion process, possible actions can be performed to overcome this arising problem. Bacterium has unique characteristics and its properties play an important role as one of the factors that contribute to the severity of the adhesion (Katsikogianni & Missirlis, 2004). Therefore, the bacterial characterization tests such as gram staining, bacterial size, bacterial surface hydrophobicity and bacterial surface charge test have been performed to provide a better insight on the roles of the bacterial properties towards the adhesion phenomenal.

#### 4.3.1 Gram Staining

Gram staining is a fundamental step to segregate bacteria into Gram positive or Gram negative, dictates by the ability of the bacteria to retain the crystal violet (purple) stain. Gram positive bacteria will show violet (purple) colour while bacteria that decolourized and give red/pink colour after counterstain with safranin was categorized as Gram negative (Beveridge, 2000; Luan et al., 2018). Figure 4.9 shows the image of Gram stained of *E. coli* ATCC 8739 and *S. aureus* ATCC 6838 under the light microscope. Based on the image, *E. coli* ATCC 8739 can be observed as Gram negative bacteria and *S. aureus* ATCC 6838 is Gram positive as the stain colour was red/pink and violet, respectively. Study by Méndez-Pfeiffer et al. (2019) and Günther et al. (2017) also had mentioned that *E. coli* is a Gram negative bacteria while *S. aureus* is a Gram positive. This staining response relies on the structural make-up of the bacterial cell wall (Beveridge, 2001). Gram negative bacteria which is *E. coli* ATCC 8739 has thin peptidoglycan layers and also thin outer membrane (Figure 2.2) which makes the bacteria cell wall was easily disrupted during the decolorization step and cannot retain the crystal

violet dye (Beveridge, 2001; Yazdankhah et al., 2001). In contrast, *S. aureus* ATCC 6838 was capable to retain the crystal violet stain due to the thick and impermeable wall which composed of thick peptidoglycan (Figure 2.3) and secondary polymer layers which help to resist the ethanol decolorization process (Yazdankhah et al., 2001).

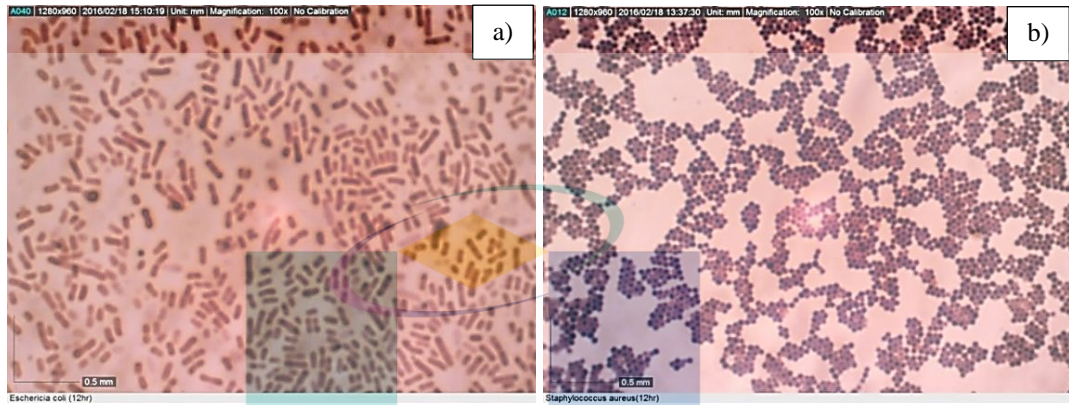


Figure 4.9 Image of Gram stained of a) *E. coli* ATCC 8739 (red colour), b) *S. aureus* ATCC 6838 (violet/purple colour) under 100x magnification of light microscope

#### 4.3.2 Bacterial Size and Shape

*E. coli* ATCC 8739 and *S. aureus* ATCC 6838 have different sizes and shapes. SEM was used to measure the bacterial size assisted by ImageJ software. ImageJ is a Java-based image processing program designed for scientific multidimensional images. A total 100 free cells (non-adhered bacteria) from the SEM images (Figure 4.10) were selected randomly to measure their average size. The size of *E. coli* ATCC 8739 was ranged between  $0.98 \mu\text{m} - 2.24 \mu\text{m}$  (length) and  $0.19 \mu\text{m} - 0.75 \mu\text{m}$  (width) while *S. aureus* ATCC 6838 was between  $0.41 \mu\text{m} - 0.727 \mu\text{m}$ . Both bacterial sizes obtained were approximately similar to other studies which found that *E. coli* dimension is about  $1 \mu\text{m} - 2 \mu\text{m}$  long by  $0.25 \mu\text{m} - 1 \mu\text{m}$  wide (Gangan & Athale, 2017; Idalia & Bernardo, 2017) and *S. aureus* is  $0.5 \mu\text{m} - 1 \mu\text{m}$  (Gnanamani et al., 2017; Madsen et al., 2018). Besides that, the SEM images at Figure 4.10 also shows the shape of each bacterium where *E. coli* ATCC 8739 can be seen is a rod shape bacteria and *S. aureus* ATCC 6838 is in spherical or cocci shape.

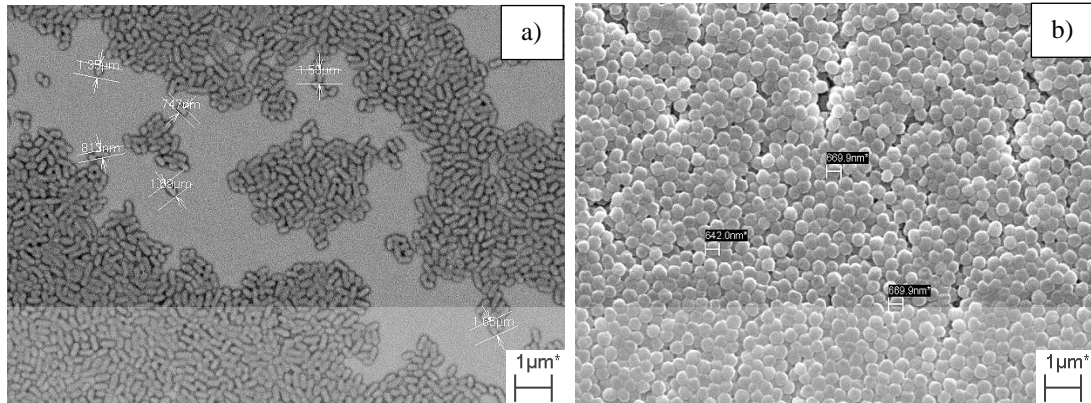


Figure 4.10 Size and shape of bacterial under scanning electron microscope a) *E. coli* ATCC 8739 b) *S. aureus* ATCC 6838 at 4000x of magnification

### 4.3.3 Bacterial Hydrophobicity

Surface hydrophobicity of bacteria is one of the factors that govern the bacterial adhesion to various surfaces. There are numbers of method to determine the surface hydrophobicity of bacteria such as bacterial adherence to hydrocarbon (BATH), hydrophobic interaction chromatography (HIC), salt aggregation test (SAT), contact angle measurement (CAM) and partitioning of cells in two phase system (TPP) (Chakraborty et al., 2010; Rosenberg, 1984; Zita & Hermansson, 1997). In this study surface hydrophobicity for *E. coli* ATCC 8739 and *S. aureus* ATCC 6838 was determined by bacterial adherence to hydrocarbon (BATH) technique and salt aggregation test (SAT) technique. These two methods were applied because it is simple, rapid technique to determine surface hydrophobicity, reasonably reproducible and widely acceptance by the researchers (Hui & Dykes, 2012; Rosenberg, 1984). BATH technique was performed by using three different types of hydrocarbon which are hexane ( $C_6H_{14}$ ), hexadecane ( $C_{16}H_{34}$ ) and xylene ( $C_8H_{10}$ ) (Mei et al., 1995). Hydrocarbons (non-polar) are hydrophobic substances and cells which possessed high surface hydrophobicity will have ability to attached to the hydrocarbon droplets. The purpose of using three hydrocarbons is to provide relative and quantitative comparison for the bacterial surface hydrophobicity property.

Referring to Bohinc et al. (2016) and Nostro et al. (2004) cells are categorized as highly hydrophobic when the hydrophobicity is greater than 70 %, moderate at 50 % - 70 % and hydrophilic when it is lower than 50 %. Table 4.4 indicates that the percentage

hydrophobicity of live cells of *E. coli* ATCC 8739 for all types of hydrocarbon was varied between 4.42 % - 23.43 % while *S. aureus* ATCC 6838 was between 75.18 % - 92.57 %. Hence, it showed that *S. aureus* ATCC 6838 has highly hydrophobic surface while *E. coli* ATCC 8739 are highly hydrophilic. This is in line with finding from Mirani et al. (2018) and Gogra et al. (2010) which also found that *S. aureus* has hydrophobic surface while *E. coli* has hydrophilic surface based on the BATH test, with 78.25 % and 46.50 % of percentage hydrophobicity, respectively. The surface hydrophobicity was dictated by the amount of protein available (proteinaceous) on the surface, while the hydrophilic character was often contributed by the polysaccharides components (Krasowska & Sigler, 2014). For instance, the presence of protein constituent at the surface (peptidoglycan) of *S. aureus* ATCC 6838 such as fibrinogen and fibronectin make the cell surface has high affinity towards hydrocarbons compared to *E. coli* ATCC 8739 (Mamo, 1989). Similarly, at old culture both bacterial cells still showed surfaces with high hydrophobic for *S. aureus* ATCC 6338 (% hydrophobicity > 70%) and hydrophilic for *E. coli* ATCC 8739 (% hydrophobicity < 50%).

Apart from that, salt aggregation test (SAT) was also conducted to compare the results achieved from the BATH technique. Three different of ammonium sulphate concentration were used which are 0.2 M, 1.8 M and 3.2 M as salting out agent to induce cells aggregation. Obuekwe et al. (2009) and Qiao et al. (2012) reported that bacteria have hydrophobic surface when the cell clumping appeared at the lowest molarity of the salt concentration. Referring to Table 4.4 *S. aureus* ATCC 6838 was observed to have hydrophobic surface because the cell aggregation occurred at low salt concentration with the SAT value is 0.1 for living cells and 0.9 for old cells. Meanwhile *E. coli* ATCC 8739 (live and old cells) did not aggregate even at a very high salt concentration (3.2 M) which indicates that it has a highly hydrophilic surface. Study from Ljungh et al. (1985) also identified that *S. aureus* as an auto aggregating strain when 135 of *S. aureus* strain tested, 123 strains showed cell clumping at low salt concentration with the SAT value  $\leq 0.1$ . The existence of protein A, fibronectin-binding surface protein and lipoteichoic acid (LTA) which mostly found at *S. aureus* ATCC 6838 surface are the main components that contribute to the auto aggregating process and surface hydrophobicity of the bacteria cell (Jonsson & Wadstrom, 1984; Ljungh et al., 1985).

#### 4.3.4 Bacterial Surface Charge

Adhesion of bacteria onto a surface is influenced by many physicochemical interactions and one of them is electrostatic interaction which mediated to surface charge. According to Carlsson (2012) surface charge plays an important role in the interaction of bacteria with ions, particles, and surfaces (Wilson et al., 2001) for optimal cell function. The ionizations of bacteria proton-active functional group such as carboxyl, amino, phosphate and hydroxyl groups at the cell surface and also the adsorption of ions from the surrounding solution contributed to the bacteria surface charge (Poortinga et al., 2002). The surface charge of *E. coli* ATCC 8739 and *S. aureus* ATCC 8638 in this study was analyzed based on zeta potential value (Wilson et al., 2001) measured by zeta potential analyzer machine at pH of 4, 7.4 and 9 and the results showed that both bacteria have a negative surface charge. The results supported by Han et al. (2016) and Halder et al. (2015) which also stated that most bacteria possess a net negative surface charge. Table 4.4 depicted the value of zeta potential of both bacteria was in a similar trend but it can be seen that *E. coli* ATCC 8739 has highly negative surface charge than *S. aureus* ATCC 6838 at all pH value. Previous findings (Arakha et al., 2015; Halder et al., 2015) also found the similar results where *E. coli* has higher negative potential than *S. aureus*. The existence of additional layer of negatively charged lipopolysaccharides (LPS) on *E. coli* ATCC 8739 has ascribed a higher negative charge compare to *S. aureus* ATCC 6838 (Halder et al., 2015). The highest negative zeta potential of *E. coli* ATCC 8739 and *S. aureus* ATCC 6838 were registered at pH 4 and pH 9 with recorded reading was  $-41.27 \pm 0.54$  mV and  $-45.63 \pm 1.08$  mV for *E. coli* ATCC 8736 and  $-26.77 \pm 0.49$  mV and  $-28.40 \pm 0.65$  mV for *S. aureus* ATCC 6838, respectively. While at more neutral environment (pH 7.4), both live and old cells surfaces have weaker negative charge with approximately similar zeta potential which is  $-24.78 \pm 0.26$  mV and  $-25.16 \pm 0.30$  mV for *E. coli* ATCC 8739 and  $-13.11 \pm 0.21$  mV and  $-17.20 \pm 0.27$  mV for *S. aureus* ATCC 6838, respectively. The increase of the negative surface charge at pH 4 and pH 9 are attributed to the deprotonation of the surface functional group at the bacterial cell wall (Dziubakiewicz et al., 2013).

In term of colloid system, Carlsson (2012) indicated that, bacteria with zeta potential more positive than +30 mV or more negative than -30 mV is considered to be in a stable condition and tend to repel or avoiding each other while, it will become

unstable if the zeta potential is between the range of -30 mV and +30 mV. As shown in the Table 4.4 the zeta potentials of *S. aureus* ATCC 6838 at all pH (4, 7.4, 9) were less than -30 mV, indicating the unstable condition where the *S. aureus* ATCC 8739 cells might tend to attract each other and flocculate and possibly can form biofilm easily compare to *E. coli* ATCC 8739.

Table 4.4 All characterizations of *E. coli* ATCC 8739 and *S. aureus* ATCC 6838

Bacterial Characteristics	<i>E. coli</i> ATCC 8739	<i>S. aureus</i> ATCC 6838
Gram Types	Negative	Positive
Shape	Rod	Spherical/cocci
Cell Size (µm)	0.98 - 2.24 (Length) 0.19 - 0.75 (Width)	0.41 - 0.72
Hydrophobicity		
1) BATH (%)		
Live Cells		
- Hexane	4.42 ± 0.86	92.57 ± 1.20
- Hexadecane	11.90 ± 4.75	75.18 ± 7.41
- Xylene	23.43 ± 0.87	88.78 ± 1.51
Old Cells		
- Hexane	30.49 ± 1.44	83.88 ± 1.81
- Hexadecane	12.48 ± 0.91	77.70 ± 3.93
- Xylene	40.77 ± 0.80	88.36 ± 1.90
2) SAT	> 1.6	0.1
SAT (Old cells)	> 1.6	≥ 0.9
Zeta Potential (mV)		
- pH 4	-41.27 ± 0.54	-26.77 ± 0.49
- pH 7.4	-24.78 ± 0.26	-13.11 ± 0.21
- pH 7.4 (Old Cells)	-25.16 ± 0.30	-17.20 ± 0.27
- pH 9	-45.63 ± 1.08	-28.40 ± 0.65

\*Live cells: 10 hours of culture; Old cells: 36 hours of culture.

\*All data are represented as average taken from three replications with ±10% of standard error.

#### 4.4 Summary

All characterizations involving metals and bacterial surfaces have been studied. The results obtained indicates that, when compare to polish, grinding and millisecond laser surfaces, most of samples fabricated by the ultrafast laser have rougher surfaces with  $S_q$  between 190 nm – 720 nm for SS and 190 nm – 910 nm for TT when the laser power had increased from 0.04 W to 0.12 W. Correspondingly, only U1 samples had hydrophobic surface where most of the CAM value is more than 100° except at U1-0.04

while, P, G and MI samples each were reported to have hydrophilic and slightly hydrophobic surfaces. Besides that, based on the SEM images of surface morphologies of all fabricated surfaces, ultrafast laser treatment had generated features called LIPSS and nano-sized irregular grains. These special features were believed had become the main factors that influenced the surface roughness and CAM of the SS and TT surfaces.

Besides that, bacterial surface characterizations also have been investigated. *E. coli* ATCC 8739 was identified as Gram-negative bacteria with length between 0.984  $\mu\text{m}$  – 2.243  $\mu\text{m}$  and width 0.198  $\mu\text{m}$  – 0.753  $\mu\text{m}$  while *S. aureus* ATCC 6838 is a Gram-positive bacterium with size between 0.414  $\mu\text{m}$  – 0.727  $\mu\text{m}$ . The surface hydrophobicity test of both bacterial had identified that *E. coli* ATCC 8739 has hydrophilic surface while *S. aureus* ATCC 6838 has hydrophobic surface. The selection of the hydrophilic and hydrophobic bacteria was evaluated to conclude the effect of hydrophobic-hydrophobic/hydrophilic-hydrophilic interaction as one of the contributing factors for increased or decreased bacteria surface interaction. Furthermore, both bacteria also were observed to have negative surface charge where *E. coli* ATCC 8739 has highly negative surface charge than *S. aureus* ATCC 6838 at all pH value (4, 7.4, 9). All these results in this chapter have been further evaluated on its effect towards mitigation of bacterial adhesion.

اونيور سيني مليسيا قهغ

UNIVERSITI MALAYSIA PAHANG

## CHAPTER 5

### ASSESSMENT OF BACTERIAL ADHESION

#### 5.1 Introduction

The fabricated surfaces were tested with the bacterial adhesion tests for 4 hours and the number of bacterial adhere per centimeter square (cm<sup>2</sup>) viewed under the fluorescence microscope were calculated using the Image J software. Prior to viewing process, the samples were stained by SYTO9 dye which diffuses into the cells (both live and dead cells) and fluoresces upon binding nucleic acids in green fluorescence (Sheng et al., 2007). Figure 5.1 illustrates the example images of stained bacteria adhered on metal surface after 4 hours of adhesion under the fluorescence microscope.

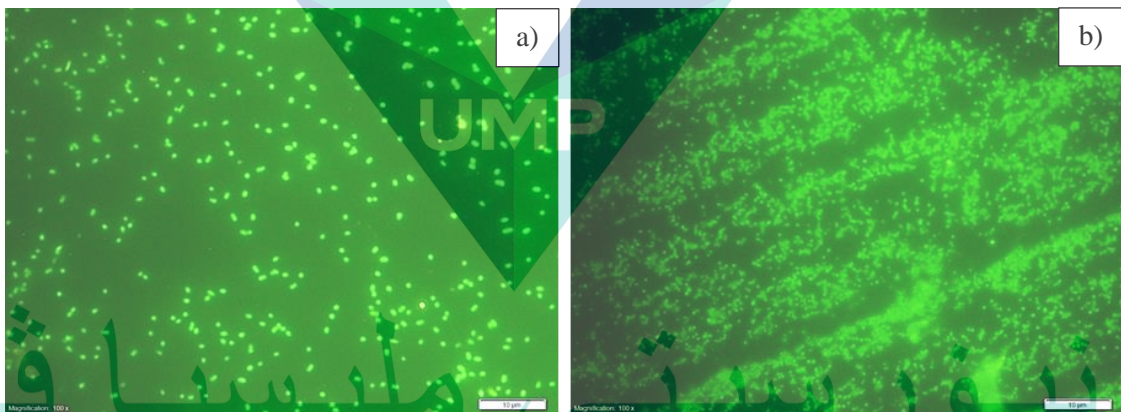


Figure 5.1 Fluorescence image of a) *E. coli* ATCC 8739 and b) *S. aureus* ATCC 6838 on UI-SS-0.11 after 4 hours of adhesion at 100x magnification

Many factors had contributed to the bacterial adhesion on the surfaces and this study was aligned to focus on certain elements related to the bacterial properties, surface properties and environmental factors. The properties of bacteria and surfaces have been discussed in the previous chapter while the details discussion about the effect of surrounding (environment) and surface fabrication on the *E. coli* ATCC 8739 and *S. aureus* ATCC 6838 adhesion will be explained in this chapter. The first subtopic described how pH and salt concentration (salinity) can influence the adhesion on the polished (controlled) surfaces of stainless steel AISI 316L and Grade 5 titanium alloys.



Next, is the discussion about the effect of grinding, millisecond laser and ultrafast laser fabrication towards the number of bacterial adhesions on both metals. Lastly, is the overall summarization about the correlation between the surface properties with respect to adhesion rate and a conclusive remark was made regarding the type of surface finishing (properties) that has the ability to prevent the initial adhesion of the bacteria on both stainless steel and titanium.

## 5.2 Effect of Environmental Condition (pH and salt concentration) on the Bacterial Adhesion

### 5.2.1 Bacterial Adhesion on Stainless Steel

Adhesion of *E. coli* ATCC 8739 and *S. aureus* ATCC 6838 on P-SS surface was investigated at different pH of bacterial suspension which are 4, 5, 6, 7.4 and 9 and the number of bacterial counts per centimeter square ( $\text{cm}^2$ ) was shown in Figure 5.2. The number of bacteria adhered on P-SS for both bacteria decreased with increasing pH value. A much lower adhesion for both *E. coli* ATCC 8739 and *S. aureus* ATCC 6838 were observed at pH 7.4 with bacterial count of  $14.50 \times 10^5/\text{cm}^2$  and  $158.95 \times 10^5/\text{cm}^2$ , respectively (Figure 5.2). On the other hand, bacterial adhesion is high at pH 4 and pH 9 with the bacterial counts of  $34.72 \times 10^5/\text{cm}^2$  and  $23.35 \times 10^5/\text{cm}^2$  for *E. coli* ATCC 8739 while  $282.41 \times 10^5/\text{cm}^2$  and  $171.89 \times 10^5/\text{cm}^2$  for *S. aureus* ATCC 6838, respectively. Similar trend also was found in Sheng et al. (2008) study where less bacteria adhesion on stainless steel AISI 316L at pH 7 and more adhesion at pH 3 and 9. Referring to the results of surface charge in chapter 4, at pH 7.4 both *E. coli* ATCC 8739 and *S. aureus* ATCC 6838 have low surface charge (*E. coli*:  $-24.78 \text{ mV} \pm 0.26$ ; *S. aureus*:  $-13.11 \text{ mV} \pm 0.21$ ) and higher surface charge at both pH 4 (*E. coli*:  $-41.27 \text{ mV} \pm 0.54$ ; *S. aureus*:  $-26.77 \text{ mV} \pm 0.49$ ) and pH 9 (*E. coli*:  $-45.63 \text{ mV} \pm 1.08$ ; *S. aureus*:  $-28.40 \text{ mV} \pm 0.65$ ). According to Sheng et al. (2008) SS has positively charged surface therefore, the high adhesion of both bacteria at pH 4 and 9 are presumably due to the strong electrostatic attraction force between the SS surface and the bacteria. On the other hand, it is reported that bacteria with strong negative charged surface were highly attracted to positively charged surface (Oh et al., 2018). However, in this study it showed the opposite result where the adhesion of *E. coli* ATCC 8739 (strong negative charge) on P-SS can be seen less than *S. aureus* ATCC 6838. Based on Gottenbos et al. (2002), this situation happened

because of the strong binding through electrostatic attraction force impeded the elongation of *E. coli* ATCC 8736 which necessary for cell division, resulting in low reading of adhered bacteria when comparing to *S. aureus* ATCC 6838 (up to ~7-fold of differences) in all metal tested. Meanwhile, Gram positive bacteria which is *S. aureus* ATCC 6838 is less affected to the electrostatic forces due to the structure of the thicker cell wall and rigid peptidoglycan (Pajerski et al., 2019).

Different of salt concentration or sodium chloride (NaCl) was used to study the effect of ionic strength towards the bacterial adhesion (Busalmen & Sanchez, 2001). Figure 5.3 depicted the adhesion of *E. coli* ATCC 8739 and *S. aureus* ATCC 6838 on P-SS at various salt concentrations, ranging from 0.001 mol/L to 0.2 mol/L. As implant-associated infection is always related with the bacterial adhesion (Wang & Tang, 2019), 0.135 mol/L of NaCl which is a normal salt concentration in human body was specifically chosen for studying the influence of ionic strength on the bacterial adhesion in the human body. High adhesion of *E. coli* ATCC 8739 was observed on P-SS at 0.2 mol/L of salt concentration (highest concentration) compare to low salt concentration (0.001 mol/L) with the number of bacterial counts are  $50.88 \times 10^5/\text{cm}^2$  and  $2.87 \times 10^5/\text{cm}^2$ , respectively (Figure 2.3). Similar trend was also reported by Subramani and Hoek (2008). Habimana et al. (2014) indicated that, solution with high ionic strength tend to enhance the adhesion of bacteria due to the reduction of bacterial electrical double layer (EDL). EDL (Figure 5.4) is an ionic layer formed by the bacterial surface charge and its counter ions, forming an ionic cloud surrounding the bacteria (Tadros, 2013). The NaCl ions in the solution resulted in charge neutralization thus, reduced the thickness EDL and the bacteria became less negative charge (Chen & Walker, 2007). Subsequently, promoted the adhesion because the electrostatic forces and adhesion barrier between P-SS and bacteria become weaker. Furthermore, Zulfakar et al. (2013) also informed that the presence of high NaCl ions in a solution affects the electrostatic interaction between the surface and the bacterial by shielding the charged surface material. This enables the negatively charged bacterium to move closer to the target surface, thus increasing the opportunities to initiate adhesion through the action of attractive van der Waals forces or via specific surface receptors (adhesin).

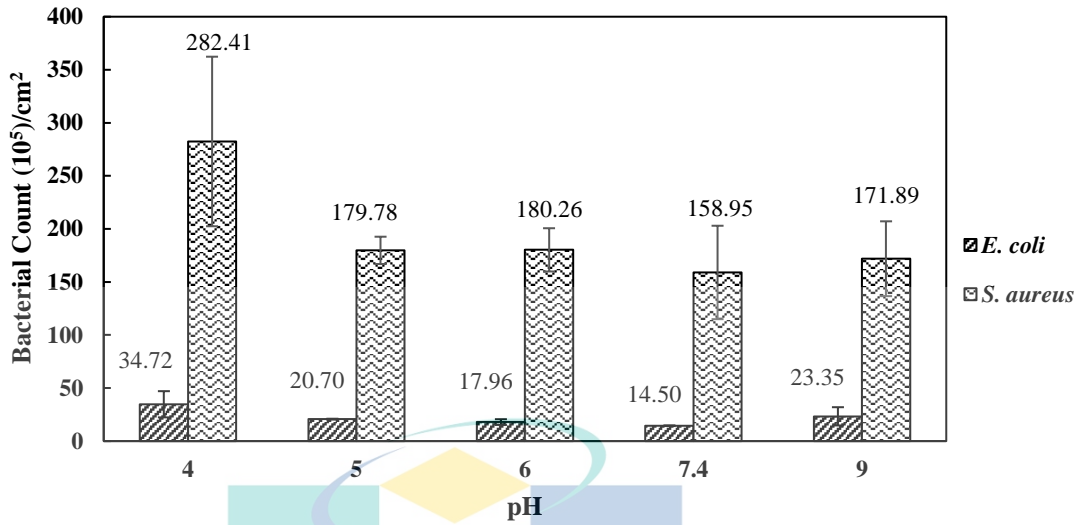


Figure 5.2 Effect of pH on the adhesion of *E. coli* ATCC 8739 and *S. aureus* ATCC 6838 on P-SS in the PBS solution with shaking 70 rpm for 4 hours

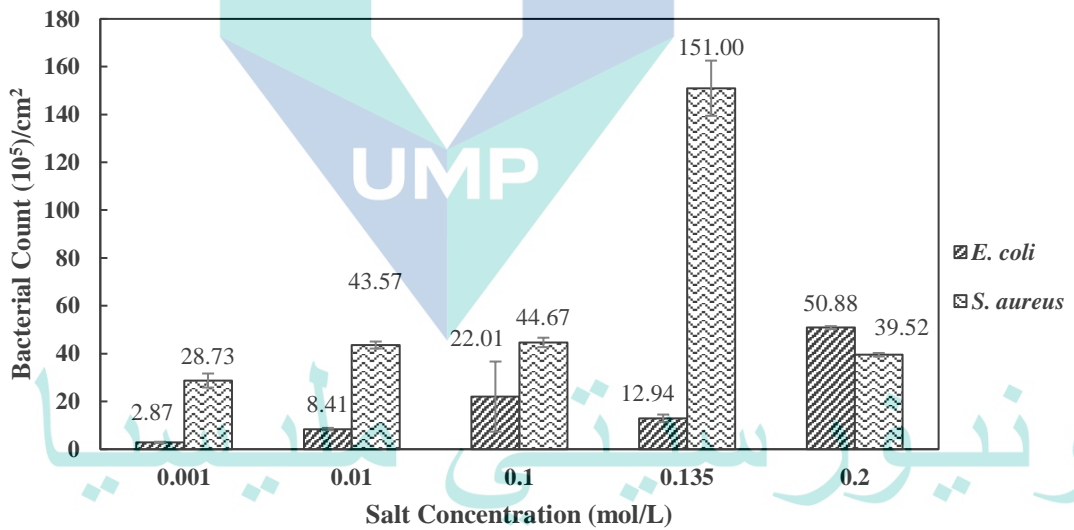


Figure 5.3 Effect of salt concentration (mol/L) on the adhesion of *E. coli* ATCC 8739 and *S. aureus* ATCC 6838 on P-SS in the PBS solution with shaking 70 rpm for 4 hours

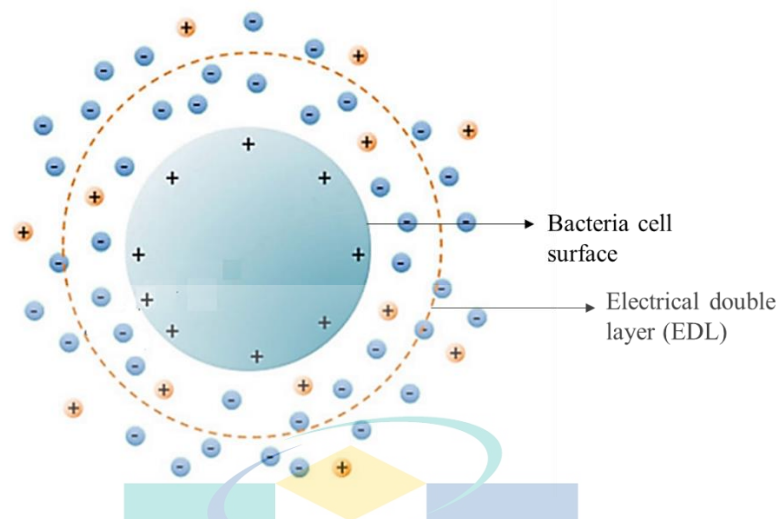


Figure 5.4 Diagram of electrical double layer (EDL) around positively charged bacteria (depends on the bacterial strain)

Source: Tadros (2013)

### 5.2.2 Bacterial Adhesion Titanium

Number of bacteria adhere on P-TT which regards to the effect of pH showed the similar results as on P-SS where the number of bacterial adhered was decreased when the pH increases from 4 to 9. The adhered bacteria at Figure 5.5 were reduced from  $31.11 \times 10^5/\text{cm}^2$  to  $15.80 \times 10^5/\text{cm}^2$  for *E. coli* ATCC 8739 and from  $334.58 \times 10^5/\text{cm}^2$  to  $102.58 \times 10^5/\text{cm}^2$  for *S. aureus* ATCC 6838. Sheng et al. (2008) displayed a similar reduction and indicated that the change in the number of bacterial adhesions measured as function of pH is possibly due to the change in ionization state of bacterial cell surface (cell wall) functional group such as carboxyl group, amino group and hydroxyl group (Liu et al., 2017). Generally, when pH increases the ionization of the carboxylate group at the cell surface become strong thus, the presence of negatively charged carboxylate ion ( $\text{COO}^-$ ) will increase the electrostatic forces in the solution (Sheng et al., 2008). Titanium was found to have slightly negative surface charge (Qiao et al., 2012). Therefore, as pH increase the number of both bacterial adhered on P-TT are less due to the electrostatic repulsion forces existed between the negatively charge bacteria (refer Table 4.4) and the P-TT surface.

A similar response as on P-SS was observed for the effect of salt concentration on the adhesion on P-TT (Figure 5.6). An intense adhesion of *E. coli* ATCC 8739 was recorded at 0.2 mol/L salt concentration ( $17.69 \times 10^5/\text{cm}^2$ ) compared to 0.001 mol/L ( $6.68$

$\times 10^5/\text{cm}^2$ ). Meanwhile, *S. aureus* ATCC 6838 showed higher adhesion at 0.135 mol/L salt concentration ( $223.77 \times 10^5/\text{cm}^2$ ) than at 0.001 mol/L ( $19.45 \times 10^5/\text{cm}^2$ ). As explained before bacterial will adhere more in the solution with high ionic strength however, *S. aureus* ATCC 6838 experienced a slight reduction of adhesion at 0.2 mol/L (high ionic strength) on both P-TT and P-SS (Figure 5.3). Some studies said that, different types of bacteria might show different results (Habimana et al., 2014; Hoogmoed et al., 1997) and for this case Busalmen and Sanchez (2001) expressed that, bacterial adhesion at ionic strength higher than 0.1 mol/L cannot be explained by EDL and others mechanisms also must be taking into account.

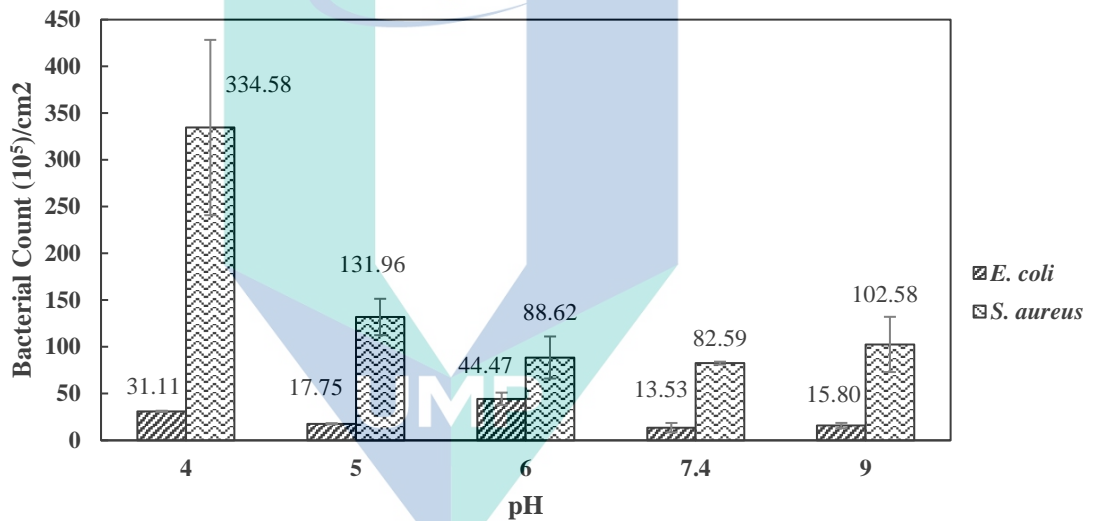


Figure 5.5 Effect of pH on the adhesion of *E. coli* ATCC 8739 and *S. aureus* ATCC 6838 on P-TT in the PBS solution with shaking 70 rpm for 4 hours

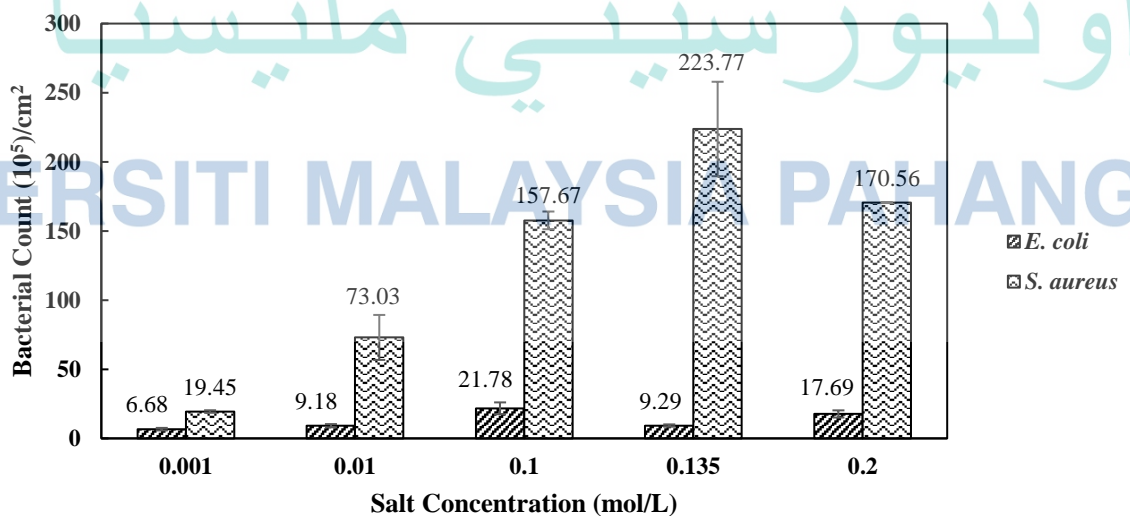


Figure 5.6 Effect of salt concentration (mol/L) on the adhesion of *E. coli* ATCC 8739 and *S. aureus* ATCC 6838 on P-TT in the PBS solution with shaking 70 rpm for 4 hours

### 5.2.3 Comparative Assessment of Bacterial Adhesion on Stainless Steel and Titanium

Changes of pH and ionic strength in a solution does affected the number of *E. coli* ATCC 8739 and *S. aureus* ATCC 6838 adhesion on P-TT and P-SS surfaces. In term of pH, the bacterial adhesion on P-SS and P-TT decrease when the pH in the solution increase and a slight increase at pH 9 due to the strong negatively charge on both bacterial surfaces. Generally, the ionization of carboxylate group occurs in all solutions which experienced the increasing of pH where the producing of more negatively charge ion ( $\text{COO}^-$ ) increases the electrostatic force in the solution. Therefore, at P-TT (negatively charged) high electrostatic repulsion force occurs between the surface and the bacterial thus, reducing the adhesion when pH increase. Meanwhile, as P-SS is a positively charged surface, a strong attractive force existed between the surface and the negatively charged bacteria, thereby enhance the adhesion but, it still showed the same trend like P-TT when the pH increased. It has been pointed out before, bacterial adhesion process is governed by many factors and presumably bacterial hydrophobicity may also affected the adhesion. As stated by Katsikogianni and Missirlis (2004), changes of pH in a solution will also influence the hydrophobicity of a bacterium. In general, when pH increased from pH 4 to pH 9, the reduction of *E. coli* ATCC 8739 and *S. aureus* ATCC 6838 at P-SS is about 58% and 44% while on P-TT is about 57% and 75%, respectively.

Besides that, the difference of salt concentration had affected the ionic strength in a solution whereas the change of ionic strength had influenced the EDL of bacteria. Based on the previous discussion, when the ionic strength increases the bacterial adhesion also increase due to the neutralization of charge and reduction of EDL. A similar trend for both bacteria and metal surfaces were observed. In conclusion, increase of NaCl from 0.001 mol/L to 0.2 mol/L had increased the adhesion of *E. coli* ATCC 8739 and *S. aureus* 6838 on P-SS about 10-fold and 4-fold while on P-TT about 1-fold and 10-fold, respectively. Next subtopic is the main study of this research where the effect of surface fabrication on the bacterial adhesion has been investigated. The pH and the salt concentration were already fixed to pH 7.4 and 0.0137 mol/L (Table 3.3), respectively.

## 5.3 Effect of Surface Fabrication on the Bacterial Adhesion

### 5.3.1 Bacterial Adhesion on Stainless Steel

#### a) Grinding

Grinding is the fabrication process using SiC abrasive paper with five different types of grit size which are 180 (courser), 600, 800, 1200 and 1500 (finer) followed by the adhesion test for four hours. Current study showed that the used of grit number from 180 to 1500 during grinding process increased the hydrophobicity of the G-SS surfaces from hydrophilic to slightly hydrophobic (CAM: 79.20° – 96.10°), while reducing its  $S_q$  (269.48 nm – 175.15 nm) and  $S_a$  (207.14 nm – 132.89 nm) (Figure 5.7). A reduction between 76% - 90% was observed for *S. aureus* ATCC 6838 with highest reduction over control surface P-SS ( $158.95 \times 10^5/\text{mm}^2$ ) was obtained with G-SS-1500 ( $15.17 \times 10^5/\text{cm}^2$ ). Referring to Table 5.1, increasing the grit scale in grinding produced surfaces with lower surface roughness ( $S_q$ ,  $S_a$ ). Generally, it has been reported that surface with high surface roughness promote bacterial adhesion for example Bohinc et al. (2016) showed the highest attachment of *E. coli* on grinded surface with  $S_q$  about 990 nm. This also supported by Truong et al. (2010) which also found that surface irregularities enhanced the initial adhesion of bacteria due to the presence of scratches, pits and grooves thus, increases the surface area. A parallel reduction of  $S_{dr}$  (% of additional surface area) was observed with the decreasing of  $S_q$  and  $S_a$  (Table 5.1). Consequently, adhesion of *S. aureus* ATCC 6838 on G-SS was reduced by 76% - 90% from  $31.02 \times 10^5/\text{cm}^2$  to  $15.17 \times 10^5/\text{cm}^2$  as the  $S_q$  decrease from 269.48 nm to 175.15 nm. Lesser bacterial colonization has been reported after post treatment where the surfaces are having less scratches or pits (Yoda et al., 2014). It is best to note that the hydrophobicity of the surface was increased with increased grit number, but the adhesion preference towards contact angle does not show any significant patterns. It can be concluded that the effect of reducing the roughness (additional binding point) might has surpassing the effect of hydrophobic-hydrophobic interaction (Katsikogianni & Missirlis, 2004).

Interestingly, *E. coli* ATCC 8739 showed the opposite results where the number of *E. coli* ATCC 8739 adhered on G-SS (G-600 until G-1500) is higher than on P-SS with the highest attachment was on G-800 ( $29.79 \times 10^5/\text{cm}^2$ ) with 1-fold of increment (Figure 5.7). *E. coli* ATCC 8739 is a hydrophilic bacterium while *S. aureus* ATCC 6838 is a

hydrophobic bacterium. Increased number of adhesion was observed with in agreement with general rule stated that hydrophobic bacteria will adhere on hydrophobic surfaces and vice versa (Katsikogianni & Missirlis, 2004). Therefore, at G-180 until G-800, *E. coli* ATCC 8739 (hydrophilic) do not show any reduction of adhesion even when  $S_q$  and  $S_a$  decrease possibly because it has high affinity towards hydrophilic surface (Table 5.1) thus, produce a stronger attachment with the surfaces compared to *S. aureus* ATCC 6838. Thereby, it was expected that *E. coli* ATCC 8739 secured a stronger adhesion towards this grinded samples compares to *S. aureus* ATCC 6838, where attraction towards the similar surface affinities wash out the effect of the reduction of surface area due to removal of scratches, pitches and peaks. This is in line with study from De-la-Pinta et al. (2019) which also found high adhesion of *E. coli* on hydrophilic surface and highlighted that, certain *E. coli* is prone to adhere on hydrophilic surface regardless of whatever magnitude of surface roughness. However, the number of *E. coli* ATCC 8739 started to decrease as hydrophilic surfaces of G-SS had turned to slightly hydrophobic at G-1200 and G-1500 (Table 5.1). Hydrophilic *E. coli* ATCC 8739 showed a slight repulsion when the surface is slightly hydrophobic. Therefore, at this state it can be described that *E. coli* ATCC 8739 is a hydrophobicity-dependence bacterium.

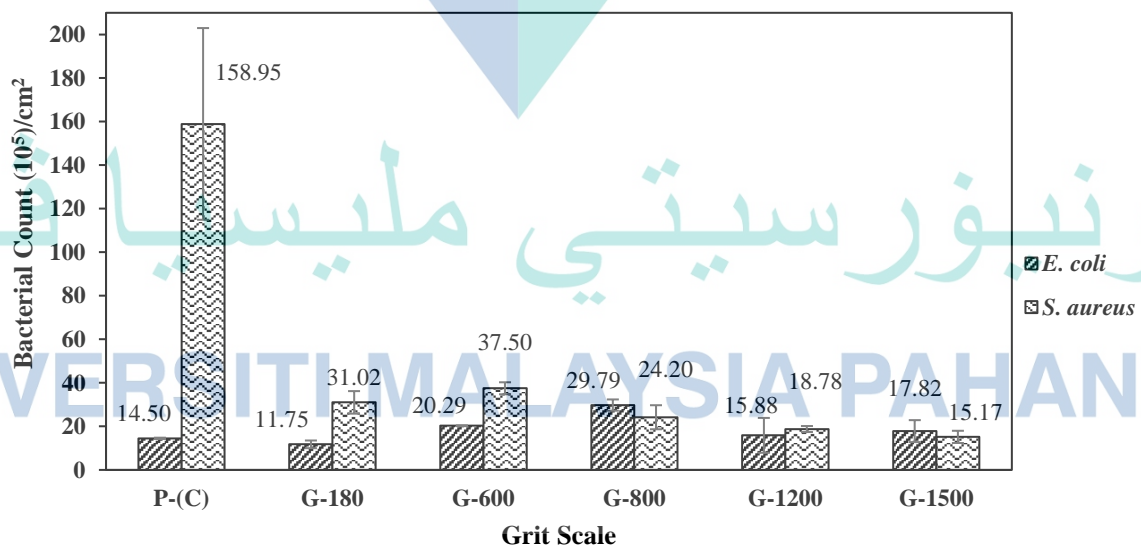


Figure 5.7 Number of *E. coli* ATCC 8739 and *S. aureus* ATCC 6838 adhesion on G-SS surface at different types of grit size after 4 hours of adhesion in the PBS solution with 70 rpm of shaking (pH 7.4 and 0.0137 mol/L of NaCl)



Table 5.1 Data of bacterial adhesion on G-SS and surface parameters

Samples	CAM (°)	Condition	S <sub>q</sub> (nm)	S <sub>a</sub> (nm)	S <sub>dr</sub> (%)	<i>E. coli</i> (10 <sup>5</sup> /cm <sup>2</sup> )	<i>S. aureus</i> (10 <sup>5</sup> /cm <sup>2</sup> )
P-(C)	83.00	Hydrophilic	97.26	68.41	0.08	14.50	158.95
G-180	79.20	Hydrophilic	269.48	207.14	0.49	11.75	31.02
G-600	84.30	Hydrophilic	265.72	207.42	0.28	20.29	37.50
G-800	89.10	Hydrophilic	212.55	163.15	0.36	29.79	24.20
G-1200	92.30	S. hydrophobic	176.60	131.97	0.31	15.88	18.78
G-1500	96.10	S. hydrophobic	175.15	132.89	0.31	17.82	15.17

\*All data are represented as average taken from three replications with ±10% of standard error.

\*S. hydrophobic stands for slightly hydrophobic.

#### b) Millisecond Laser

Five different power (4.2 W, 5.1 W, 6.0 W, 7.0 W, 7.8 W) were used in surface fabrication of MI-SS using millisecond laser machine. Figure 5.8 demonstrated that, MI surfaces had promoted the *E. coli* ATCC 8739 adhesion on MI-SS with 2-7-folds of increment compare to P-SS. Meanwhile, *S. aureus* ATCC 6838 also showed about 27% - 37% of increment at MI-SS-6.0, MI-SS-7.0 and MI-SS-7.8 except at MI-SS-4.2 and MI-SS-5.1 which had a slight reduction of bacteria around 8% -38% when compared to P-SS. Data in Table 5.2 shows that the increasing power in MI treatments also had increased the roughness of the surfaces from 98.34 nm to 358.8 nm for S<sub>q</sub> and from 67.58 nm to 256.28 nm for S<sub>a</sub>. Therefore, compare to *E. coli* ATCC 8736, the adhesion of *S. aureus* ATCC 6838 on MI-SS still affected by the surface roughness, where the number of bacterial counts increased parallelly to the increment of S<sub>q</sub> and S<sub>a</sub>. Other studies that showed similar trends are Yoda et al. (2014) and Stadnyk et al. (2019) which showed high adhesion of *S. epidermis* on rougher surface (S<sub>q</sub> = 7.2 nm) of stainless steel AISI 316L and also high *S. aureus* adhesion on stainless steel 800 nm of S<sub>q</sub> than at 400 nm, respectively. This condition all due to the increasing of surface area that might give a chance to bacteria to retain on the surface. Nevertheless, at MI-SS-7.8, the adhesion of *S. aureus* ATCC 6838 (216.68 x 10<sup>5</sup>/cm<sup>2</sup>) observed was almost similar to MI-7.0 even though the S<sub>q</sub> and S<sub>a</sub> are the highest. It is presumably due to sudden change of surface properties from slightly hydrophobic (CAM: 94°) to hydrophilic (CAM: 88.80°) which led to a slight reduction of *S. aureus* ATCC 6838 (0.4%). Nevertheless, the reduction of *S. aureus* ATCC 6838 caused by CAM is comparatively are very low. Thus, it can be concluded that at MI-SS, *S. aureus* ATCC 6838 was significantly affected by the S<sub>q</sub> and S<sub>a</sub>, which showed similarity towards the grinding process.

The adhesion of *E. coli* ATCC 8739 on MI surfaces were still failed to show any significant improvement over the P surfaces (Figure 5.8). In MI treatments, the roughness of the surfaces was increased from 98.34 nm to 358.57 nm for  $S_q$  and from 67.58 nm to 256.28 nm for  $S_a$  (controlled adequately without surpassing the bacterial size) but still not able to prevent the adhesion. CAM can be said still influenced the adhesion of *E. coli* ATCC 8739 on ML-SS because the retaining bacterial on the surfaces from MI-4.2 to MI-7.8 were consistence with the CAM rules, as Katsikogianni and Missirlis (2004) said hydrophilic bacteria will be attracted more to hydrophilic surface. However, it is observed that there is high reduction of *E. coli* ATCC 8739 which is about 38% from MI-5.1 to MI-6.0. It is examined that, beside of CAM changes (hydrophilic to slightly hydrophobic surface) there is another factor that influenced the reduction. Hence, to obtain a deeper observation other surface parameter like  $S_{sk}$ ,  $S_{ku}$ ,  $S_{dr}$  and  $S_{ds}$  were used to relate between the surface characteristics and the bacterial adhesion (Chan et al., 2017). Based on Table 5.2,  $S_{ku}$  observed at MI-6.0 is extremely high ( $S_{ku}$ : 50.15) which indicates that it has a spiky surface (can also be referred at Table 4.1). Pogodin et al. (2013) informed that spikier surfaces tend to reduce bacterial as it can pierce the cell membrane, leading to cell rupture and lysis. Therefore, it showed that *E. coli* ATCC 8739 is affected by these features as it is Gram negative bacteria with thin membrane layer (*S. aureus* ATCC 6838 is Gram positive with thicker membrane cell) which are very fragile to bruise. Study from Valquier-Flynn et al. (2017) and Ahmad et al. (2017) also reported that, a slightly larger value of  $S_{ku}$  reduced the bacterial adhesion and this is in line with the observation at MI-SS-5.1 and MI-SS-6.0.

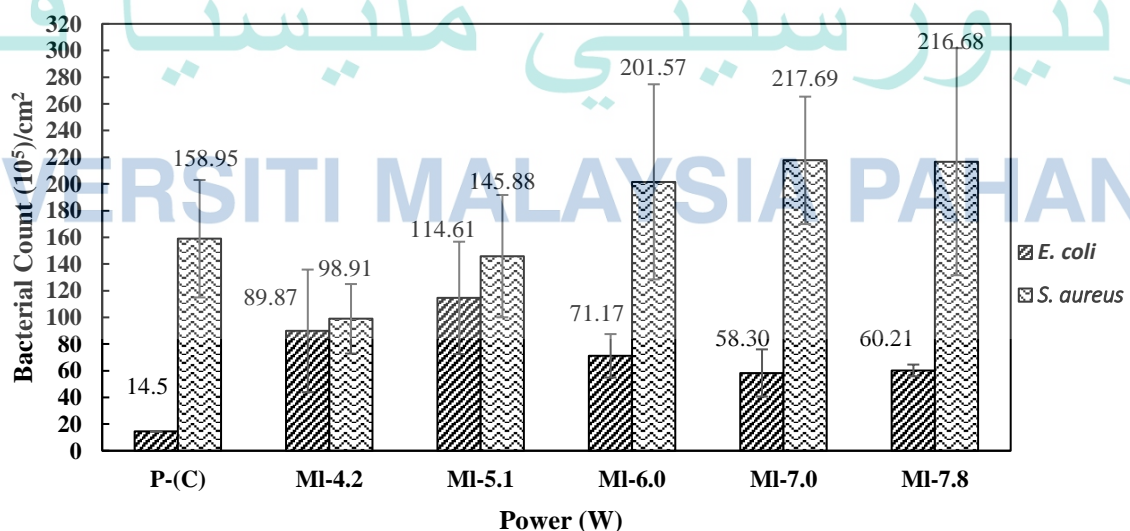


Figure 5.8 Number of *E. coli* ATCC 8739 and *S. aureus* ATCC 6838 adhesion on MI-SS surface at different types of power after 4 hours of adhesion in the PBS solution with 70 rpm of shaking (pH 7.4 and 0.0137 mol/L of NaCl)

Table 5.2 Data of bacterial adhesion on MI-SS and surface parameters

Samples	CAM (°)	Condition	S <sub>q</sub> (nm)	S <sub>a</sub> (nm)	S <sub>sk</sub>	S <sub>ku</sub>	<i>E. coli</i> (10 <sup>5</sup> /cm <sup>2</sup> )	<i>S. aureus</i> (10 <sup>5</sup> /cm <sup>2</sup> )
P-(C)	83.00	Hydrophilic	97.26	68.41	0.85	7.61	14.50	158.95
MI-4.2	83.20	Hydrophilic	98.34	67.58	0.65	17.07	89.87	98.91
MI-5.1	85.50	Hydrophilic	99.47	70.76	0.52	25.73	114.61	145.88
MI-6.0	90.70	S. hydrophobic	115.64	73.20	-1.52	50.15	71.17	201.57
MI-7.0	94.00	S. hydrophobic	207.17	139.80	-0.28	23.63	58.30	217.69
MI-7.8	88.80	Hydrophilic	358.57	256.28	-0.29	3.97	60.21	216.68

\*All data are represented as average taken from three replications with ±10% of standard error.

\*S. hydrophobic stands for slightly hydrophobic.

### c) Ultrafast Laser

Stainless steel surfaces fabricated with ultrafast laser machine also had been tested with different power which are 0.04 W, 0.10 W, 0.11 W and 0.12 W, produced a hydrophobic surface (89.40° - 145.70°) with S<sub>q</sub> and S<sub>a</sub> ranged from 190 nm – 720 nm and 140 nm – 650 nm, respectively. The difference between MI and UI treatment is the ability of the proposed method to produce nanoparticles on its surface, which is expected to be beneficial to reduce bacteria adhesion. This study found out that, the UI surfaces had been able to repel adhesion with number of adhered bacteria (both *E. coli* ATCC 8739 and *S. aureus* ATCC 6838) were much lower than on P-SS surface. Based on Figure 5.9, *E. coli* ATCC 8739 adhesion was reduced by 65% - 98% over P-SS surface with UI-0.10 observed to be the best surfaces that prevented the adhesion. Meanwhile, only UI-0.12 promoted a slightly increase of *E. coli* ATCC 8739 when compared to P-SS, with bacterial count 18.25 x 10<sup>5</sup>/cm<sup>2</sup>. Lowest *S. aureus* ATCC 6838 adhesion was also achieved with UI-0.10, reduced by 78% when compared to P-SS. Meanwhile other surfaces like UI-0.04, UI-0.11 and UI-0.12 also had reduction of *S. aureus* ATCC 6838 adhesion around 19% - 60%. This is in agreement with study from Chen et al. (2020) which showed an obvious decrease of *E. coli* (98%) and *S. aureus* (75%) adhesion on glass treated by femtosecond laser compared to flat surfaces. Study from Schwibbert et al. (2019) also achieved a reduction of *E. coli* (only 12% of coverage) on femtosecond laser-modified polyethylene.

Referring to Table 4.2 (Chapter 4) and also Table 5.3, the increasing of ultrafast laser power had drastically increased the surface roughness of UI-SS from 190 nm to 720 nm and from 140 nm to 650 nm for  $S_q$  and  $S_a$ , respectively. Although the roughness of the surfaces was increased with increased laser power, the additional surface area imparts by the presence of the additional LIPSS does not support the adhesion. Surprisingly, both bacterial adhesions especially *S. aureus* ATCC 6828 which previously observed was influenced by surface roughness ( $S_q$ ,  $S_a$ ) were reduced instead of bacterial proliferation especially at UI-0.10 which showed the highest depletion when compare to other surfaces like G-SS and MI-SS. Study from Du et al. (2020) also showed a reduction of *E. coli* (57%) and *S. aureus* (40%) on surface treated by femtosecond laser when  $S_q$  increased from 68 nm – 79 nm (polished surfaces) to 119 nm – 142 nm. Besides that, ultrafast laser texturing also had significantly produced SS with high hydrophobics surfaces, almost reaching the super-hydrophobic region ( $CAM > 150$ ) especially at UI-0.11 ( $CAM: 145.70^\circ$ ) (Jeevahan et al., 2018). Similar to previous findings at G-SS and MI-SS, *E. coli* ATCC 8739 which has hydrophilic character was greatly influenced by the CAM as it showed high repellence towards hydrophobic surface of UI-SS especially at UI-0.10. On the other hand, the adhesion of *S. aureus* ATCC 6838 was comparatively higher than *E. coli* ATCC 8739 on the same surfaces (Table 5.3 and Figure 5.8) with highest preference ( $128.65 \times 10^2/cm^2$ ) was obtained on the most hydrophobic surface (UI-0.11), but still 19% lower than the control surfaces. Preference on this surface might suggested a very strong hydrophobic-hydrophobic interaction between the bacteria and UI-0.11.

Furthermore, ultrafast laser surface texturing had affected the  $S_{ds}$  (summit density/peaks) parameters where the values are significantly increased from 16171.76/  $mm^2$  to 26945.58/  $mm^2$  which is about 4 times higher than G-SS and ML-SS surfaces. Referring to the SEM images in Figure 4.8, LIPSS and the additional of nano-sized irregular grains were produced during the ultrafast laser texturing and it is believed that the existing of both features contributed to the increasing of peaks ( $S_{ds}$ ) as well as roughness ( $S_q$  and  $S_a$ ). Therefore, the reduction of both bacterial on UI-SS was believed due to the dense peaks (LIPSS, nano-sized irregular grains) that reduced the contact area between the original SS surfaces and the bacterial then, inhibited the bacterial retention (Truong et al., 2010). The results also supported by Cunha et al. (2016) which also found that ultrafast laser texturing can inhibit the bacterial attachment due to the existing of special features like LIPSS on the substratum surfaces. Meanwhile UI-0.10 was reported

to have less bacterial colonization than other surfaces possibly because it has low  $S_{dr}$  (4.65%) which also referred as low percentage of additional surface area compared to other surfaces.

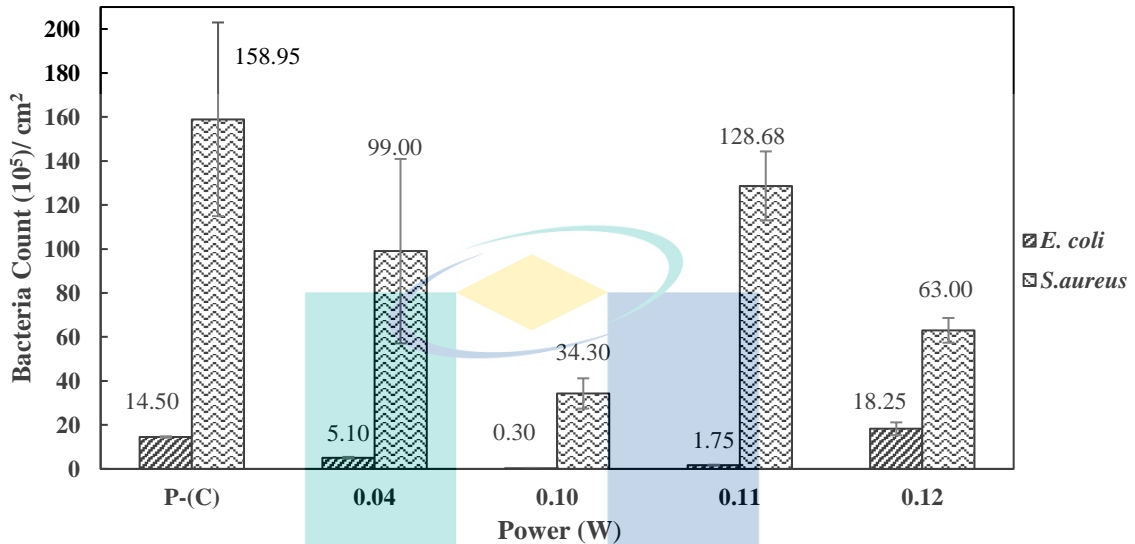


Figure 5.9 Number of *E. coli* ATCC 8739 and *S. aureus* ATCC 6838 adhesion on UI-SS surface at different types of power after 4 hours of adhesion in the PBS solution with 70 rpm shaking (pH 7.4 and 0.0137 mol/L of NaCl)

Table 5.3 Data of bacterial adhesion on UI-SS and surface parameters

Samples	CAM (°)	Condition	$S_q$ (nm)	$S_a$ (nm)	$S_{dr}$ (%)	$S_{ds}$ ( $1/mm^2$ )	<i>E. coli</i> ( $10^5/cm^2$ )	<i>S. aureus</i> ( $10^5/cm^2$ )
P-(C)	83.00	Hydrophilic	97.26	68.41	0.08	4230.62	14.50	158.95
UI-0.04	89.40	Hydrophilic	190.00	140.00	5.30	16171.76	5.10	99.00
UI-0.10	140.22	Hydrophobic	298.00	264.00	4.65	17039.43	0.30	34.30
UI-0.11	145.70	Hydrophobic	650.00	510.00	30.80	19868.05	1.75	128.68
UI-0.12	129.50	Hydrophobic	720.00	650.00	60.83	26945.58	18.25	63.00

\*All data are represented as average taken from three replications with  $\pm 10\%$  of standard error.

### 5.3.2 Bacterial Adhesion on Titanium

#### a) Grinding

The adhesion of *E. coli* ATCC 8739 on G-TT at different grit size of SiC paper (180, 600, 800, 1200, 1500) showed an increment about 5% to 1-fold when compare to P-TT and the highest adhesion was recorded at G-600 (1-fold) with bacterial count on the surface is  $29 \times 10^5/\text{cm}^2$  (Figure 5.8). Meanwhile, adhesion of *S. aureus* ATCC 6838 reduced by 58% to 84% when compare against P-TT, presumably contributed by lowering the surface roughness (Bohinc et al., 2016; Xing et al., 2015). Similar observation towards G-SS before, the adhesion of *E. coli* ATCC 8739 on G-TT failed to produce any significant trends with regards to effect of  $S_q$  and  $S_a$  ( $S_q$ : 365.01 nm – 204.10 nm,  $S_a$ : 287.69 nm – 157.15 nm). It is due to the strong hydrophilic-hydrophilic interaction between *E. coli* ATCC 8736 and G-TT which a hydrophilic surface thus, contributed to the increasing of *E. coli* ATCC 8739, surpassing the effect of reduced surface area for adhesion. However, a small reduction of *E. coli* ATCC8739 can be seen at G-1200 and G-1500 as the surfaces become slightly hydrophobic with 33% to 34% of reduction, thereby contributed to the surface repulsion between bacteria and TT surfaces, resulting in lower bacteria adhesion.

On the other hand, adhesion of *S. aureus* ATCC 6838 on G-TT reduced from  $42.44 \times 10^5/\text{cm}^2$  to  $13.37 \times 10^5/\text{cm}^2$  which can be considered due to the decreasing surface roughness from 365.01 nm to 204.10 nm for  $S_q$  and from 287.69 nm to 157.15 nm for  $S_a$  which also similar to G-SS. Therefore, it can be concluded that TT fabricated by grinding technique facilitates the adhesion of *E. coli* ATCC 8739 due to CAM changes and reduces *S. aureus* ATCC 6838 which caused by surface roughness ( $S_q$ ,  $S_a$ ).

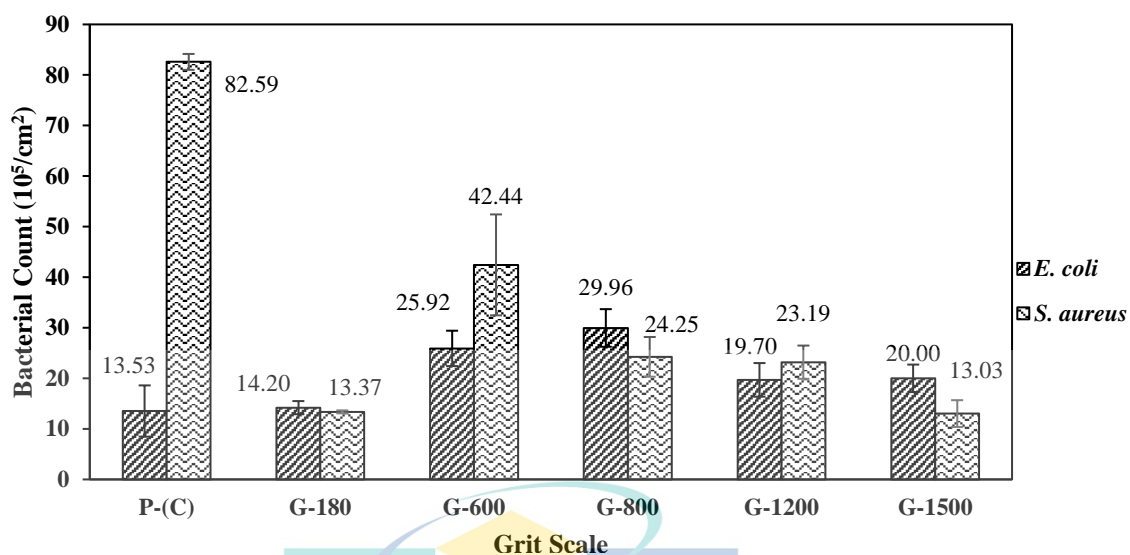


Figure 5.10 Number of *E. coli* ATCC 8739 and *S. aureus* ATCC 6838 adhesion on G-TT surface at different types of grit size after 4 hours of adhesion in the PBS solution with 70 rpm shaking (pH 7.4 and 0.0137 mol/L of NaCl)

Table 5.4 Data of bacterial adhesion on G-TT and surface parameters

Samples	CAM (°)	Condition	S <sub>q</sub> (nm)	S <sub>a</sub> (nm)	<i>E. coli</i> ( $10^5/\text{cm}^2$ )	<i>S. aureus</i> ( $10^5/\text{cm}^2$ )
P-(C)	72.70	Hydrophilic	90.80	51.30	13.53	82.59
G-180	72.30	Hydrophilic	365.01	287.69	14.20	13.37
G-600	79.90	Hydrophilic	254.70	195.27	25.92	42.44
G-800	84.80	Hydrophilic	226.33	175.18	29.96	24.25
G-1200	93.20	S. hydrophobic	205.66	159.60	19.70	23.19
G-1500	95.30	S. hydrophobic	204.10	157.15	20.00	13.03

\*All data are represented as average taken from three replications with  $\pm 10\%$  of standard error.

\*S. hydrophobic stands for slightly hydrophobic

## b) Millisecond Laser

Figure 5.11 showed that, as power increase from 3.0 W to 7.8 W in surface fabrication of TT using millisecond laser, the number of *E. coli* ATCC 8739 adhesion showed a reduction about 17% - 40% while, *S. aureus* ATCC 6838 increased with the highest increment about 1-fold compared to P-TT. Adhesion of *S. aureus* ATCC 6838 on MI-TT and MI-SS (Figure 5.8) showed similar trends where both surfaces promoted the bacterial adhesion when compare to P-TT and P-SS surfaces. Thus, based on the results, MI texturing was proven can stimulates the *S. aureus* ATCC 6838 adhesion on both SS and TT surfaces.

Previously, the adhesion of *S. aureus* ATCC 6838 on MI-SS was reported significantly influenced by  $S_q$  and  $S_a$  from the beginning but it showed differently on MI-TT (refer table 5.5). Changes of surface roughness from 88.92 nm to 270 nm for  $S_q$  and from 48.19 nm to 209 nm for  $S_a$  did not remarkably affect the adhesion at MI-TT-3.0 until MI-TT-7.8 where the number of *S. aureus* ATCC 6838 count on the surfaces are decreased even though the roughness increased. As mentioned from study by Valquier-Flynn et al. (2017), deeper observations of surface topography such as  $S_{sk}$ ,  $S_{ku}$  and  $S_{ds}$  must be considered other than  $S_q$  and  $S_a$ . The fabrication of TT using MI approach had also significantly impacted the  $S_{sk}$ ,  $S_{ku}$  and  $S_{ds}$  of the surfaces. Most of the MI-TT surfaces have negative  $S_{sk}$  which are -5.62, -4.06, -1.24 and -0.46 for MI-TT-3.0, MI-TT-4.2, MI-TT-5.4 and MI-TT-6.6, respectively (Table 5.5). Hence, it indicates that the surfaces have more valleys and pits (can also be referred at Figure 4.7) and also very spiky as all the  $S_{ku}$  is more than 3 ( $S_{ku} > 3$ ). The higher the negativity value of  $S_{sk}$  indicates the deeper the valleys, which means that more bacteria can be trapped within the cracks and voids that was generated during laser treatments and contributed to the increasing of *S. aureus* ATCC 6838 adhesion. The negativity of the  $S_{sk}$  reduced from -5.62 to 0.27 when the power was increased from 3.0 W to 7.8 W, which reflected a surface becomes less waviness with reduced valleys. This is supported with reduced number of adhered *S. aureus* ATCC 6838 from  $206.77 \times 10^5/\text{cm}^2$  to  $158.25 \times 10^5/\text{cm}^2$ . The size of *S. aureus* ATCC 6838 are within  $0.414 \mu\text{m} - 0.727 \mu\text{m}$ , (Table 4.4) and there is high chance that the existing of valleys and pits had trapped and lodged the *S. aureus* ATCC 6838 between the cavities and increased the bacterial colonies (Whitehead et al., 2005). This is also supported by Crawford et al. (2012) which investigated that, large valley and pits offered



better shelter to small and coccus-shaped cells compare to large and rod-shaped cells. With all the observations, the decreasing of *S. aureus* ATCC 6838 adhesion on MI-TT surfaces with respect to the power of MI are now relatable.

Besides that, there is a contradict results between two metal types which regarding the adhesion of *E. coli* ATCC 8739 on MI-TT and MI-SS. Adhesion of *E. coli* ATCC 8739 on MI-TT was reduced while MI-SS showed the addition of bacteria when compare to P-TT and P-SS. Previously, *E. coli* ATCC 8739 adhesion on G-SS, MI-SS, UI-SS and G-TT was observed significantly influenced by the surface hydrophobicity (CAM) but, at MI-TT the factor did not notably affect the adhesion. The adhesion was reduced about 17% - 40% when compared to P-TT even though all MI-TT surfaces (MI-3.0 -MI-7.8) are hydrophilic (Table 5.5). By looking at different point of view, MI-TT surfaces were full of deeper valleys and pits (negative  $S_{sk}$ ) while *E. coli* ATCC 8739 is a large (0.984  $\mu\text{m}$  – 2.243  $\mu\text{m}$ ) (Table 4.4) and rod-shaped bacterium. Therefore, it is possibly *E. coli* ATCC 8739 have difficulties to re-position itself to fill in the deeper valleys and pits at MI-TT surfaces compared to MI-SS which have shallower and broader valleys. Hence, it will avoid the surfaces and subsequently contributed to the reduction of bacteria. Moreover, the same condition also used to explain why the adhesion of *E. coli* ATCC 8739 on ML-TT (MI-3.0, MI-4.2, MI-5.4) increased from  $9.01 \times 10^5/\text{cm}^2$  to  $11.54 \times 10^5/\text{cm}^2$  as the  $S_{sk}$  slowly approaching zero (asymmetrical surface) aside from the influenced of  $S_q$ ,  $S_a$  and CAM. Study from Ahmad et al. (2017) also had described the similar results where a strong bacterial binding occurred on steel with negative skewness ( $S_{sk} = - 0.8$ ) due to the presence of holes and valleys which facilitates the adhesion. However, there is a slight reduction of *E. coli* ATCC 8739 at MI-TT-6.6 and MI-TT-7.8 and at this stage probably  $S_{ds}$  had played it roles. As explained before high  $S_{ds}$  reduced the contact area between the bacteria and metal surfaces due to the existence of dense peaks on the surface then, caused bacterial reduction. Thereby, it can be concluded that the surface with negative skewness ( $S_{sk}$ ) can repels the addition of *E. coli* ATCC 8739 and enhances the adhesion of *S. aureus* ATCC 6838 due to difference of bacterial size and shape.

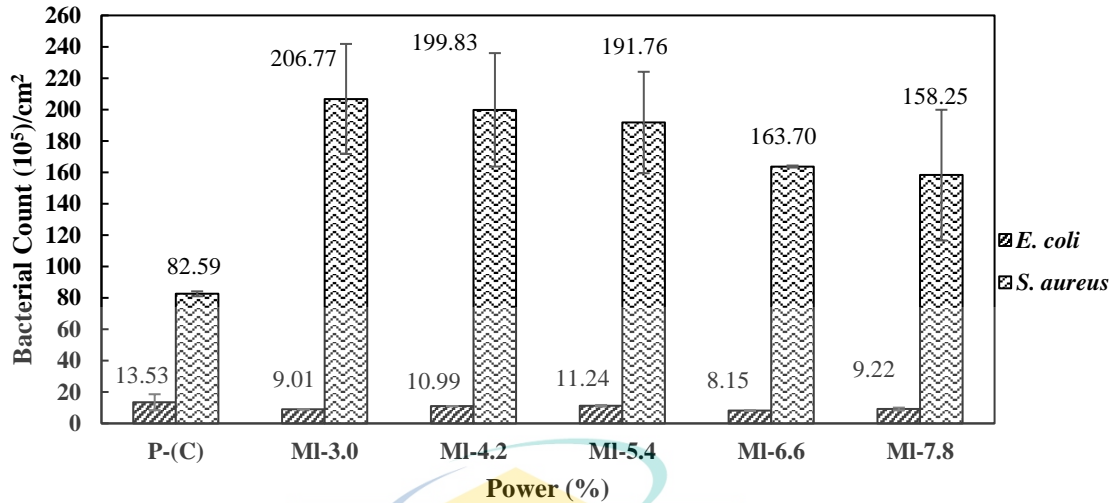


Figure 5.11 Number of *E. coli* ATCC 8739 and *S. aureus* ATCC 6838 adhesion on MI-TT surface at different types of power after 4 hours of adhesion in the PBS solution with 70 rpm shaking (pH 7.4 and 0.0137 mol/L of NaCl)

Table 5.5 Data of bacterial adhesion on MI-TT and surface parameters

Samples	CAM (°)	Condition	S <sub>q</sub> (nm)	S <sub>a</sub> (nm)	S <sub>sk</sub>	S <sub>ku</sub>	S <sub>ds</sub> (1/mm <sup>2</sup> )	<i>E. coli</i> (10 <sup>5</sup> /cm <sup>2</sup> )	<i>S. aureus</i> (10 <sup>5</sup> /cm <sup>2</sup> )
P-(C)	72.70	Hydrophilic	90.80	51.30	-4.51	37.04	3346.27	13.53	82.59
MI-3.0	79.70	Hydrophilic	88.92	48.19	-5.62	68.17	2965.94	9.01	206.77
MI-4.2	80.90	Hydrophilic	92.40	52.79	-4.06	45.45	4912.55	10.99	199.83
MI-5.4	82.70	Hydrophilic	146.75	96.11	-1.24	11.47	7086.16	11.24	191.76
MI-6.6	87.50	Hydrophilic	213.01	161.00	-0.46	4.22	8053.78	8.15	163.70
MI-7.8	86.00	Hydrophilic	270.26	208.64	0.27	3.75	7458.29	9.22	158.25

\*All data are represented as average taken from three replications with ±10% of standard error.

### c) Ultrafast laser

The power used in fabricating titanium surfaces using ultrafast laser machine was carried out between 0.10 W to 0.12 W. Figure 5.12 presents the adhesion of bacterial on UI-TT surfaces experienced a reduction about 20% - 96% for *E. coli* ATCC 8739 and 12% - 33% for *S. aureus* ATCC 6838 over the P-TT surface. Similar to UI-SS less adhesion was found on UI-0.10 with number of bacteria count is  $0.50 \times 10^6/\text{cm}^2$  and  $55.70 \times 10^6/\text{cm}^2$  for *E. coli* ATCC 8739 and *S. aureus* ATCC 6838, respectively. Based on Table 5.3 and Table 5.6, both surfaces which are UI-SS and UI-TT have similar trend on the *E. coli* ATCC 8739 and *S. aureus* ATCC 6838 adhesion. On the other hand, *S. aureus* ATCC

6838 adhesion was a greater colonizer than *E. coli* ATCC 8739, with higher adhesion of *S. aureus* ATCC 6838 was observed on UI-TT compare to *E. coli* ATCC 8739 due to its strong hydrophobic-hydrophobic interaction (Habimana et al., 2014).

Ultrafast laser surface texturing increased the surface roughness of UI-TT from 190 nm to 910 nm for  $S_q$  and 155 nm to 700 nm for  $S_a$  but, the increasing of surface roughness not always increased the adhesion of *E. coli* ATCC 8739 and *S. aureus* ATCC 6838 instead it is inhibiting the adhesion when compare to P-TT. This is in line with other studies related to the bacterial adhesion on ultrafast laser which also reported reduction of bacterial when the surface roughness increased. Shaikh et al. (2017) reported a 98% of *P. aeruginosa* and *E. coli* rejection on glass surface when  $S_q$  increased from 0.32  $\mu\text{m}$  to 7.74  $\mu\text{m}$  and Rajab et al. (2018) showed high reduction of *E. coli* (76%) on titanium when  $S_q$  increased from 0.02  $\mu\text{m}$  to 1.31  $\mu\text{m}$ . The ultrafast laser texturing contributed to high  $S_{ds}$  on both UI-SS and UI-TT due to the presence of LIPSS and nano-sized irregular grains on the surfaces which was 2-3 times higher than on G-TT and MI-TT. The existing of the special features are believed inhibit or resist the bacterial adhesion on its surface. In addition, it is best to note that both UI-SS-0.10 and UI-TT-0.10 surfaces recorded very minimal *E. coli* ATCC 8739 and *S. aureus* ATCC adhesion among other surface fabrication. However, the ultimate repulsion of bacterial on UI surfaces was achieved with *E. coli* ATCC 8738 which recorded the lowest adhesion on UI-SS-0.10 ( $0.30 \times 10^5/\text{cm}^2$ ) and UI-TT-0.10 ( $0.50 \times 10^5/\text{cm}^2$ ) across the current study.

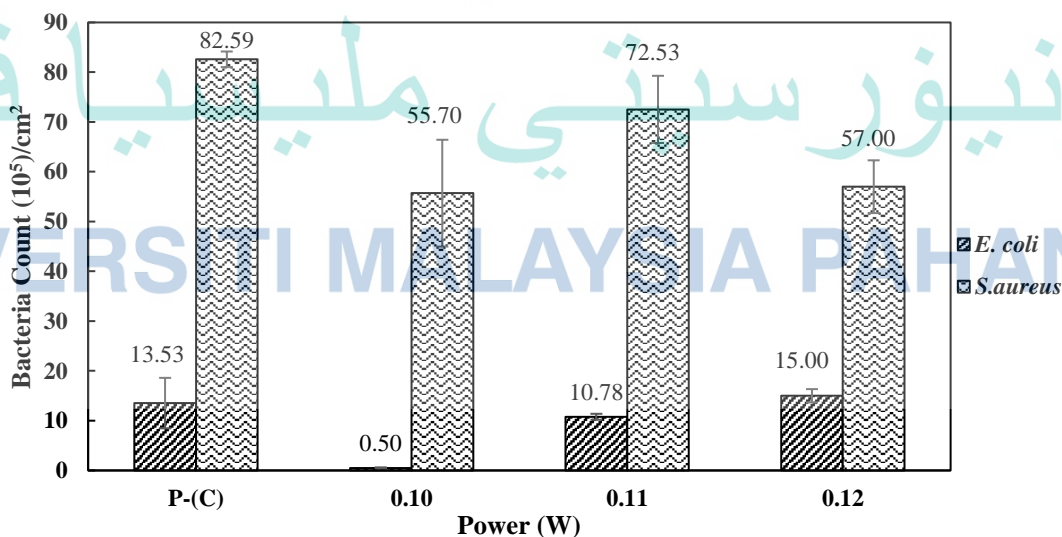


Figure 5.12 Number of *E. coli* ATCC 8739 and *S. aureus* ATCC 6838 adhesion on UI-TT surface at different types of power after 4 hours of adhesion in the PBS solution with 70 rpm shaking (pH 7.4 and 0.0137 mol/L of NaCl)

Table 5.6 Data of bacterial adhesion on UI-TT and surface parameters

Samples	CAM (°)	Condition	S <sub>q</sub> (nm)	S <sub>a</sub> (nm)	S <sub>ds</sub> (1/mm <sup>2</sup> )	<i>E. coli</i> (10 <sup>5</sup> /cm <sup>2</sup> )	<i>S. aureus</i> (10 <sup>5</sup> /cm <sup>2</sup> )
P-(C)	72.70	Hydrophilic	90.80	51.30	3346.27	13.53	82.59
UI-0.10	100.65	Hydrophobic	210.00	175.00	16456.30	0.50	55.70
UI-0.11	130.10	Hydrophobic	910.00	700.00	20670.31	10.78	72.53
UI-0.12	134.20	Hydrophobic	630.00	490.00	19031.06	15.00	57.00

\* All data are represented as average taken from three replications with ±10% of standard error.

### 5.3.3 Comparative Assessment of Bacterial Adhesion on Stainless Steel and Titanium

The degree of improvement or severity of bacterial adhesion on surfaces undergone grinding, millisecond and ultrafast laser fabrications were compared with polished surfaces as the control specimen. Overall, grinding technique increased the adhesion of *E. coli* ATCC 8739 on both G-SS and G-TT with 22% - 1-fold and 5% - 1-fold of increment each meanwhile, reduced the *S. aureus* ATCC 6838 adhesion on G-SS and G-TT with 76% - 90% and 58% - 84% of reduction, respectively. On the other hand, millisecond laser treatment promoted *S. aureus* ATCC 6838 on both MI-SS and MI-TT with increment about 27% - 37% and 91% - 1-fold each whereas *E. coli* ATCC 8739 experienced an increase of adhesion on MI-SS by 27% - 37% and a reduction at MI-TT by 17% to 40%. Besides that, ultrafast laser surfaces experienced a bacterial reduction at both UI-SS and UI-TT. *E. coli* ATCC 8739 adhesion was reduced about 65% - 98% at UI-SS and 20% - 96% at UI-TT while *S. aureus* ATCC 6838 reduced by 19% - 78% at UI-SS and 12%-33% at UI-TT. Therefore, it is shown that ultrafast laser is the only technique that can produce surfaces with the reduction of *E. coli* ATCC 8739 and *S. aureus* ATCC 6838 at both SS and TT when compared to control (polished) surfaces with the least bacterial adhesion was found at UI-SS-0.10 ( $S_q = 298$  nm,  $S_{ds} = 17039.43/\text{mm}^2$ ) and UI-TT-0.10 ( $S_q = 210$  nm,  $S_{ds} = 16456.30/\text{mm}^2$ ). The details comparison between all the surface fabrications (grinding, millisecond laser, ultrafast laser) with regards to the bacterial has been discussed in the next paragraph. Figure 5.13 showed the average summation of the bacterial count on different surface fabrications.

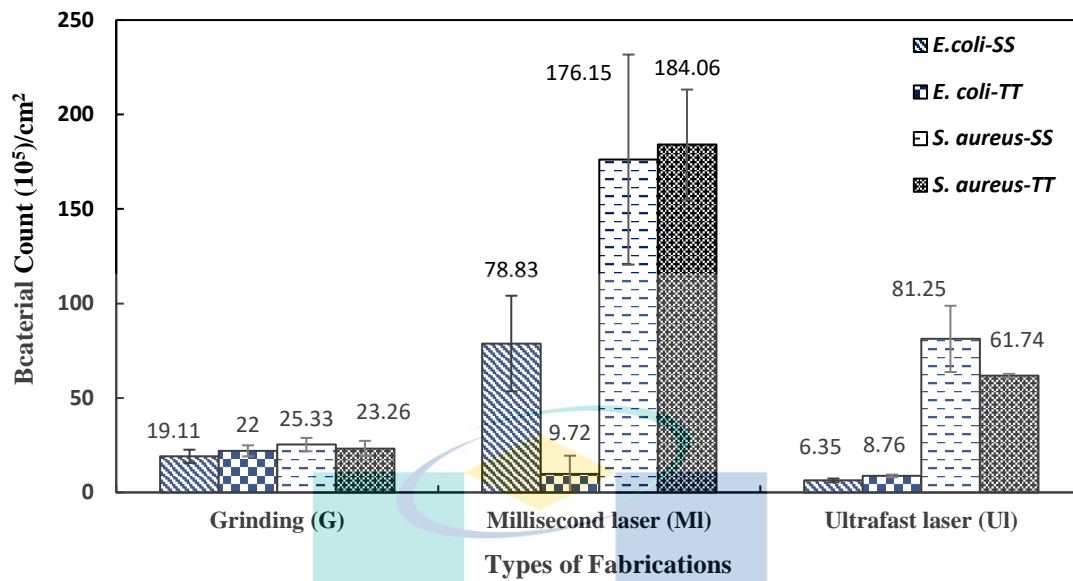


Figure 5.13 The average summation of *E. coli* ATC 8739 and *S. aureus* ATCC 6838 adhesion on SS and TT which undergone different surface fabrications

Based on the graph at Figure 5.13, UI had proved can reduce the number of *E. coli* ATCC 8739 as it had the lowest adhesion on both SS and TT than at G and MI surfaces with 10% to 91% (compared to G and MI surfaces) of reduction. Meanwhile, *S. aureus* ATCC 6838 showed a slightly different results where the lowest adhesion was observed on G (62% - 87% of reduction compare to MI and UI) not on UI surfaces. Nevertheless, number of *S. aureus* ATCC 6838 on UI still fewer than on MI surfaces (53% - 66% of reduction compare to MI). UI texturing produced surfaces with high CAM  $S_q$  and  $S_{ds}$  value compared to other fabrication techniques. Most of UI surfaces are hydrophobic (CAM: 100° - 145.70°) except at UI-SS-0.04 (Table 4.1). Therefore, it is believed that *E. coli* ATCC 8739 which is a hydrophilic bacterium (Table 4.4) encountered a huge depletion on UI surfaces probably because both surfaces (bacterial and UI) tend to repel each other due to the different in surface hydrophobicity (Krasowska & Sigler, 2014; Lorenzetti et al., 2015). Meanwhile, adhesion of *S. aureus* ATCC 6838 which is a hydrophobic bacterium (Table 4.4) was slightly augmented on UI surfaces due to strong hydrophobic-hydrophobic interaction (Gusnaniar et al., 2017). However, UI surfaces still able to prevent the adhesion better than MI surfaces even though the hydrophobic interaction is really strong. Bohinc et al. (2016) stated that, bacterial adhesion is the results of interplay between different factors. Their study revealed that stainless steel (hydrophobic surface) resisted the adhesion of hydrophilic bacteria which

is *E. coli* but *L. monocytogenes* which also a hydrophilic bacterium adhered the best on the stainless steel and it is because of surface roughness and surface chemistry factors that washed away the hydrophobic or hydrophilic interaction. Therefore, in this study UI surfaces still managed to reduce *S. aureus* ATCC 6838 adhesion probably due to high  $S_q$  and  $S_{ds}$  (Table 4.2 and Table 4.3) generated after ultrafast laser texturing which reduces the binding strength and lead to easy removal caused by hydrodynamic forces. The  $S_q$  (190 nm – 910 nm) and  $S_{ds}$  (16171.76/mm<sup>2</sup> – 26945.58/mm<sup>2</sup>) on UI surfaces were drastically changed owing to the formation of LIPSS (ripples) and nano-sized irregular grain on the surfaces which reduced the *E. coli* ATCC 8739 and *S. aureus* ATCC adhesion by minimizing the contact point between the bacteria and the metal surfaces. On the other hand, G surface managed to reduce *E. coli* ATCC 8739 and *S. aureus* ATCC 6838 adhesion on both SS and TT. However, it was reported that grinding surfaces are susceptible to the corrosion problem (Zhou, 2018). Every metal that exposed to the air will be oxidized and formed an oxide layer on it which can protect the surface from corrosion. But, the mechanical processing like grinding had damaged the oxide layer and subsequently enhanced the corrosion process (Zhou, 2018). Therefore, grinding samples are not suitable to use in human body and for industrial equipment as its surface can corrode easily. Thus, UI is the best surface which can reduce the bacterial adhesion especially *E. coli* ATCC 8739 as well as safe to use.

Figure 5.14 and Figure 5.15 displayed the SEM images of bacterial adhesion on P, G, MI and UI surfaces. Surfaces with full of grooves, ripples and pits enhance bacterial colonization by providing protection from shear stress or any hydrodynamic forces (Gu et al., 2016). Based on the SEM images at Figure 5.15 (c) and (d), UI treatment had produced micro and nanoscale surface topography way smaller than the size of sample bacteria. The sizes of *E. coli* ATCC 8739 (length: 0.984  $\mu\text{m}$  – 2.243  $\mu\text{m}$ ; width: 0.198  $\mu\text{m}$  – 0.753  $\mu\text{m}$ ) and *S. aureus* ATCC 6838 (0.414  $\mu\text{m}$  – 0.727  $\mu\text{m}$ ) are bigger than LIPSS (0.20  $\mu\text{m}$ ) and the nano-sized irregular grains (0.083  $\mu\text{m}$  - 0.112  $\mu\text{m}$ ) (Figure 5.15). The size of valleys, pits and crevices produced on UI surfaces are smaller (0.086  $\mu\text{m}$  – 0.29  $\mu\text{m}$ ) than those on G and MI surfaces (Figure 5.14). The production of these features on the UI surfaces resisted the penetration of both *E. coli* ATCC 8739 and *S. aureus* ATCC 6838 into the valleys or voids to provide stable bond with the original surfaces thus, inhibit the adhesion by reducing the area of contact interface between bacteria and the original metal surfaces (Cunha et al., 2016). Therefore, this finding is supported by Gu et

al. (2016) which also found that bacterial adhesion can be reduced when the grooves, ripples or valleys are smaller than the bacterial size and the same finding also mentioned in Schwibbert et al. (2019) study. Meanwhile, the surface topography on G is larger than the bacterial size and as can be seen at Figure 5.14 (c) and (d) *E. coli* ATCC 8739 and *S. aureus* ATCC 6838 prone to locate themselves between the grooves and scratches which believed can secure their position (Dantas et al., 2016).

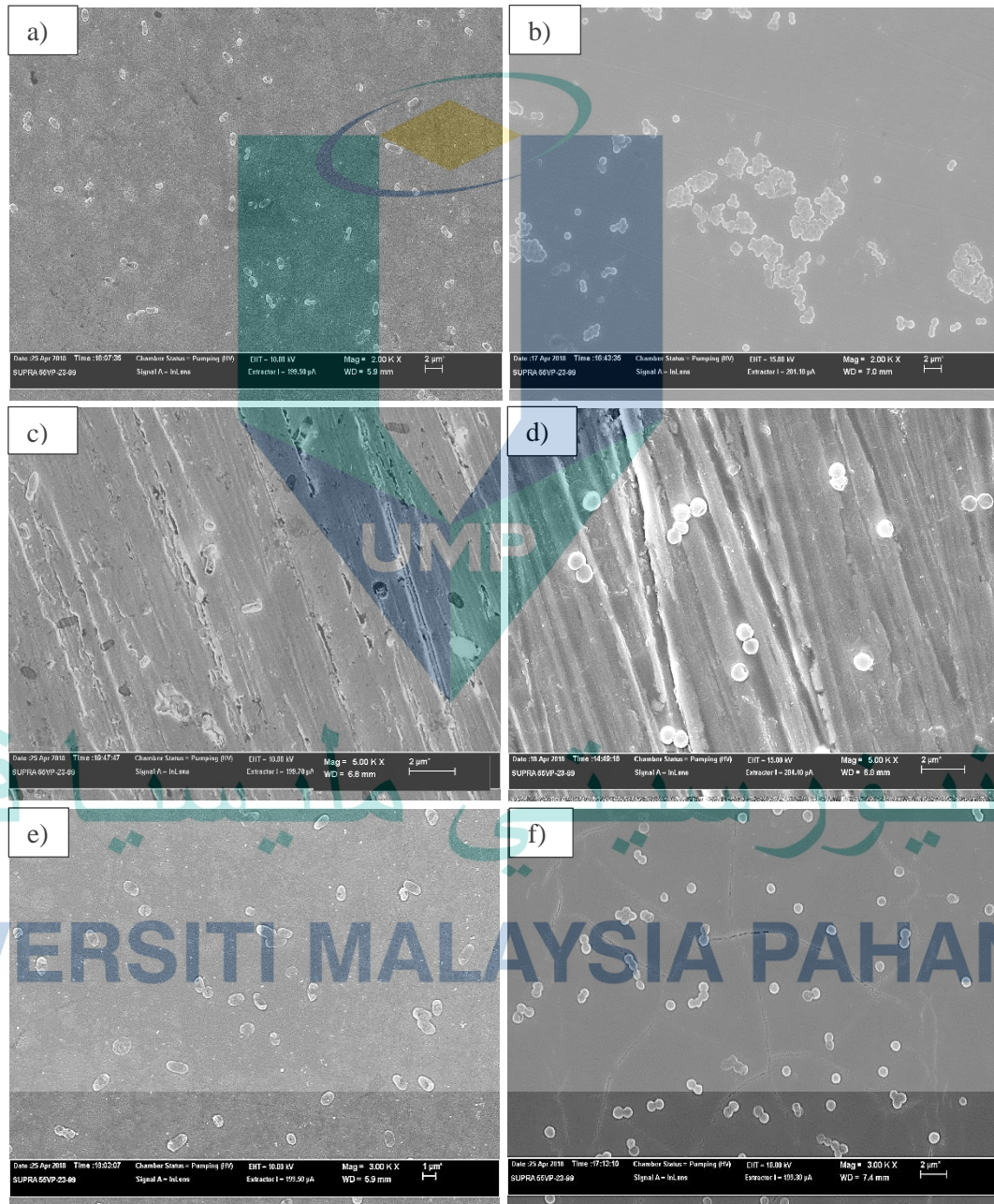


Figure 5.14 SEM micrographs of *E. coli* ATCC 8736 adhesion on a) P-SS c) G-SS-180 e) MI-SS-6.0 and *S. aureus* ATCC 6838 adhesion on b) P-SS d) G-SS-180 f) MI-SS-6.0

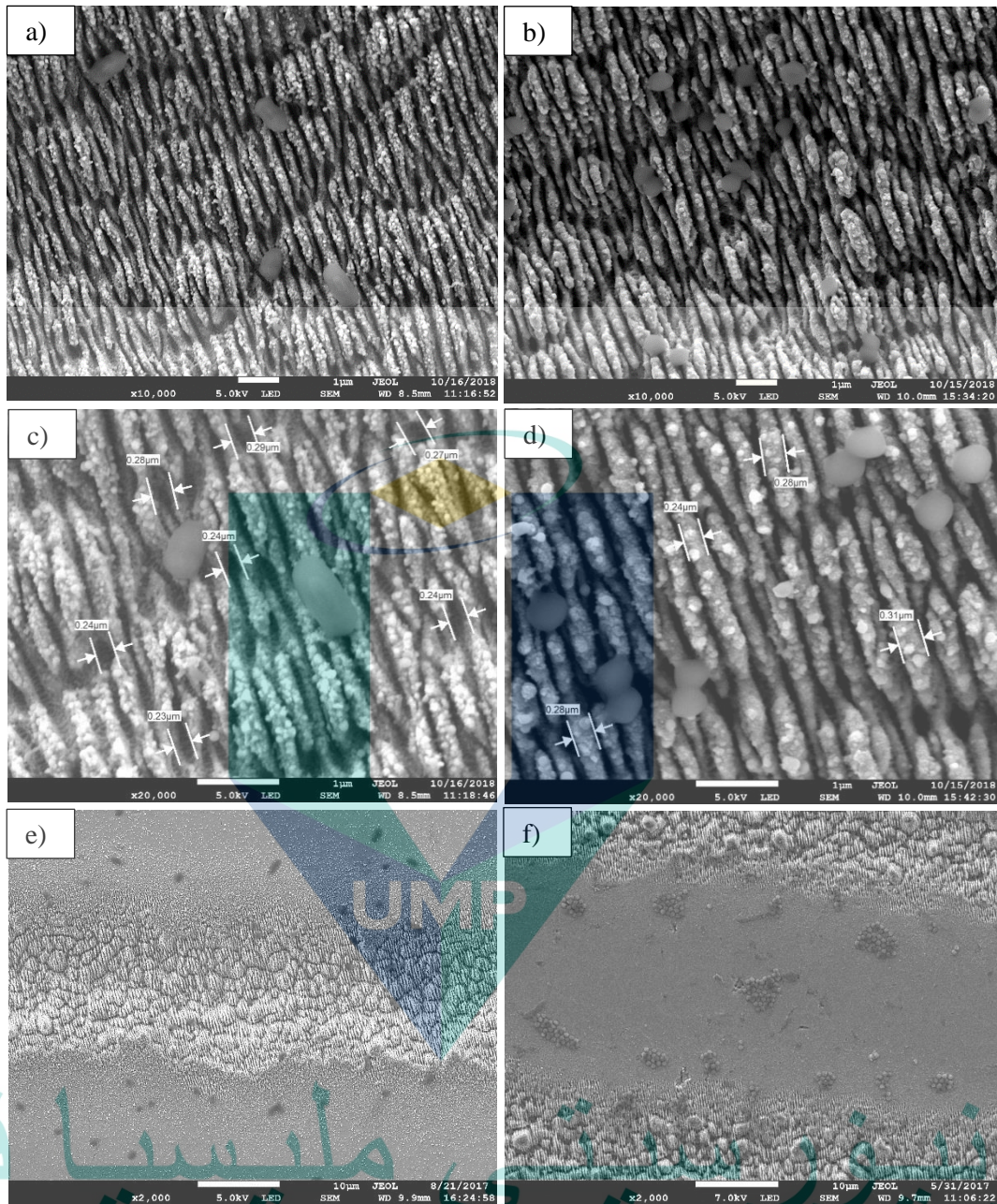


Figure 5.15 SEM micrographs of *E. coli* ATCC 8739 (a), (c), (e) and *S. aureus* ATCC 6838 (b), (d), (f) adhesion on different parts of UI-SS with different magnifications

*E. coli* ATCC 8739 have more difficulties in positioning themselves on the UI surfaces, it needs to aligned itself on the protruding structures and some of them intersect with the contour lines where the maximum contact area can be attained (Figure 5.15). However, the position is not strong enough to overcome the shear stress or hydrodynamic forces and easily detached during the 4 hours of adhesion (Schwibbert et al., 2019). The valleys and crevices are too small for these rod-shaped bacteria to penetrate into the spaces. Furthermore, only single separated *E. coli* ATCC 8739 cells were found on the



UI surfaces (Figure 5.15 (a)) and the same observation could be found on all UI-SS and UI-TT surfaces. In contrast, due to different in size, *S. aureus* ATCC 6838 adhered easily at the grooves or valleys between the LIPSS. The presence of the valley serves as a basin which trapped the bacteria, thus providing additional protections from shear stress while strengthening the bonding (Oh et al., 2016). However, it is interesting to observe that only 2-3 of *S. aureus* ATCC 6838 cells appeared between the LIPSS, while only single cell on top of the contour line and no cells cluster formed (Figure 5.15 (b)). It is believed that the structure of the LIPSS might prevent the cells-cells interaction and subsequently eliminates the formation of the cell cluster or colonies. Figure 5.15 (e) and (f) proved that the colonies of *S. aureus* ATCC 6838 was formed on the unstructured surfaces and similar observation for *E. coli* ATCC 8739 where more cells were attached outside the laser line. This common view was also observed on all UI-TT surfaces for both bacterial. On the other hand, the existence of nano-sized irregular grains on all UI surfaces presumably can ruptures the cell membranes (bactericidal effect) of both bacteria especially *E. coli* ATCC 8739 which composed of thin peptidoglycan compare to *S. aureus* ATCC 6838 that has thicker peptidoglycan (Habimana et al., 2014). Therefore, it is noted that all features on UI surfaces such as LIPSS, valleys/crevices and the formation of nano-sized irregular grains were proved to successfully reduce the *E. coli* ATCC 8739 adhesion about 10% to 91% compared to G and MI surfaces. Besides, it also able to inhibit the formation of *S. aureus* ATCC 6838 clusters on all UI-SS and UI-TT surfaces. It is mentioned in the earlier discussion that *S. aureus* ATCC 6838 adhesion on both UI-SS and UI-TT surfaces is higher than on G surfaces due to high surface hydrophobicity ( $100^{\circ}$  -  $145^{\circ}$ ) thus, created strong hydrophobic-hydrophobic interaction. However, it is interesting to discuss that, if the UI surfaces become superhydrophobic ( $CAM > 150^{\circ}$ ) the adhesion of *S. aureus* ATCC 6838 might be reduced more (Jalil et al., 2020; Zhang et al., 2013). This is due to the repulsion of water (bacterial solution) which can limit the access of bacteria onto the superhydrophobic surfaces (Epperlein et al., 2017) subsequently contribute to the reduction of bacterial.

In this study, the adhesion of *E. coli* ATCC 8739 and *S. aureus* ATCC 6838 on different surface fabrication mostly influenced by CAM and  $S_q$  or  $S_a$  (Subtopic 5.3). Table 5.7 represents the average number of bacterial counts on different surface fabrication (G, MI, UI) with respect to the CAM. The CAM value was divided into two phase which are hydrophilic ( $< 90^{\circ}$ ) and hydrophobic ( $> 90^{\circ}$ ). Denser *E. coli* ATCC 8739 and *S. aureus*

ATCC 6838 population were seen on hydrophilic compared to hydrophobic surfaces on both G and MI surfaces. *E. coli* ATCC 8739 which also known as hydrophilic bacteria (refer Chapter 4.3) were influenced by CAM. The attached bacteria decreased when the surface become hydrophobic for both G ( $43.97 \times 10^5/\text{cm}^2$  to  $36.70 \times 10^5/\text{cm}^2$ ) and MI ( $97.95 \times 10^5/\text{cm}^2$  to  $64.77 \times 10^5/\text{cm}^2$ ) surfaces. However, *S. aureus* ATCC 6838 which is a hydrophobic bacterium (refer Chapter 4.3) reported otherwise. Based on the general rule regarding the hydrophobic/ hydrophilic interaction the number of *S. aureus* ATCC 6838 should be increased when the surface become more hydrophobic but instead it decreased at both G ( $60.93 \times 10^5/\text{cm}^2 - 35.09 \times 10^5/\text{cm}^2$ ) and MI ( $337.88 \times 10^5/\text{cm}^2 - 209.63 \times 10^5/\text{cm}^2$ ) surfaces. At this point, the surfaces roughness ( $S_q$  and  $S_a$ ) might be one of the controlling factors that contributed to the adhesion. However, at UI samples the surfaces become extremely hydrophobic ( $> 100^\circ$ ) which affected the degree of adhesion for *S. aureus* ATCC 6838. It was observed that when CAM is more than  $100^\circ$  the number of bacterial count increased from  $99 \times 10^5/\text{cm}^2$  to  $137.07 \times 10^5/\text{cm}^2$ . Meanwhile, the adhesion of *E. coli* ATCC 8739 still governed by CAM because it recorded the lowest cell number at hydrophobic UI surfaces compare to G and MI surfaces, although the increased of surface roughness are visible (Figure 4.6, 4.7, 4.8). Therefore, it can be concluded that in this study *E. coli* ATCC 8739 was strongly influenced by the CAM value while *S. aureus* ATCC 6838 was affected by the surface topography ( $S_q$ ,  $S_a$ ,  $S_{sk}$ ,  $S_{ku}$ ,  $S_{dr}$  and  $S_{ds}$ ) and become significantly influenced to CAM when the value of CAM is more than  $100^\circ$ .

Table 5.7 Average number of bacterial count based on the contact angle measurement (CAM) at different surface fabrication

		Number of bacterial count ( $10^5/\text{cm}^2$ )		
CAM ( $^\circ$ )		G	MI	UI
<b>&lt; 90</b> <b>(Hydrophilic)</b>	<i>E. coli</i> ATCC 8739	43.97	97.95	5.10
	<i>S. aureus</i> ATCC 6838	60.93	337.88	99.00
<b>&gt; 90</b> <b>(Hydrophobic)</b>	<i>E. coli</i> ATCC 8739	36.70	64.77	16.56
	<i>S. aureus</i> ATCC 6838	35.09	209.63	137.07

\*All data are represented as average taken from three replications with  $\pm 10\%$  of standard error.

Figure 5.16 displayed the differences of *E. coli* ATCC 8739 and *S. aureus* ATCC 6838 adhesion on SS and TT surfaces. Overall, *S. aureus* ATCC 6838 recorded the highest number on all SS and TT surfaces while *E. coli* ATCC 8739 became the less adhesive bacteria on the metal surfaces. Slullitel et al. (2018) also came out with the similar finding where *E. coli* was found to have weak adherence on all biomaterial surfaces (i.e: cobalt chromium, ceramic and polyethylene). Referring to Table 4.4 in Chapter 4, at pH 7.4 the zeta potential of *E. coli* ATCC 8739 and *S. aureus* ATCC 6838 is  $-24.78 \pm 0.26$  mV and  $-13.11 \pm 0.21$  mV, respectively. Meanwhile, SS has positive surface charge (Sheng et al., 2008) and TT surface is slightly negative (Qiao et al., 2012).

When observation on the overall number of attached bacteria on those surfaces, it was revealed that *E. coli* ATCC 8739 on SS is only around  $524.78 \times 10^5/\text{cm}^2$  while *S. aureus* ATCC 6838 is doubled, approximately  $1332.37 \times 10^5/\text{cm}^2$ . When referring to the difference in surface charge, the number of *E. coli* ATCC 8739 should be higher than *S. aureus* ATCC 6838 due to strong electrostatic attraction force between *E. coli* ATCC 8739 and SS surface. But, the strong electrostatic attraction force had hindered the elongation of *E. coli* ATCC 8739 which necessary for cell division (Gottenbos et al., 2002) thus, reduced the *E. coli* ATCC 8739 adhesion on SS surfaces (Subtopic 5.2.1). *S. aureus* ATCC 6838 which has thicker and rigid peptidoglycan compares to *E. coli* ATCC 8739 was less affected by the electrostatic forces (Pajerski et al., 2019). Furthermore, *E. coli* ATCC 8739 adhesion on TT (highly negative surface) reduced almost half than those on SS due to additional resistance for attachment, predominantly caused by strong electrostatic repulsion forces occurred between both surfaces. Similarly, adhesion of *S. aureus* ATCC 6838 on TT reduced about 8% compared to SS which also caused by the electrostatic repulsion. Nevertheless, the adhesion of *S. aureus* ATCC 6838 was still higher than *E. coli* ATCC 8739 as the surface charge of *S. aureus* ATCC 6838 is lower than the surface charge of *E. coli* ATCC 8739. On the other hand, Ma et al. (2012) also mentioned that hydrophobic bacteria adhere to a greater extent than hydrophilic bacteria.

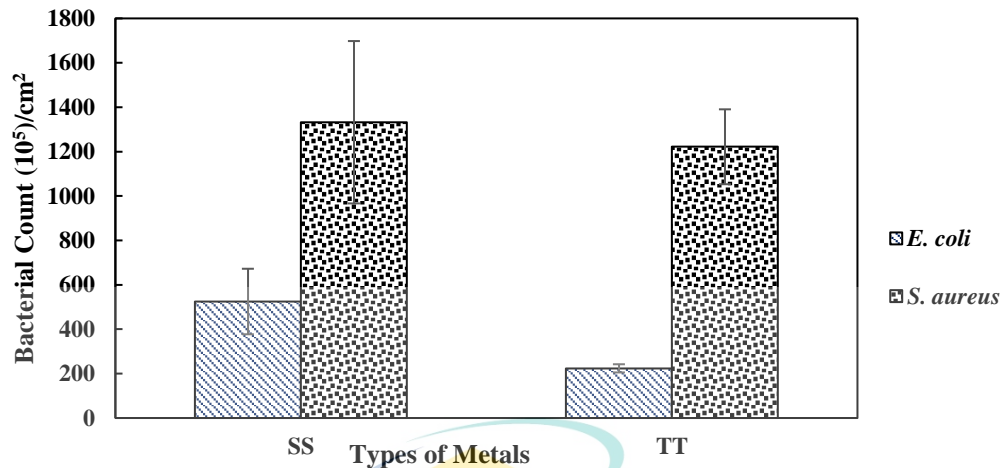


Figure 5.16 The summations of *E. coli* ATCC 8739 and *S. aureus* ATCC 6838 on SS and TT at all surface fabrication after 4 hours of adhesion

#### 5.3.4 Bacterial Adhesion on Ultrafast Laser Surfaces Fabricated under Argon Gas

Surface chemical composition can influence the bacterial adhesion (Han et al., 2016). Laser treatment was carried out in air and it is believed that the change of surface topography was accompanied with the existence of oxide layer (Damiati et al., 2018). The probability of the TT metal to change to TiO, TiO<sub>2</sub> or Ti<sub>2</sub>O<sub>3</sub> upon exposure to air during laser treatment were off very high probability and also can be partially hydrolyzed to become TiOH (Han et al., 2016). The oxide surfaces are electrically charged in the liquid due to the interaction of -OH with the hydroxide ion in the aqueous solution (Han et al., 2016). The net charge of the surface (either positive or negative) is depending on the isoelectric point (IEP) of the metal surfaces and the pH of the environment and then will become factor that will attract or repulse the bacteria to the surface. The presence of oxide layer on the metals during the laser treatments might be contributed to the bacterial adhesion due to the existing of surface charge of the metals when placed in the aqueous solution. Cunha et al. (2016) has reported that, the native oxide film on the titanium surface had significantly facilitated the bacterial adhesion on a surface. Meanwhile, Pazuza et al. (2019) informed that significant changes of surface chemistry was not observed for lasered surfaces exposed to argon gas because there is no oxidation occur.

Therefore, laser treatments by using UI machine have been performed under argon gas for both SS and TT in order to study the effect of argon gas towards the bacterial adhesion by preventing the formation of possible oxide layer during fabrication process. Table 5.8 presents the number bacterial adhesion on UI (SS and TT) surfaces fabricated under argon gas (Ar) in comparison to normal air. The UI-SS and UI-TT parameters like CAM,  $S_q$  and  $S_{ds}$  were set to become approximately similar at both conditions (air and argon). Adhesion of *S. aureus* ATCC 6838 on the surface fabricated under argon gas had further reduced about 88% on UI-SS and 21% on UI-TT compared to normal air (Table 5.8). Meanwhile, adhesion of *E. coli* ATCC 8739 on UI-TT had reduced about 19% and there is no reduction reported on UI-SS and it is possibly due to the difference of CAM (Air: 145.70°, Ar: 135.70°). Consequently, it can be concluded that laser treatments under argon gas suppressed the oxidation from occur thus, no oxide layer was formed on the surfaces subsequently increased the detachment of the bacterial adhesion. Therefore, by performing the UI treatment under argon gas the adhesion of *S. aureus* ATCC 6838 on both SS and TT could be further reduced.

Table 5.8 Number of *E. coli* ATCC 8739 and *S. aureus* ATCC 6838 adhesion on UI-SS and UI-TT surfaces fabricated under argon gas

Samples	CAM (°)	$S_q$ (nm)	$S_{ds}$ (1/mm <sup>2</sup> )	<i>E. coli</i> ATTC 8739 (10 <sup>5</sup> /cm <sup>2</sup> )	<i>S. aureus</i> ATCC 6838 (10 <sup>5</sup> /cm <sup>2</sup> )
UI-SS (Air)	145.70	650	19868	1.75	128.68
UI-SS (Ar)	135.70	670	25000	9.90	17.00
UI-TT (Air)	134.20	630	19031	24.00	57.00
UI-TT (Ar)	135.80	600	24800	19.40	45.20

\*All data are represented as average taken from three replications with  $\pm 10\%$  of standard error.

#### 5.4 Summary

pH and ionic strength (salt concentration) had prominent effects towards the adhesion of *E. coli* ATCC 8739 and *S. aureus* ATCC 6838 on polished surfaces which are P-SS and P-TT. Observation of five level pH (pH 4 to pH 9) and salt concentration (0.001 – 0.2 mol/L) were tested in this study. In term of pH, both P-SS and P-TT recorded similar trend where the bacterial adhesion decreased when the pH increased from pH 4 to pH 9. Overall, when pH increased from pH 4 to pH 9, the reduction of *E. coli* ATCC

8739 and *S. aureus* ATCC 6838 at P-SS is about 58% and 44% while on P-TT is about 57% and 75%, respectively. Besides that, it has been reported that salt concentration had affected the ionic strength in a solution. When the ionic strength in the solution increased, more adhesion occurred due to the neutralization of charge and reduction of EDL. In general, adhesion of *E. coli* ATCC 8739 and *S. aureus* 6838 on P-SS and P-TT had increased about 4-fold to 10-fold and 1-fold - 10-folds, respectively when NaCl increased from 0.001 mol/L to 0.2 mol/L. Therefore, it can be concluded that any slight changes of pH and salt concentration in the surrounding will affect the number of bacterial adhesions on the SS and TT surfaces.

The number of bacterial adhesions on grinding, millisecond laser and ultrafast laser surfaces have been compared to control (polished). It was shown that ultrafast laser is the only technique that can produce surfaces with the reduction of *E. coli* ATCC 8739 (20% - 98%) and *S. aureus* ATCC 6838 (12% - 78%) at both SS and TT when compared to control (polished) surfaces with the lesser bacterial adhesion was found at UI-SS-0.10 ( $S_q = 298$  nm,  $S_{ds} = 17039.43/\text{mm}^2$ ) and UI-TT-0.10 ( $S_q = 210$  nm,  $S_{ds} = 16456.30/\text{mm}^2$ ). Besides that, based on three different types of surface fabrication techniques that have been performed (grinding, millisecond laser, ultrafast laser), surface fabricated by UI treatment experienced the lowest adhesion of *E. coli* ATCC 8739 by 10% to 91% of reduction (compared to G and MI) on both SS and TT. Lowest adhesion of *S. aureus* ATCC 6838 was found on G (62% - 87% of reduction compare to MI an UI) surfaces but, UI still managed to reduce *S. aureus* ATCC 6838 (53% - 66% of reduction compare to MI) adhesion better than MI surfaces. On the other hand, it has been concluded that *E. coli* ATCC 8739 was strongly influenced by the contact angle measurement (CAM) while *S. aureus* ATCC 6838 adhesion was affected by the difference in surface topography like  $S_q$ ,  $S_a$ ,  $S_{sk}$ ,  $S_{ku}$ ,  $S_{dr}$  and  $S_{ds}$ . However, CAM will have considerable effect on the adhesion of *S. aureus* ATCC 6838 when the value of CAM is more than  $100^\circ$ . Lastly, it has been found that *S. aureus* ATCC 6838 has the highest adhesion on both SS and TT while *E. coli* ATCC 6838 was the less adhesive bacteria for both metals. It is due to the difference in surface charge and also the physiological of each bacterium. UI surfaces which treated under argon gas had reduced *E. coli* ATCC 8739 adhesion about 19% on TT when compared to UI-TT treated under normal air, while *S. aureus* ATCC 6838 on UI-SS and UI-TT showed 88% and 21% of reduction, respectively compared to surface (SS and TT) treated under normal air.

## CHAPTER 6

### CONCLUSION AND RECOMMENDATIONS

#### 6.1 Conclusion

The adhesion of *E. coli* ATCC 8739 and *S. aureus* ATCC 6838 on stainless steel AISI316L and Grade 5 titanium alloys were successfully investigated in this research. The overall conclusion that can be drawn from this study are as follows:

Fabrication of stainless steel AISI316L (SS) and Grade 5 titanium alloys (TT) by polishing (control) (P), grinding (G), millisecond laser (MI) and ultrafast laser (UI) texturing were successfully performed. Characterizations and the properties of both metal and bacterial surfaces have been investigated. Based on the CAM results, both metals structured by the ultrafast laser have hydrophobic surfaces ( $CAM > 100^\circ$ ) with an exception for UI-0.04 (SS and TT) which have hydrophilic surface. Meanwhile, metals fabricated with polishing, grinding and millisecond laser were identified to have slightly hydrophobic ( $CAM: 90^\circ - 100^\circ$ ) and hydrophilic surfaces ( $CAM < 90^\circ$ ) respectively. After the fabrication process, P samples were found to have finer and smooth surface structures compared to G and MI which surfaces were full of grooves and heavy scratches. On the other hand, ultrafast laser treatment had produced surfaces with laser induced periodic surface structures (LIPSS) and nano-sized irregular grains (power  $> 0.10$  W). Both features had influenced the UI samples to have surfaces with high roughness ( $S_q$  reached 900 nm), high summit density ( $S_{ds} > 16000/\text{mm}^2$ ) and hydrophobic surface. Besides that, bacterial characterization tests revealed that *E. coli* ATCC 8739 is a hydrophilic bacterium with highly negative surface charge (-24.73 mV, pH 7.4) and *S. aureus* ATCC 6838 is a highly hydrophobic bacterium with less negative surface charge (-13.11 mV, pH 7.4).

Study on the effect of environmental condition (pH, salt concentration) towards the bacterial adhesion on P-SS and P-TT surfaces showed that, the adhesion reduced when the pH increased from 4 to 9 with less bacterial adhesion was at pH 7.4. *E. coli*

ATCC 8739 adhesion on P-SS reduced about 58% and 57% on P-TT while *S. aureus* ATCC 6838 reported 44% of reduction on P-SS and 75% on P-TT. The ionization of the bacterial cell surface functional group and the differences of the bacterial negative charge are the reasons for to the reduction of bacterial. Besides that, the increasing of salt concentration (0.001 mol/L - 0.2 mol/L) had increased the number of both bacterial adhesions. *E. coli* ATCC was increased about 10-fold on P-SS and 1-fold on P-TT while *S. aureus* ATCC 6838 had 4-fold of increment on P-SS and 10-fold on P-TT. Solution with high salt concentration consisted of strong ionic strength in which can enhance the bacterial adhesion through the reduction of bacterial electrical double layer (EDL).

Furthermore, the effect of surface fabrication towards the bacterial adhesion also has been analyzed in detail. When compared to P (control) surfaces, the ultimate achievement was observed with UI surfaces which undergone a bacterial reduction at both UI-SS and UI-TT. *E. coli* ATCC 8739 and *S. aureus* ATCC 6838 were reduced from 20% to 98% and 12% to 78% respectively. Then, when compared to all different surface fabrication (G, MI, UI), UI surfaces have the lowest adhesion of *E. coli* ATCC 8736 where the bacteria were reduced about 10% - 91% on SS and TT. Therefore, it can be concluded that, UI surfaces can reduce the bacterial adhesion on both SS and TT with the highest achievement was on UI-SS-0.10 and UI-TT-0.10 surfaces with roughness ( $S_q$ ) is 298 nm and 210 nm respectively. This indicated that the range of a roughness ( $S_q$ ) of a metal must be maintained from 200 nm to 300 nm and the summit density ( $S_{ds}$ ) from 15000/ mm<sup>2</sup> to 18000/ mm<sup>2</sup> in order to control the adhesion. If the value of  $S_q$  and  $S_{ds}$  are different from the required range, the other topographic parameters ( $S_{sk}$ ,  $S_{ku}$ ,  $S_{dr}$ ) and the CAM value of the UI surface might change thus, can affect the bacterial adhesion. The existence of LIPSS and nano-sized irregular grains on UL surfaces become the main factors that contributed to the reduction of the bacterial adhesion.

Bacterial adhesion on solid surfaces is a natural phenomenon that is influenced by interaction of multiple factors, i) bacteria properties (size, hydrophobicity, charge), ii) solid surface properties (topography, hydrophobicity, charge) and iii) environmental condition (pH, salinity). Current observation had identified that the *E. coli* ATCC 8739 adhesion on both SS and TT was significantly affected by the change of CAM (hydrophobicity) while *S. aureus* ATCC 6838 was influenced by the surface topography but when the value of CAM is more than 100°, the adhesion of *S. aureus* ATCC will be



highly governed by the CAM value. Lastly, it has been found that UI surfaces treated under argon gas could further reduced the *E. coli* ATCC 8739 adhesion about 19% on TT compares to adhesion on the same surface fabricated using air as a shield gas. Similar observation was observed for the adhesion of *S. aureus* ATCC 6838 where 88% reduction was obtained on UI-SS and 21% on UI-TT. Overall, fabrication by the ultrafast laser machine is the best method to produce surface with less bacterial adhesion (within specific range) and the application must be applied in both medical and industrial sectors.

## 6.2 Recommendations

The following are the recommendations that can be made for future works.

- 1) The zeta potential test for metal surfaces must be performed in order to study the metal surface charge. Therefore, the relationship between the bacterial adhesion and metal surfaces in term of surface charge can be discussed in more detail.
- 2) The fabrication of superhydrophobic surfaces ( $CAM > 150^\circ$ ) towards the bacterial adhesion on the ultrafast laser surfaces should be carried out because it could be one of the factors that can reduce the bacterial adhesion especially for *S. aureus* ATCC 6838.
- 3) An extensive research about the effect of argon gas towards bacterial adhesion should be carried out more as it has tendency in producing surface with antibacterial properties. The analysis can be further extend using the AFM to study the strength of adhesion between the bacteria and the metal surfaces.
- 4) This study should be employed in the medical industry to control the implant-associated infection problem among the implant recipients by modifying the surface at the specific range of roughness ( $S_q$ : 200 nm – 300 nm) using ultrafast laser machine.

## REFERENCES

- Abraham, S. N., Sharon, N., Ofek, I., & Schwartzman, J. D. (2015). Adhesion and Colonization. *Molecular Medical Microbiology*, 4, 409-421
- Achinas, S., Charalampogiannis, N., & Euverink, G. J. W. (2019). A Brief Recap of Microbial Adhesion and Biofilms. *Applied Sciences*, 9, 2801
- Agripa, H., & Botef, I. (2019). Modern Production Methods for Titanium Alloys: A Review. *Titanium Alloys - Novel Aspects of Their Manufacturing and Processing*, 2, 1-15
- Ahmad, M., Liu, S., Mahmood, N., Mahmood, A., Ali, M., Zheng, M., & Ni, J. (2017). Effects of porous carrier size on biofilm development, microbial distribution and nitrogen removal in microaerobic bioreactors. *Bioresour Technol*, 234, 360-369
- AlAbbas, F. M., Spear, J. R., Kakpovbia, A., Balhareth, N. M., Olson, D. L., & Mishra, B. (2012). Bacterial Attachment to Metal Substrate and Its Effects on Microbiologically-influenced Corrosion in Transporting Hydrocarbon Pipelines. *The Journal of Pipeline Engineering*, 1, 63-72
- An, Y. H., & Friedman, R. J. (2000). Handbook of Bacterial Adhesion. *Principles, Methods and Application*, 1-20
- Anikieieva, M., & Gordiyenko, O. (2014). Influence of a medium pH and ionic strength on the adhesion of *Streptococcus thermophilus* microorganisms to human. *Periodicum Biologorum*, 116, 89–93
- Arakha, M., Saleem, M., Mallick, B. C., & Jha, S. (2015). The effects of interfacial potential on antimicrobial propensity of ZnO nanoparticle. *Scientific Reports*, 5
- Arciola, C. R., Campoccia, D., Gamberini, S., Donati, M. E., & Montanaro, L. (2004). Presence of fibrinogen-binding adhesin gene in *Staphylococcus epidermidis* isolates from central venous catheters-associated and orthopaedic implant-associated infections. *Biomaterials*, 25, 4825-4829
- Armentano, I., Arciola, C. R., Fortunati, E., Ferrari, D., Mattioli, S., Amoroso, C. F., Rizzo, J., Kenny, J. M., Imbriani, M., & Visai, L. (2014). The Interaction of Bacteria with Engineered Nanostructured Polymeric Materials: A Review. *The Scientific World Journal*, 2014, 1-18
- Arnold, J. W., & Bailey, G. W. (2000). Surface finishes on stainless steel reduce bacterial attachment and early biofilm formation: scanning electron and atomic force microscopy study. *Poult Sci*, 79, 1839-1845
- Bachirraho, G., & Abouni, B. (2017). *Escherichia coli* and *Staphylococcus aureus* most common source of infection. *The Battle Against Microbial Pathogens: Basic Science, Technological Advances and Educational Programs*, 637-648

- Bagherifard, S., Hickey, D. J., de Luca, A. C., Malheiro, V. N., Markaki, A. E., Guagliano, M., & Webster, T. J. (2015). The influence of nanostructured features on bacterial adhesion and bone cell functions on severely shot peened 316L stainless steel. *Biomaterials*, *73*, 185-197
- Barros, J., Melo, L. D. R., Poeta, P., Igrejas, G., Ferraz, M. P., Azeredo, J., & Monteiro, F. J. (2019). Lytic bacteriophages against multidrug-resistant *Staphylococcus aureus*, *Enterococcus faecalis* and *Escherichia coli* isolates from orthopaedic implant-associated infections. *International Journal of Antimicrobial Agents*, *54*, 329-337
- Beveridge. (2001). Use of the Gram stain in microbiology. *Biotechnic & Histochemistry*, *76*, 111-118
- Bezek, K., Nipič, D., Torkar, K. G., Oder, M., Dražić, G., Abram, A., Žibert, J., Raspor, P., & Bohinc, K. (2019). Biofouling of stainless steel surfaces by four common pathogens: the effects of glucose concentration, temperature and surface roughness. *Biofouling*, *35*, 273-283
- Blateyron, F. (2013). The Areal Field Parameters. *Characterisation of Areal Surface Texture*, 15-43
- Bohinc, K., Dražić, G., Abram, A., Jevšnik, M., Jeršek, B., Nipič, D., Kurinčič, M., & Raspor, P. (2016). Metal surface characteristics dictate bacterial adhesion capacity. *International Journal of Adhesion and Adhesives*, *68*, 39-46
- Bollenl, C. M. L., Lambrechts, P., & Quirynen, M. (1997). Comparison of surface roughness of oral hard materials to the threshold surface roughness for bacterial plaque retention: A review of the literature. *Dent Mate*, *13*, 258-269
- Boulangé-Petermann, L., Rault, J., & Bellon-Fontaine, M. N. (1997). Adhesion of streptococcus thermophilus to stainless steel with different surface topography and roughness. *Biofouling*, *11*, 201-216
- Buividas, R., Mikutis, M., Kudrius, T., Greičius, A., Šlekys, G., & Juodkazis, S. (2012). Femtosecond Laser Processing- A New Enabling Technology. *Lithuanian Journal of Physics*, *52*, 301-311
- Busalmen, J. P., & Sanchez, S. R. (2001). Influence of pH and Ionic Strength on Adhesion of Wild Strain of *Pseudomonas* sp. to Titanium. *Journal of Industrial Microbiology and Biotechnology*, *26*, 303-308
- Calignano, F., Manfredi, D., Ambrosio, E. P., Iuliano, L., & Fino, P. (2012). Influence of process parameters on surface roughness of aluminum parts produced by DMLS. *The International Journal of Advanced Manufacturing Technology*, *67*, 2743-2751
- Callow, J. A., & Callow, M. E. (2011). Trends in the development of environmentally friendly fouling-resistant marine coatings. *Nat Commun*, *2*, 244

- Carlos, A. T., Hernández, N., Galeano, A., Novoa-Aponte, L., & Soto, C.-Y. (2013). Zeta potential as a measure of the surface charge of mycobacterial cells. *Annals of Microbiology*, 64, 1189-1195
- Carlsson, S. (2012). *Surface Characterization of Gram-Negative Bacteria and their Vesicles*. (Master of Chemistry), University Umea, Sweden.
- Carvalho, I., Henriques, M., & Carvalho, S. (2013). New Strategies to Fight Bacterial Adhesion. *Microbial pathogens and strategies for combating them: science, technology and education* (A. Méndez-Vilas, Ed.), 170-178
- Chakraborty, S., Mukherji, S., & Mukherji, S. (2010). Surface hydrophobicity of petroleum hydrocarbon degrading Burkholderia strains and their interactions with NAPLs and surfaces. *Colloids Surf B Biointerfaces*, 78, 101-108
- Chan, C.-W., Carson, L., Smith, G. C., Morelli, A., & Lee, S. (2017). Enhancing the antibacterial performance of orthopaedic implant materials by fibre laser surface engineering. *Applied Surface Science*, 404, 67-81
- Chantal, G., Malek, K., Pfleging, W., & Roth, R. (2011). *Laser Micromachining of Polymers*.
- Charville, G. W., Hetrick, E. M., Geer, C. B., & Schoenfisch, M. H. (2008). Reduced bacterial adhesion to fibrinogen-coated substrates via nitric oxide release. *Biomaterials*, 29, 4039-4044
- Chen, C., Enrico, A., Pettersson, T., Ek, M., Herland, A., Niklaus, F., Stemme, G., & Wagberg, L. (2020). Bactericidal surfaces prepared by femtosecond laser patterning and layer-by-layer polyelectrolyte coating. *J Colloid Interface Sci*, 575, 286-297
- Chen, G., & Walker, S. L. (2007). Role of Solution Chemistry and Ion Valence on the Adhesion Kinetics of Groundwater and Marine Bacteria. *Langmuir*, 23, 7162-7169
- Chen, M., Yu, Q., & Sun, H. (2013). Novel Strategies for the Prevention and Treatment of Biofilm Related Infections. *International Journal of Molecular Sciences*, 14, 18488-18501
- Cheng, Y., Feng, G., & Moraru, C. I. (2019). Micro- and Nanotopography Sensitive Bacterial Attachment Mechanisms: A Review. *Frontiers in Microbiology*, 10
- Cheung, H. Y., Chan, G. K. L., Cheung, S. H., Sun, S. Q., & Fong, W. F. (2007). Morphological and chemical changes in the attached cells of Pseudomonas aeruginosa as primary biofilms develop on aluminium and CaF<sub>2</sub> plates. *Journal of Applied Microbiology*, 102, 701-710
- Cowell, B. A., Willcox, M. D. P., & Schneider, R. P. (1998). A relatively small change in sodium chloride concentration has a strong effect on adhesion of ocular bacteria to contact lenses. *Journal of Applied Microbiology*, 84, 950-958

- Crawford, R. J., Webb, H. K., Truong, V. K., Hasan, J., & Ivanova, E. P. (2012). Surface topographical factors influencing bacterial attachment. *Adv Colloid Interface Sci*, 179-182, 142-149
- Crémet, L., Corvec, S., Bémer, P., Bret, L., Lebrun, C., Lesimple, B., Miegerville, A.-F., Reynaud, A., Lepelletier, D., & Caroff, N. (2012). Orthopaedic-implant infections by *Escherichia coli*: Molecular and phenotypic analysis of the causative strains. *Journal of Infection*, 64, 169-175
- Cunat, P. J. (2004). Alloying Elements in Stainless Steel and Other Chromium-Containing Alloys. *International Chromium Development Association*, 1-24
- Cunha, A., Elie, A.-M., Plawinski, L., Serro, A. P., Botelho do Rego, A. M., Almeida, A., Urdaci, M. C., Durrieu, M.-C., & Vilar, R. (2016). Femtosecond laser surface texturing of titanium as a method to reduce the adhesion of *Staphylococcus aureus* and biofilm formation. *Applied Surface Science*, 360, 485-493
- Cunliffe, D., Smart, C. A., Alexander, C., & Vulfson, E. N. (1999). Bacterial Adhesion at Synthetic Surfaces. *APPLIED AND ENVIRONMENTAL MICROBIOLOGY*, Vol. 65, 4995-5002
- Damiati, L., Eales, M. G., Nobbs, A. H., Su, B., Tsimbouri, P. M., Salmeron-Sanchez, M., & Dalby, M. J. (2018). Impact of surface topography and coating on osteogenesis and bacterial attachment on titanium implants. *Journal of Tissue Engineering*, 9, 1-16
- Dantas, L. C., da Silva-Neto, J. P., Dantas, T. S., Naves, L. Z., das Neves, F. D., & da Mota, A. S. (2016). Bacterial Adhesion and Surface Roughness for Different Clinical Techniques for Acrylic Polymethyl Methacrylate. *Int J Dent*, 2016, 8685796
- Darouiche, R. O. (2004). Treatment of Infections Associated with Surgical Implants. *The new england journal of medicine*, 350, 1422-1429
- De-la-Pinta, I., Cobos, M., Ibarretxe, J., Montoya, E., Eraso, E., Guraya, T., & Quindos, G. (2019). Effect of biomaterials hydrophobicity and roughness on biofilm development. *J Mater Sci Mater Med*, 30, 77
- De Giorgi, C., Furlan, V., Demir, A. G., Tallarita, E., Candiani, G., & Previtali, B. (2016). Laser Micro-polishing of Stainless Steel for Antibacterial Surface Applications. *Procedia CIRP*, 49, 88-93
- Deltombe, R., Kubiak, K. J., & Biggerelle, M. (2014). How to select the most relevant 3D roughness parameters of a surface. *Scanning*, 36, 150-160
- Desrousseaux, C., Sautou, V., Descamps, S., & Traoré, O. (2013). Modification of the surfaces of medical devices to prevent microbial adhesion and biofilm formation. *Journal of Hospital Infection*, 85, 87-93

- Dewasthale, S., Mani, I., & Vasdev, K. (2018). Microbial biofilm: current challenges in health care industry. *Journal of Applied Biotechnology & Bioengineering*, 5
- Donald, H. (2017). *The Effects of Nanopattern Surface Technology and Targeted Metabolic Therapies on Orthopaedic Implant Related Infections*. (MRCS, MBChB, BSc (Hons)), University of Glasgow, Glasgow Theses Service.
- Du, C., Wang, C., Zhang, T., Yi, X., Liang, J., & Wang, H. (2020). Reduced bacterial adhesion on zirconium-based bulk metallic glasses by femtosecond laser nanostructuring. *Proc Inst Mech Eng H*, 234, 387-397
- Duarte, P. M., Reis, A. F., de Freitas, P. M., & Ota-Tsuzuki, C. (2009). Bacterial Adhesion on Smooth and Rough Titanium Surfaces After Treatment With Different Instruments. *Journal of Periodontology*, 80, 1824-1832
- Dunne, W. M., Jr. (2002). Bacterial adhesion: seen any good biofilms lately? *Clin Microbiol Rev*, 15, 155-166
- Dziubakiewicz, E., Hryniewicz, K., Walczyk, M., & Buszewski, B. (2013). Study of charge distribution on the surface of biocolloids. *Colloids and Surfaces B: Biointerfaces*, 104, 122-127
- Eick, S., Kindblom, C., Mizgalska, D., Magdon, A., Jurczyk, K., Sculean, A., & Stavropoulos, A. (2017). Adhesion of Porphyromonas gingivalis and Tannerella forsythia to dentin and titanium with sandblasted and acid etched surface coated with serum and serum proteins - An in vitro study. *Arch Oral Biol*, 75, 81-88
- Eid, A. (2016). Infected orthopedic implants. *The Egyptian Orthopaedic Journal*, 51, 187
- Elbourne, A., Chapman, J., Gelmi, A., Cozzolino, D., Crawford, R. J., & Truong, V. K. (2019). Bacterial-nanostructure interactions: The role of cell elasticity and adhesion forces. *J Colloid Interface Sci*, 546, 192-210
- Eni, A. O., Oluwawemitan, I. A., & Solomon, O. U. (2010). Microbial quality of fruits and vegetables sold in Sango Ota, Nigeria. *African Journal of Food Science*, Vol. 4, 291-296
- Epperlein, N., Menzel, F., Schwibbert, K., Koter, R., Bonse, J., Sameith, J., Krüger, J., & Toepel, J. (2017). Influence of femtosecond laser produced nanostructures on biofilm growth on steel. *Applied Surface Science*, 418, 420-424
- Fabre, A., Raynaud, S., & Brenier, B. (2011). Effect of measurement conditions on three-dimensional roughness values, and development of measurement standard. *Journal of Physics: Conference Series*, 311, 012008
- Farmer, J. J., Farmer, M. K., & Holmes, B. (2010). The Enterobacteriaceae: General characteristics. *Bacteriology Organisms and Their Biology*, 5, 1-39
- Fernandes, D. J., Elias, C. N., & Valiev, R. Z. (2015). Properties and Performance of Ultrafine Grained Titanium for Biomedical Applications. *Materials Research*, 18, 1163-1175

- Fletcher, M. (1994). Bacterial biofilms and biofouling. *Bacterial biofilms and biofouling Fletcher*, 5, 302-306
- Flint, S. H., Brooks, J. D., & Bremer, P. J. (2000). Properties of the stainless steel substrate, influencing the adhesion of thermo-resistant streptococci. *Journal of Food Engineering*, 43, 235-242
- Floyd, K. A., Eberly, A. R., & Hadjifrangiskou, M. (2017). Adhesion of bacteria to surfaces and biofilm formation on medical devices. *Biofilms and Implantable Medical Devices*, 10, 47-95
- Gadelmawla, E. S., Koura, M. M., Maksoud, T. M. A., Elewa, L. M., & Soliman, H. H. (2002). Roughness Parameters. *Journal of Materials Processing Technology*, 123, 133-145
- Gangan, M. S., & Athale, C. A. (2017). Threshold effect of growth rate on population variability of Escherichia coli cell lengths. *Royal Society Open Science*, 4, 160417
- Garrett, T. R., Bhakoo, M., & Zhang, Z. (2008). Bacterial adhesion and biofilms on surfaces. *Progress in Natural Science*, 18, 1049-1056
- Giannuzzi, G., Gaudioso, C., Di Mundo, R., Mirengi, L., Fraggelakis, F., Kling, R., Lugarà, P. M., & Ancona, A. (2019). Short and long term surface chemistry and wetting behaviour of stainless steel with 1D and 2D periodic structures induced by bursts of femtosecond laser pulses. *Applied Surface Science*, 494, 1055-1065
- Gnanamani, A., Hariharan, P., & Paul-Satyaseela, M. (2017). Staphylococcus aureus: Overview of Bacteriology, Clinical Diseases, Epidemiology, Antibiotic Resistance and Therapeutic Approach. *Frontiers in Staphylococcus Aureus*, 1, 3-28
- Goebel, M., Bachmann, J., Woche, S. K., Fischer, W. R., & Horton, R. (2004). Water Potential and Aggregate Size Effects on Contact Angle and Surface Energy. *SOIL SCI. SOC. AM. J.*, 68, 383-393
- Gogra, A. B., Yao, J., Sandy, E. H., Zheng, S., Zaray, G., Koroma, B. M., & Hui, Z. (2010). Cell surface hydrophobicity (CSH) of Escherichia coli, Staphylococcus aureus and Aspergillus niger and the biodegradation of Diethyl Phthalate (DEP) via Microcalorimetry. *Journal of American Science*, 6, 78-88
- Gottenbos, B., Bussher, H. J., & Van Der Mei, H. C. (2002). Pathogenesis and Prevention of Biomaterial Centered Infections. *Journal of Materials Science: Material in Medicine*, 13, 717-722
- Gu, H., Chen, A., Song, X., Brasch, M. E., Henderson, J. H., & Ren, D. (2016). How Escherichia coli lands and forms cell clusters on a surface: a new role of surface topography. *Sci Rep*, 6, 29516

- Günther, J., Petzl, W., Bauer, I., Ponsuksili, S., Zerbe, H., Schubert, H.-J., Brunner, R. M., & Seyfert, H.-M. (2017). Differentiating *Staphylococcus aureus* from *Escherichia coli* mastitis: *S. aureus* triggers unbalanced immune-dampening and host cell invasion immediately after udder infection. *Scientific Reports*, 7
- Gusnaniar, N., van der Mei, H. C., Qu, W., Nuryastuti, T., Hooymans, J. M. M., Sjollema, J., & Busscher, H. J. (2017). Physico-chemistry of bacterial transmission versus adhesion. *Adv Colloid Interface Sci*, 250, 15-24
- Habimana, O., Semião, A. J. C., & Casey, E. (2014). The role of cell-surface interactions in bacterial initial adhesion and consequent biofilm formation on nanofiltration/reverse osmosis membranes. *Journal of Membrane Science*, 454, 82-96
- Halder, S., Yadav, K. K., Sarkar, R., Mukherjee, S., Saha, P., Haldar, S., Karmakar, S., & Sen, T. (2015). Alteration of Zeta potential and membrane permeability in bacteria: a study with cationic agents. *Springerplus*, 4, 672
- Hamad, A. H. (2016). Effects of Different Laser Pulse Regimes (Nanosecond, Picosecond and Femtosecond) on the Ablation of Materials for Production of Nanoparticles in Liquid Solution.
- Hamadi, F., Latrache, H., Mabrouki, M., Elghmari, A., Outzourhit, A., Ellouali, M., & Chtaini, A. (2005). Effect of pH on distribution and adhesion of *Staphylococcus aureus* to glass. *Journal of Adhesion Science and Technology*, 19, 73-85
- Han, A., Tsoi, J. K. H., Rodrigues, F. P., Leprince, J. G., & Palin, W. M. (2016). Bacterial adhesion mechanisms on dental implant surfaces and the influencing factors. *International Journal of Adhesion and Adhesives*, 69, 58-71
- Harimawan, A., & Ting, Y. P. (2016). Investigation of extracellular polymeric substances (EPS) properties of *P. aeruginosa* and *B. subtilis* and their role in bacterial adhesion. *Colloids Surf B Biointerfaces*, 146, 459-467
- Harris, L. G., Meredith, D. O., Eschbach, L., & Richards, R. G. (2007). *Staphylococcus aureus* adhesion to standard micro-rough and electropolished implant materials. *J Mater Sci Mater Med*, 18, 1151-1156
- Harris, L. G., & Richards, R. G. (2006). *Staphylococci* and implant surfaces: a review. *Injury*, 37, S3-S14
- Harvey, P. D. (2011). Engineering Properties of Steel. *ASM International*, 1, 1-4
- Herman-Bausier, P., El-Kirat-Chatel, S., Foster, T. J., Geoghegan, J. A., & Dufrene, Y. F. (2015). *Staphylococcus aureus* Fibronectin-Binding Protein A Mediates Cell-Cell Adhesion through Low-Affinity Homophilic Bonds. *mBio*, 6, e00413-00415
- Hermawan, H., Ramdan, D., & Djuansjah, J. R. P. (2011). Metals for Biomedical Applications. *Biomedical Engineering – From Theory to Applications*, 17, 411-430



- Hilbert, L. R., Bagge-Ravn, D., Kold, J., & Gram, L. (2003). Influence of surface roughness of stainless steel on microbial adhesion and corrosion resistance. *International Biodeterioration & Biodegradation*, 52, 175-185
- Hoogmoed, C. G., Mei, H. C., & Busscher, H. J. (1997). The influence of calcium on the initial adhesion of *S. thermophilus* to stainless steel under flow studied by metallurgical microscopy. *Biofouling*, 11, 167-176
- Hou, Z. B., & Komanduri, R. (2003). On the mechanics of the grinding process – Part I. Stochastic nature of the grinding process. *International Journal of Machine Tools and Manufacture*, 43, 1579-1593
- Hsieh, P. H., Lee, M. S., Hsu, K. Y., Chang, Y. H., Shih, H. N., & Ueng, S. W. (2009). Gram-Negative Prosthetic Joint Infections: Risk Factors and Outcome of Treatment. *Clinical Infectious Diseases*, 49, 1036-1043
- Huang, J., Wei, S., Zhang, L., Yang, Y., Yang, S., & Shen, Z. (2018). Effect of Laser Texturing Parameters on Wettability of Nickel Surface. *Journal of Materials Science and Chemical Engineering*, 06, 163-168
- Huhtamaki, T., Tian, X., Korhonen, J. T., & Ras, R. H. A. (2018). Surface-wetting characterization using contact-angle measurements. *Nat Protoc*, 13, 1521-1538
- Hui, Y. W., & Dykes, G. A. (2012). Modulation of cell surface hydrophobicity and attachment of bacteria to abiotic surfaces and shrimp by Malaysian herb extracts. *J Food Prot*, 75, 1507-1511
- Idalia, V.-M. N., & Bernardo, F. (2017). *Escherichia coli* as a Model Organism and Its Application in Biotechnology. *Escherichia coli - Recent Advances on Physiology, Pathogenesis and Biotechnological Applications*, 13, 253-274
- Indira, K., Sylvie, C., Zhongke, W., & Hongyu, Z. (2016). Investigation of Wettability Properties of Laser Surface Modified Rare Earth Mg Alloy. *Procedia Engineering*, 141, 63-69
- Jaeggi, B., Neuenschwander, B., Schmid, M., Muralt, M., Zuercher, J., & Hunziker, U. (2011). Influence of the Pulse Duration in the ps-Regime on the Ablation Efficiency of Metals. *Physics Procedia*, 12, 164-171
- Jalil, S. A., Akram, M., Bhat, J. A., Hayes, J. J., Singh, S. C., ElKabbash, M., & Guo, C. (2020). Creating superhydrophobic and antibacterial surfaces on gold by femtosecond laser pulses. *Applied Surface Science*, 506, 144952
- Jalil, S. A., Akram, M., Bhat, J. A., Hayes, J. J., Singh, S. C., ElKabbash, M., & Guo, C. (2020). Creating superhydrophobic and antibacterial surfaces on gold by femtosecond laser pulses. *Appl Surf Sci*, 506, 144952

- Jamai, L., Sendide, K., Ettayebi, K., Errachidi, F., Hamdouni-Alami, O., Tahra-Jouti, M. A., McDermott, T., & Ettayebi, M. (2001). Physiological difference during ethanolfermentation between calcium alginate-immobilized *Candida tropicalis* and *Sacchromyces cervivisae*. *FEMS Microbiol Letters*, *204*, 375-379
- Jang, Y., Choi, W. T., Johnson, C. T., García, A. J., Singh, P. M., Breedveld, V., Hess, D. W., & Champion, J. A. (2018). Inhibition of Bacterial Adhesion on Nanotextured Stainless Steel 316L by Electrochemical Etching. *ACS Biomaterials Science & Engineering*, *4*, 90-97
- Jaritngam, P., Tangwarodomnukun, V., Qi, H., & Dumkum, C. (2020). Surface and subsurface characteristics of laser polished Ti6Al4V titanium alloy. *Optics & Laser Technology*, *126*, 106102
- Jeevahan, J., Chandrasekaran, M., Britto Joseph, G., Durairaj, R. B., & Mageshwaran, G. (2018). Superhydrophobic surfaces: a review on fundamentals, applications, and challenges. *Journal of Coatings Technology and Research*, *15*, 231-250
- Jonsson, P., & Wadstrom, T. (1984). Cell Surface Hydrophobicity of *Staphylococcus aureus* Measured by the Salt Aggregation Test (SAT). *Current Microbiology*, *10*, 203-210
- Kalin, M., & Polajnar, M. (2014). The wetting of steel, DLC coatings, ceramics and polymers with oils and water: The importance and correlations of surface energy, surface tension, contact angle and spreading. *Applied Surface Science*, *293*, 97-108
- Kashi, A. M., Tahermanesh, K., Moradi, F., Beyranvand, S. P., Tavangar, S. M., Anvari-Yazdi, A. F., Chaichian, S., Najafabadi, A. S. M., Abed, S. M., Joghataei, M. T., & Lotfibakhshaiesh, N. (2014). How to Prepare Biological Samples and Live Tissues for Scanning Electron Microscopy (SEM) *Galen Medical Journal*, *3*, 63-80
- Katsikogianni, M., & Missirlis, Y. F. (2004). Concise review of mechanisms of bacterial adhesion to biomaterials and of techniques used in estimating bacteria-material interactions. *Eur Cell Mater*, *8*, 37-57
- Keskin, D., Mergel, O., van der Mei, H. C., Busscher, H. J., & van Rijn, P. (2019). Inhibiting Bacterial Adhesion by Mechanically Modulated Microgel Coatings. *Biomacromolecules*, *20*, 243-253
- Khare, S. K., & Agarwal, S. (2015). Predictive Modeling of Surface Roughness in Grinding. *Procedia CIRP*, *31*, 375-380
- Khatoon, Z., McTiernan, C. D., Suuronen, E. J., Mah, T.-F., & Alarcon, E. I. (2018). Bacterial biofilm formation on implantable devices and approaches to its treatment and prevention. *Heliyon*, *4*, e01067

- Klotzbach, U., Washio, K., Arnold, C. B., Zheng, Y., An, Z., Smyrek, P., Seifert, H. J., Kunze, T., Lang, V., Lasagni, A. F., & Pflieger, W. (2016). Direct laser interference patterning and ultrafast laser-induced micro/nano structuring of current collectors for lithium-ion batteries. *9736*, 97361B
- Kobayashi, N., Procop, G. W., Krebs, V., Kobayashi, H., & Bauer, T. W. (2008). Molecular identification of bacteria from aseptically loose implants. *Clin Orthop Relat Res*, *466*, 1716-1725
- Kokare, C. R., Chakraborty, S., Khopade, A. N., & Mahadik, K. R. (2008). Biofilm: Importance and applications. *Indian Journal of Biotechnology*, *8*, 159-168
- Krasowska, A., & Sigler, K. (2014). How microorganisms use hydrophobicity and what does this mean for human needs? *Front Cell Infect Microbiol*, *4*, 112
- Kumar, S. S., & Hiremath, S. S. (2019). Effect of surface roughness and surface topography on wettability of machined biomaterials using flexible viscoelastic polymer abrasive media. *Surface Topography: Metrology and Properties*, *7*, 015004
- Kuntiya, A., Nicolella, C., Pyle, L., & Poosaran, N. (2005). Effect of sodium chloride on cell surface hydrophobicity and formation of biofilm in membrane bioreactor. *Songklanakarin J. Sci. Technol*, *27*, 1073-1082
- Kwak, J.-S. (2005). Application of Taguchi and response surface methodologies for geometric error in surface grinding process. *International Journal of Machine Tools and Manufacture*, *45*, 327-334
- Li, B., & Logan, B. E. (2004). Bacterial adhesion to glass and metal-oxide surfaces. *Colloids Surf B Biointerfaces*, *36*, 81-90
- Li, Y. H., & Tian, X. (2012). Quorum sensing and bacterial social interactions in biofilms. *Sensors (Basel)*, *12*, 2519-2538
- Lima, M. S. F., & Almeida, I. (2017). Surface Modification of Ti6Al4V Alloy by Pulsed Lasers: Microstructure and Hydrophobic Behavior. *Materials Research*, *20*, 8-14
- Lin, Y. C., & Kao, C. H. (2004). A study on surface polishing of SiC with a tribochemical reaction mechanism. *The International Journal of Advanced Manufacturing Technology*, *25*, 33-40
- Liu, M., Dong, F., Zhang, W., Nie, X., Wei, H., Sun, S., Zhong, X., Liu, Y., & Wang, D. (2017). Contribution of surface functional groups and interface interaction to biosorption of strontium ions by *Saccharomyces cerevisiae* under culture conditions. *RSC Advances*, *7*, 50880-50888
- Ljungh, A., Huerten, S., & Wadstrom, T. (1985). High Surface Hydrophobicity of Autoaggregating *Staphylococcus aureus* Strains Isolated from Human Infections Studied with the Salt Aggregation Test. *Infection and Immunity*, *47*, 522-526

- Löberg, J., Mattisson, I., Hansson, S., & Ahlberg, E. (2010). Characterisation of Titanium Dental Implants I: Critical Assessment of Surface Roughness Parameters. *The Open Biomaterials Journal*, 2, 18-35
- Long, P. H. (2008). Medical Devices in Orthopedic Applications. *Toxicologic Pathology*, 36, 85-91
- Lorenzetti, M., Dogsa, I., Stosicki, T., Stopar, D., Kalin, M., Kobe, S., & Novak, S. (2015). The influence of surface modification on bacterial adhesion to titanium-based substrates. *ACS Appl Mater Interfaces*, 7, 1644-1651
- Lorite, G. S., Rodrigues, C. M., de Souza, A. A., Kranz, C., Mizaikoff, B., & Cotta, M. A. (2011). The role of conditioning film formation and surface chemical changes on *Xylella fastidiosa* adhesion and biofilm evolution. *Journal of Colloid and Interface Science*, 359, 289-295
- Lu, A., Gao, Y., Jin, T., Luo, X., Zeng, Q., & Shang, Z. (2020). Effects of surface roughness and texture on the bacterial adhesion on the bearing surface of bio-ceramic joint implants: An in vitro study. *Ceramics International*, 46, 6550-6559
- Lu, N., Zhang, W., Weng, Y., Chen, X., Cheng, Y., & Zhou, P. (2016). Fabrication of PDMS surfaces with micro patterns and the effect of pattern sizes on bacteria adhesion. *Food Control*, 68, 344-351
- Luan, Y., Liu, S., Pihl, M., van der Mei, H. C., Liu, J., Hizal, F., Choi, C.-H., Chen, H., Ren, Y., & Busscher, H. J. (2018). Bacterial interactions with nanostructured surfaces. *Current Opinion in Colloid & Interface Science*, 38, 170-189
- Ma, Y., Chen, M., Jones, J. E., Ritts, A. C., Yu, Q., & Sun, H. (2012). Inhibition of *Staphylococcus epidermidis* biofilm by trimethylsilane plasma coating. *Antimicrob Agents Chemother*, 56, 5923-5937
- Madsen, A. M., Kurdi, I., Feld, L., & Tendal, K. (2018). Airborne MRSA and Total *Staphylococcus aureus* as Associated With Particles of Different Sizes on Pig Farms. *Annals of Work Exposures and Health*, 62, 966-977
- Maharjan, N. (2019). *Laser Surface Hardening of Bearing Steels*. (Doctor of Philosophy), Nanyang Technological University Singapore, Nanyang Technological University Singapore. (150)
- Mamo, W. (1989). Physical and biochemical surface properties of Gram-positive bacteria in relation to adhesion to bovine mammary cells and tissues : A review of the literature. *Rev. sci. tech. Off. int.*, 8, 163-176
- Maragkaki, S., Elkalash, A., & Gurevich, E. L. (2017). Orientation of ripples induced by ultrafast laser pulses on copper in different liquids. *Applied Physics A*, 123
- McCarty, S., Jones, E. M., Finnegan, S., Woods, E., Cochrane, C. A., & Percival, S. L. (2014). Wound Infection and Biofilms. 339-358

- Medilanski, E., Kaufmann, K., Wick, L. Y., Wanner, O., & Harms, H. (2002). Influence of the Surface Topography of Stainless Steel on Bacterial Adhesion. *Biofouling*, 18, 193-203
- Mei, H. C., Belt-Gritter, B., & Busscher, H. J. (1995). Implications of microbial adhesion to hydrocarbons for evaluating cell surface hydrophobicity 2. Adhesion mechanisms. *Colloids and Surfaces B: Biointerfaces*, 5, 117-126
- Méndez-Pfeiffer, P. A., Soto Urzúa, L., Sánchez-Mora, E., González, A. L., Romo-Herrera, J. M., Gervacio Arciniega, J. J., & Martínez Morales, L. J. (2019). Damage on Escherichia coli and Staphylococcus aureus using white light photoactivation of Au and Ag nanoparticles. *Journal of Applied Physics*, 125, 213102
- Mertens, A., Reginster, S., Paydas, H., Contrepois, Q., Dormal, T., Lemaire, O., & Lecomte-Beckers, J. (2014). Mechanical properties of alloy Ti-6Al-4V and of stainless steel 316L processed by selective laser melting: influence of out-of-equilibrium microstructures. *Powder Metallurgy*, 57, 184-189
- Mirani, Z. A., Fatima, A., Urooj, S., Aziz, M., Khan, M. N., & Abbas, T. (2018). Relationship of cell surface hydrophobicity with biofilm formation and growth rate: A study on Pseudomonas aeruginosa, Staphylococcus aureus, and Escherichia coli. *Iranian Journal of Basic Medical Sciences*, 21, 760-769
- Mohamad, A. J., Zhu, X., Liu, X., Pflöging, W., & Torge, M. (2013). Effect of surface topography on hydrophobicity and bacterial adhesion of polystyrene. *2013 International Conference on Manipulation, Manufacturing and Measurement on the Nanoscale (3M-NANO)*, 13, 228-233
- Muszanska, A. K., Rochford, E. T., Gruszka, A., Bastian, A. A., Busscher, H. J., Norde, W., van der Mei, H. C., & Herrmann, A. (2014). Antiadhesive polymer brush coating functionalized with antimicrobial and RGD peptides to reduce biofilm formation and enhance tissue integration. *Biomacromolecules*, 15, 2019-2026
- Nassar, A., & Nassar, E. (2012). An Experimental Study of Ultrasonic Vibration-Assisted Grinding. *2nd International Conference on Advances in Computational Tools for Engineering Applications (ACTEA)*, 1, 1-3
- Naylor, A., Talwalkar, S. C., Trail, I. A., & Joyce, T. J. (2016). Evaluating the Surface Topography of Pyrolytic Carbon Finger Prostheses through Measurement of Various Roughness Parameters. *J Funct Biomater*, 7
- Neoh, K. G., Hu, X., Zheng, D., & Kang, E. T. (2012). Balancing osteoblast functions and bacterial adhesion on functionalized titanium surfaces. *Biomaterials*, 33, 2813-2822
- Nguyen, T., Roddick, F., & Fan, L. (2012). Biofouling of Water Treatment Membranes: A Review of the Underlying Causes, Monitoring Techniques and Control Measures. *Membranes*, 2, 804-840

- Nostro, A., Cannatelli, M. A., Crisafi, G., Musolino, A. D., Procopio, F., & Alonzo, V. (2004). Modifications of hydrophobicity, in vitro adherence and cellular aggregation of *Streptococcus mutans* by *Helichrysum italicum* extract. *Lett Appl Microbiol*, *38*, 423-427
- Nuutinen, T., Silvennoinen, M., Päiväsaari, K., & Vahimaa, P. (2012). Control of cultured human cells with femtosecond laser ablated patterns on steel and plastic surfaces. *Biomed Microdevices*, *15*, 279–288
- Obuekwe, C. O., Al-Jadi, Z. K., & Al-Saleh, E. S. (2009). Hydrocarbon degradation in relation to cell-surface hydrophobicity among bacterial hydrocarbon degraders from petroleum-contaminated Kuwait desert environment. *International Biodeterioration & Biodegradation*, *63*, 273-279
- Oh, J. K., Kohli, N., Zhang, Y., Min, Y., Jayaraman, A., Cisneros-Zevallos, L., & Akbulut, M. (2016). Nanoporous aerogel as a bacteria repelling hygienic material for healthcare environment. *Nanotechnology*, *27*, 1-24
- Oh, J. K., Yegin, Y., Yang, F., Zhang, M., Li, J., Huang, S., Verkhoturov, S. V., Schweikert, E. A., Perez-Lewis, K., Scholar, E. A., Taylor, T. M., Castillo, A., Cisneros-Zevallos, L., Min, Y., & Akbulut, M. (2018). The influence of surface chemistry on the kinetics and thermodynamics of bacterial adhesion. *Sci Rep*, *8*, 17247
- Olsen, I. (2015). Biofilm-specific antibiotic tolerance and resistance. *Eur J Clin Microbiol Infect Dis*, *34*, 877-886
- Orapiriyakul, W., Young, P. S., Damiaty, L., & Tsimbouri, P. M. (2018). Antibacterial surface modification of titanium implants in orthopaedics. *Journal of Tissue Engineering*, *9*, 204173141878983
- Ortega, M. P., Hagiwara, T., Watanabe, H., & Sakiyama, T. (2008). Factors Affecting Adhesion of *Staphylococcus epidermidis* to Stainless Steel Surface. *Japan Journal of Food Engineering*, Vol. 9, 251 - 259
- Pajerski, W., Ochonska, D., Brzychczy-Wloch, M., Indyka, P., Jarosz, M., Golda-Cepa, M., Sojka, Z., & Kotarba, A. (2019). Attachment efficiency of gold nanoparticles by Gram-positive and Gram-negative bacterial strains governed by surface charges. *Journal of Nanoparticle Research*, *21*
- Pauzona, C., Hryhaa, E., Forêt, P., & Nyborga, L. (2019). Effect of argon and nitrogen atmospheres on the properties of stainless steel 316 L parts produced by laser-powder bed fusion. *Materials and Design*, *179*, 107873
- Pfleging, W., Torge, M., Bruns, M., Trouillet, V., Welle, A., & Wilson, S. (2009). Laser- and UV-assisted modification of polystyrene surfaces for control of protein adsorption and cell adhesion. *Applied Surface Science*, *255*, 5453-5457
- Phillips, K. C., Gandhi, H. H., Mazur, E., & Sundaram, S. K. (2015). Ultrafast laser processing of materials: a review. *Advances in Optics and Photonics*, *7*, 684

- Pogodin, S., Hasan, J., Baulin, V. A., Webb, H. K., Truong, V. K., Phong Nguyen, T. H., Boshkovikj, V., Fluke, C. J., Watson, G. S., Watson, J. A., Crawford, R. J., & Ivanova, E. P. (2013). Biophysical model of bacterial cell interactions with nanopatterned cicada wing surfaces. *Biophys J*, *104*, 835-840
- Poortinga, A. T., Bos, R., Norde, W., & Busscher, H. J. (2002). Electric Double Layer Interactions in Bacterial Adhesion to Surfaces. *Surface Science Reports*, *47*, 1-32
- Prajitno, D. H., Maulana, A., & Syarif, D. G. (2016). Effect of Surface Roughness on Contact Angle Measurement of Nanofluid on Surface of Stainless Steel 304 by Sessile Drop Method. *Journal of Physics: Conference Series*, *739*, 012029
- Pratikno, H., & Titah, H. S. (2017). Bio-corrosion on Aluminium 6063 by Escherichia coli in Marine Environment. *The Journal for Technology and Science*, *28*, 55-58
- Qiao, G., Li, H., Xu, D.-H., & Il Park, S. (2012). Modified a Colony Forming Unit Microbial Adherence to Hydrocarbons Assay and Evaluated Cell Surface Hydrophobicity and Biofilm Production of *Vibrio scophthalmi*. *Journal of Bacteriology & Parasitology*, *03*
- Rajab, F. H., Liauw, C. M., Benson, P. S., Li, L., & Whitehead, K. A. (2018). Picosecond laser treatment production of hierarchical structured stainless steel to reduce bacterial fouling. *Food and Bioproducts Processing*, *109*, 29-40
- Renner, L. D., & Weibel, D. B. (2011). Physicochemical regulation of biofilm formation. *MRS Bull*, *36*, 347-355
- Ribeiro, M., Monteiro, F. J., & Ferraz, M. P. (2012). Infection of orthopedic implants with emphasis on bacterial adhesion process and techniques used in studying bacterial-material interactions. *Biomatter*, *2*, 176-194
- Ribeiro, M., Monteiro, F. J., & Ferraz, M. P. (2014). Infection of orthopedic implants with emphasis on bacterial adhesion process and techniques used in studying bacterial-material interactions. *Biomatter*, *2*, 176-194
- Rosenberg, M. (1984). Bacterial adherence to hydrocarbons: a useful technique for studying cell surface hydrophobicity. *FEMS Microbiology Letters* *2*, *22*, 289-295
- Rosernbeg, M. (1984). Bacterial adherence to hydrocarbons: a useful technique for studying cell surface hydrophobicity. *FEMS Microbiol Letters*, *22*, 289-295
- Rudawska, A. (2019). Mechanical treatment. *Surface Treatment in Bonding Technology*, 87-128
- Schwibbert, K., Menzel, F., Epperlein, N., Bonse, J., & Kruger, J. (2019). Bacterial Adhesion on Femtosecond Laser-Modified Polyethylene. *Materials (Basel)*, *12*
- Sehar, S., & Naz, I. (2016). Role of the Biofilms in Wastewater Treatment.

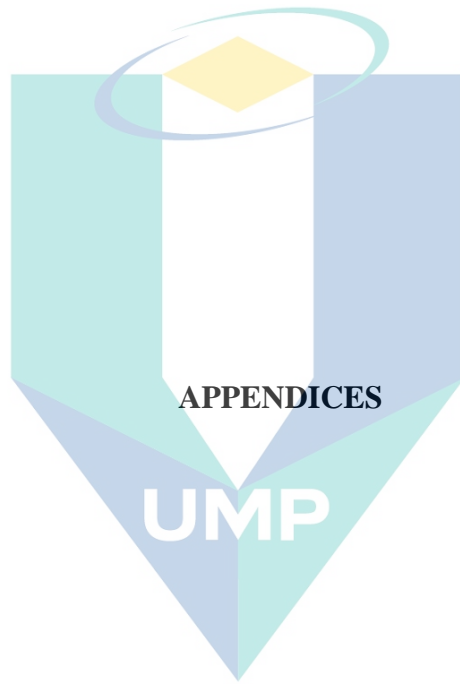
- Shaikh, S., Singhb, D., Subramanianb, M., Kediaa, S., Singh, A. K., Singhd, K., Gupta, N., & Sinhaa, S. (2017). Femtosecond laser induced surface modification for prevention of bacterial adhesion on 45S5 bioactive glass. *Journal of Non-Crystalline Solids*, 482, 63-72
- Sheng, X., Ting, Y. P., & Pehkonen, S. O. (2007). Force measurements of bacterial adhesion on metals using a cell probe atomic force microscope. *J Colloid Interface Sci*, 310, 661-669
- Sheng, X., Ting, Y. P., & Pehkonen, S. O. (2008). The influence of ionic strength, nutrients and pH on bacterial adhesion to metals. *J Colloid Interface Sci*, 321, 256-264
- Shephard, J. J., Savory, D. M., Bremer, P. J., & McQuillan, A. J. (2010). Salt modulates bacterial hydrophobicity and charge properties influencing adhesion of *Pseudomonas aeruginosa* (PA01) in aqueous suspensions. *Langmuir*, 26, 8659-8665
- Shewaramani, S., Finn, T. J., Leahy, S. C., Kassen, R., Rainey, P. B., & Moon, C. D. (2017). Anaerobically Grown *Escherichia coli* Has an Enhanced Mutation Rate and Distinct Mutational Spectra. *PLoS Genet*, 13, e1006570
- Slullitel, P. A., Buttaro, M. A., Greco, G., Onativia, J. I., Sanchez, M. L., Mc Loughlin, S., Garcia-Avila, C., Comba, F., Zanotti, G., & Piccaluga, F. (2018). No lower bacterial adhesion for ceramics compared to other biomaterials: An in vitro analysis. *Orthop Traumatol Surg Res*, 104, 439-443
- Song, F., Koo, H., & Ren, D. (2015). Effects of Material Properties on Bacterial Adhesion and Biofilm Formation. *Journal of Dental Research*, 94, 1027-1034
- Stadnyk, I., Sabadosh, G., Hushtan, T., & Yevchuk, Y. (2019). Formation of microbial biofilms on stainless steel with different surface roughness. *Potravinarstvo Slovak Journal of Food Sciences*, 13, 915-924
- Subramani, A., & Hoek, E. (2008). Direct observation of initial microbial deposition onto reverse osmosis and nanofiltration membranes. *Journal of Membrane Science*, 319, 111-125
- Suh, A. Y., Polycarpou, A. A., & Conry, T. F. (2003). Detailed surface roughness characterization of engineering surfaces undergoing tribological testing leading to scuffing. *Wear*, 255, 556-568
- Tadros, T. (2013). Electrical Double Layers. *Encyclopedia of Colloid and Interface Science*, 8, 341-457
- Taljanovic, M. S., Jones, M. D., Benjamin, J. B., Ruth, J. T., Sheppard, J. E., Hunter, T. B., & Brown, A. W. (2003). Joint Arthroplasties and Prostheses. *Radiographics*, 23, 1295 - 1314



- Tasneem, U., Yasin, N., Nisa, I., Shah, F., Rasheed, U., Momin, F., Zaman, S., & Qasim, M. (2018). Biofilm producing bacteria: A serious threat to public health in developing countries. *J Food Sci Nutr*, *1*, 25-31
- Temmler, A., & Pirch, N. (2020). Investigation on the mechanism of surface structure formation during laser remelting with modulated laser power on tool steel H11. *Applied Surface Science*, *526*, 146393
- Tolosa, I., Garciandía, F., Zubiri, F., Zapirain, F., & Esnaola, A. (2010). Study of mechanical properties of AISI 316 stainless steel processed by “selective laser melting”, following different manufacturing strategies. *The International Journal of Advanced Manufacturing Technology*, *51*, 639-647
- Truong, V. K., Lapovok, R., Estrin, Y. S., Rundell, S., Wange, J. Y., Fluke, C. J., Crawford, R. J., & Ivanova, E. P. (2010). The influence of nano-scale surface roughness on bacterial adhesion to ultrafine-grained titanium. *Biomaterials*, *31*, 3674-3683
- Tuson, H. H., & Weibel, D. B. (2013). Bacteria-surface interactions. *Soft Matter*, *9*, 4368-4380
- Valquier-Flynn, H., Wilson, C. L., Holmes, A. E., & Wentworth, C. D. (2017). Growth Rate of *Pseudomonas aeruginosa* Biofilms on Slippery Butyl Methacrylate-Co-Ethylene Dimethacrylate (BMA-EDMA), Glass and Polycarbonate Surfaces. *J Biotechnol Biomater*, *7*
- Vanhaecke, E., Remon, J. P., Moors, M., Raes, F., De Rudder, D., & Van Peteghem, A. (1990). Kinetics of *Pseudomonas aeruginosa* adhesion to 304 and 316-L stainless steel: role of cell surface hydrophobicity. *Appl Environ Microbiol*, *56*, 788-795
- Vishwakarma, V. (2020). Impact of environmental biofilms: Industrial components and its remediation. *Journal of Basic Microbiology*, *60*, 198-206
- Walker, S. L., Hill, J. E., Redman, J. A., & Elimelech, M. (2005). Influence of growth phase on adhesion kinetics of *Escherichia coli* D21g. *Appl Environ Microbiol*, *71*, 3093-3099
- Wang, L., Fan, D., Chen, W., & Terentjev, E. M. (2015). Bacterial growth, detachment and cell size control on polyethylene terephthalate surfaces. *Scientific Reports*, *5*
- Wang, M., & Tang, T. (2019). Surface treatment strategies to combat implant-related infection from the beginning. *J Orthop Translat*, *17*, 42-54
- Wassmann, T., Kreis, S., Behr, M., & Buegers, R. (2017). The influence of surface texture and wettability on initial bacterial adhesion on titanium and zirconium oxide dental implants. *Int J Implant Dent*, *3*, 32
- Wennerberg, A., Albrektsson, T., & Jimbo, R. (2015). *Overview of Surface Microtopography/Chemistry/Physics/Nano-roughness*. New York Dordrecht London: Springer Heidelberg.

- Whip, B. R. (2017). *Effect of Process on The Surface Roughness and Mechanical Performance of Additively Manufactured Alloy 718*. (Master of Science in Mechanical Engineering), Wright State University, Wright State University.
- Whitehead, K. A., Colligon, J., & Verran, J. (2005). Retention of microbial cells in substratum surface features of micrometer and sub-micrometer dimensions. *Colloids Surf B Biointerfaces*, *41*, 129-138
- Wilson, W. W., Wade, M. M., Holman, S. C., & Champlin, F. R. (2001). Status of methods for assessing bacterial cell surface charge properties based on zeta potential measurements. *Journal of Microbiological Methods*, *43*, 153-164
- Woo, J., Seo, H., Na, Y., Choi, S., Kim, S., Choi, W. I., Park, M. H., & Sung, D. (2020). Facile synthesis and coating of aqueous antifouling polymers for inhibiting pathogenic bacterial adhesion on medical devices. *Progress in Organic Coatings*, *147*, 105772
- Wu, S., Altenried, S., Zogg, A., Zuber, F., Maniura-Weber, K., & Ren, Q. (2018). Role of the Surface Nanoscale Roughness of Stainless Steel on Bacterial Adhesion and Microcolony Formation. *ACS Omega*, *3*, 6456-6464
- Wu, Y., Zitelli, J. P., TenHuisen, K. S., Yu, X., & Libera, M. R. (2011). Differential response of Staphylococci and osteoblasts to varying titanium surface roughness. *Biomaterials*, *32*, 951-960
- Xing, R., Lyngstadaas, S. P., Ellingsen, J. E., Taxt-Lamolle, S., & Haugen, H. J. (2015). The influence of surface nanoroughness, texture and chemistry of TiZr implant abutment on oral biofilm accumulation. *Clin Oral Implants Res*, *26*, 649-656
- Xu, L. C., Wo, Y., Meyerhoff, M. E., & Siedlecki, C. A. (2017). Inhibition of bacterial adhesion and biofilm formation by dual functional textured and nitric oxide releasing surfaces. *Acta Biomaterialia*, *51*, 53-65
- Yang, H., He, H., Zhou, L., Qian, J., Hao, J., & Zhu, H. (2012). Sharp transition of laser-induced periodic ripple structures. *Optica Applicata*, *4*, 795-803
- Yang, Y., Rouxhet, P. G., Chudziak, D., Telegdi, J., & Dupont-Gillain, C. C. (2014). Influence of poly(ethylene oxide)-based copolymer on protein adsorption and bacterial adhesion on stainless steel: modulation by surface hydrophobicity. *Bioelectrochemistry*, *97*, 127-136
- Yazdankhah, S. P., Sørum, H., Larsen, H. J. S., & Gogstad, G. (2001). Use of magnetic beads for Gram staining of bacteria in aqueous suspension. *Journal of Microbiological Methods*, *47*, 369-371
- Yoda, I., Koseki, H., Tomita, M., Shida, T., Horiuchi, H., Sakoda, H., & Osaki, M. (2014). Effect of surface roughness of biomaterials on Staphylococcus epidermidis adhesion. *BMC Microbiology*, *14*, 1-7

- Yuan, Y., Hays, M. P., Hardwidge, P. R., & Kim, J. (2017). Surface characteristics influencing bacterial adhesion to polymeric substrates. *RSC Advances*, 7, 14254-14261
- Yuan, Y., & Lee, T. R. (2013). Contact Angle and Wetting Properties. *51*, 3-34
- Zanatta, F. B., Valandro, L. F., Kleverlaan, C. J., Exterkate, R. A. M., Kantorski, K. Z., Pereira, G. K. R., & Dutra, D. A. M. (2017). Grinding With Diamond Burs and Hydrothermal Aging of a Y-TZP Material: Effect on the Material Surface Characteristics and Bacterial Adhesion. *Operative Dentistry*, 42, 669-678
- Žemaitis, A., Mimidis, A., Papadopoulos, A., Gečys, P., Račiukaitis, G., Stratakis, E., & Gedvilas, M. (2020). Controlling the wettability of stainless steel from highly-hydrophilic to super-hydrophobic by femtosecond laser-induced ripples and nanospikes. *RSC Advances*, 10, 37956-37961
- Zhang, B., Wu, S., Liu, Y., Suo, X., & Li, H. (2018). Influence of surface topography on bacterial adhesion: A review (Review). *Biointerphases*, 13, 060801
- Zhang, X., Wang, L., & Levänen, E. (2013). Superhydrophobic surfaces for the reduction of bacterial adhesion. *RSC Advances*, 3, 12003
- Zhao, G., & Chen, W. N. (2017). Biofouling formation and structure on original and modified PVDF membranes: role of microbial species and membrane properties. *RSC Advances*, 7, 37990-38000
- Zhou, N. (2018). Surface integrity and corrosion behavior of stainless steels after grinding operation. *Department of Chemistry Division of Surface and Corrosion Science, Doctor Philosophy*, 1-109
- Zita, A., & Hermansson, M. (1997). Determination of bacterial cell surface hydrophobicity of single cells in cultures and in wastewater in situ. *FEMS Microbiol Letters*, 152, 299-306
- Zituni, D., Schütt-Gerowitt, H., Kopp, M., Krönke, M., Addicks, K., Hoffmann, C., Hellmich, M., Faber, F., & Niedermeier, W. (2013). The growth of *Staphylococcus aureus* and *Escherichia coli* in low-direct current electric fields. *International Journal of Oral Science*, 6, 7-14
- Zulfakar, S. S., White, J. D., Ross, T., & Tamplin, M. (2013). Effect of pH, salt and chemical rinses on bacterial attachment to extracellular matrix proteins. *Food Microbiol*, 34, 369-375



اونيورسيتي ملايسيا قهغ

UNIVERSITI MALAYSIA PAHANG

## APPENDIX A: LIST OF PUBLICATIONS AND AWARDS

### Publications:

- 1) Noratiqah Chik, Wan Salwanis Wan Md. Zain, Ahmad Johari Mohamad, Mohd. Zaidi Sidek, Wan Hanisah Wan Ibrahim, Alexandra Reif, Jan Hendric Rakebrandt, Wilhelm Pfleging, Xianping Liu (2018). Bacterial Adhesion on the Titanium and Stainless-Steel Surfaces Undergone Two Different Treatment Methods: Polishing and Ultrafast Laser Treatment. *IOP Conf. Series: Material Science and Engineering*. 358, 012034. DOI: 10.1088/1757-899X/358/1/012034
- 2) Nur Hanuni Ramli, Nor Ashikin Ibrahim, Noratiqah Chik, Nur Hidayah Mat Yasin (2015). Investigation of antimicrobial activity and phytochemical analysis of thorns of *Ceiba petandra* plant. *Journal of Pure and Applied Microbiology*. 9, 519-524. ISSN: 0973-7510.

### Awards:

- 1) Silver medal at Creation, Innovation, Technology and Research Exposition (CITREX) UMP (2018). Effect of Roughness on the Adhesion of Bacteria on Lasered Surface Metal.
- 2) Bronze medal at Creation, Innovation, Technology and Research Exposition (CITREX) UMP (2015). Adhesion of Bacterial on Metal Surfaces: Effect of Surface Roughness.

اونيورسيتي ملايسيا قهغ

UNIVERSITI MALAYSIA PAHANG